Experiments with 3D Printed Coil Forms[1]
A Laboratory Notebook

Jed Marti KI7NNP

June 24, 2024

The engineer who has occasion to calculate an inductance is likely to be overwhelmed by the very wealth of formulas offered him.
Frederick W. Grover, 1946

[1] Any Artificial Intelligence used in this study was implemented entirely by the author.

Contents

List of Figures

List of Tables

1 Why?

Precision inductors are a bit of an anachronism - for small values, parasitic inductance in their circuit physicality may predominate. The inductance calculation may suffer from the geometry necessary for mechanical stability. The inductor geometry may change slightly with temperature and so on. Tuned circuits relying on fixed inductors usually have variable capacitors to make up for this lack. This may not be an option hence the need for inductors with predictable and measurable values.

Looking for precision inductors to complement the "precision" capacitors of a previous study, I went on-line to find the number of turns and geometry for my needs - 1.6 μh in a reasonable size with a modest Q. Using one of the equations I computed the number of turns, the radius and length. I printed the form using PLA, a reasonable dielectric, and got no where near the desired result. Many repeated attempts with different PLA densities, diameters, turns and lengths I finally got within 6% of the desired result but with much waste and frustration. It was clear that the geometry of the printed form was not that expected by the equation or that the equations had unspecified restrictions.

Figure 1: Some of those that were not close enough.

3D printing opens up possibilities for inductors beyond that envisioned by the approximation in the ARRL handbook[1][2]. Here $\mathscr{L}$ is the inductance in microhenries, d the coil diameter, n the number of turns and l the coil length in inches.

$$\mathscr{L} = \frac{d^2 n^2}{18d + 40l} \tag{1}$$

[2]In the text that follows, we abbreviate this equation **ARRL**

Rather than try and capture the physics behind this in an all encompassing equation, I decided on a number of experiments to capture the variables along a single dimension of change and fit multi-variable polynomials to the experimental results. This is accomplished by a multi-process, genetic optimization program. It tries billions of solutions on 150+ measured coils and finds a reasonable fit within the ranges of values allowed.

There are multivariate polynomial regression routines, notably in Python and Mathcad, but others have worked a similar mechanism where many measurements are taken [2]. The approach of averaging 30 measurements reduces the data size from over 5000 data points to a reasonable number for the available computing resources as opposed to the method proposed in [3]. The solutions examined have up to 4 variables with powers up to 5. Mostly the optimization is against the mean measured values but for restricted sets entire datasets were used.

A second program converts your inductance requirements into an STL file for 3D printing. You give it the inductance you want, set ranges for the size, wire gauge, and turns, then, after a while, an STL file is created.

2 Existing Solutions

The inductance measure is named after Joseph Henry, the units we use are micro Henries or μH, one millionth of a henry. You can see him in front of the Smithsonian (secretary from 1846 5to 1878) and as the last named mountain range in the US (in southern Utah). He was president of the National Academy of Sciences from 1868 to 1878.

Accurate solutions are feasible using Maxwell's equations and complex geometric descriptions. For example, see *Inductance Calculations* [4] or *Inductance Loop and Partial* [5]. We propose to accept simple polynomial approximations derived by experiment as have the approximations described below.

The number of different equations on the net was truly surprising until an offhand comment about them being derived from experiments rather than physics was an eye opener. It's clear that each approximation has unadvertised limits on the coil parameters. The basic parameters for a cylindrical single layer coil include:

- n the number of turns (somewhat lacking in detail),
- l the coil length (somewhat lacking in detail),
- r the coil radius to center of the wire,
- A the area of the core (somewhat lacking in detail),
- μ_r the relative permeability of the core.

After my experiments, I've identified a few other parameters that influence inductance.

- **Parasitic Geometry** The coil may be more complex than a simple helix.
- **Wire Gauge** Even with the same number of turns on the same length, the wire gauge affects the inductance.
- **Humidity** Most 3D printed plastics are hygroscopic. The inductance does vary somewhat with humidity.
- **LCR meters** No two of these read the same values.
- **Core permeability** Plastics with embedded ferromagnetic material for increased Q.
- **Core permittivity** Conductive plastics reduce coil self resonant frequency.

Figure 2 shows the kind of coil we're contemplating and some of its troublesome characteristics. Using any standard air coil approximation for this geometry is thwarted by the following:

1. The coil form extends to $\frac{1}{2}$ the wire radius - not air.

2. There's an extra small turn at each end that affects the inductance.

3. The coil core will not be a uniform cylinder. It may have a hole and the plastic interior may not be solid. The relative permeability of plain PLA is not known though probably very close to 1. 3D printing of plastic with relative permeability greater than 1.0 is affected by the density and geometry of the fill.

Here l is the distance between the center of the end of the final turns and the coil area A:

$$A = \pi(r_1^2 - r_2^2) \tag{2}$$

A is only important if μ_r is not 1.0.

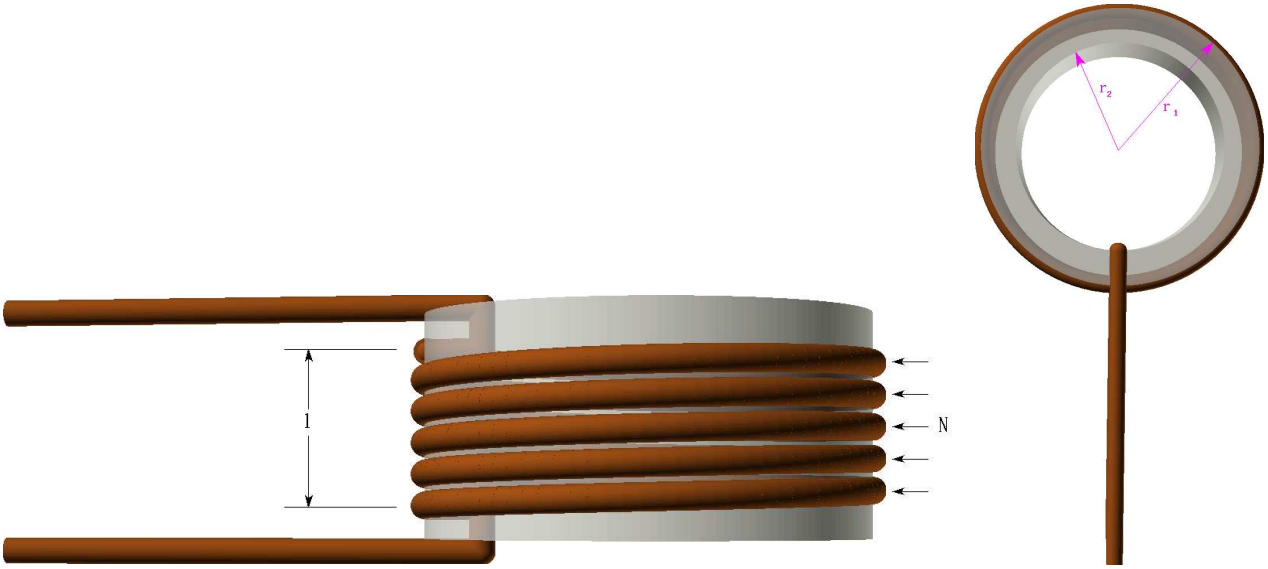

Figure 2: Important coil dimensions.

Figure 3 shows this detail from two coils taken at about 10X enlargement. As you can see on the left hand side, the winding wire track is not nearly as nice as that pictured by the CAD system.

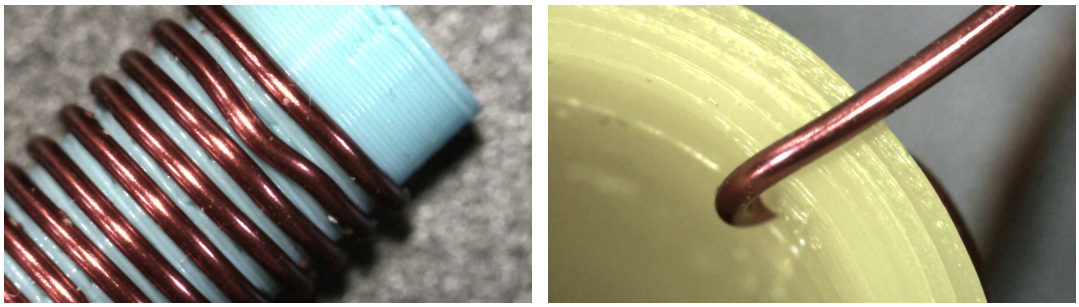

Figure 3: Sample windings under a microscope.

2.1 Some Approximations

The ARRL handbook approximation in equation 1 is reasonable as long as the coil aspect ratio is reasonable, the turns are close together and your core has μ_0 permeability. This, and other equations work better with the geometry in Figure 4.

Figure 4: Air core coil geometry.

Notice the difference between Figure 2 and Figure 4. The air coil is missing $\frac{1}{2}$ a turn but doesn't have the curl to hold the wires in place. This leads to some of the differences that we discover later on.

Another approximation caters to low and high aspect ratio air coils [6]. In what follows, we will call this equation **Russian**. For dimensions in millimeters:

$$\mathscr{L} = \begin{array}{ll} l > r & \frac{\left(\frac{d}{10}\right)^2 n^2}{4.5d+10l} \\ l \leq r & \frac{\left(\frac{d}{10}\right)^2 n^2}{4d+11l} \end{array} \tag{3}$$

The most common equation appears to come from "Basic AC Circuits" [7]. The Encyclopedia Magnetica provides a formula for non-air core inductors [8, 9]. Here $\mu_0 = 4\pi 10^{-7}$ [3] and μ_r is the relative permeability of the core material. We will use equation 4 to compute the permeability of various inductor cores. In what follows we call this equation **Basic AC**.

$$\mathscr{L} = \frac{n^2 \mu_0 \mu_r A}{l} \tag{4}$$

The following equation from [10] supposedly is accurate to 1% when $l > 0.67r$. We call equation 5 **RFC** and the units are millimeters and the result in microHenries.

$$\mathscr{L} = \frac{0.0394 r^2 n^2}{9r + 10l} \tag{5}$$

While reference [11] for $l > 0.8r$ has the same approximation expressed as a function of μ_0. For most results it corresponds closely to equation 5. We call this equation **RF1**.

$$\mathscr{L} = \frac{\pi r^2 \mu_0 n^2}{9r + 10l} \tag{6}$$

Another on-line tool from EEWeb includes the wire diameter w [12] but unfortunately, does not allow variable wire spacing. The on-line solver appears to have a bug. In metric units we have:

$$\mathscr{L} = n^2 \mu_0 \mu_r r(\ln(\frac{8d}{w}) - 2) \tag{7}$$

In the code this is called **EEWeb**.

Claimed more accurate is Lundin's approximation of Nagaoka's tables [13] 90 and avoiding the elliptic integrals of Miller's solution.

$$\mathscr{L} = \begin{array}{ll} 2r \leq l & \frac{\mu_0 n^2 \pi r^2}{l} \left\{ f_1\left(\frac{4r^2}{l^2}\right) - \frac{4}{3\pi}\frac{2r}{l} \right\} \\ 2r > l & \mu_0 n^2 r \left\{ \left[ln\left(\frac{8r}{l}\right) - \frac{1}{2} \right] f_1\left(\frac{l^2}{4r^2}\right) + f_2\left(\frac{l^2}{4r^2}\right) \right\} \end{array} \tag{8}$$

where:

$$f_1(x) = \frac{1 + 0.383901x + 0.017108x^2}{1 + 0.258952x}, 0 \leq x \leq 1 \tag{9}$$

$$f_2(x) = 0.093842x + 0.002029x^2 - 0.000801x^3, 0 \leq x \leq 1 \tag{10}$$

notice the restriction on x. In the code, this is called **LUNDIN**.

[3] In 2019, μ_0 was redefined as proportional to the fine-structure constant and is now 1.25663706127e-6. All calculations were performed with the pre-2019 value.

The final word appears to be Miller's solving elliptic integrals of the first and second kind [14]. However, it does not account for wire size. For radius r, axial length l and n turns, we have:

$$d = \sqrt{4r^2 + l^2} \tag{11}$$

$$k = \frac{2r}{d} \tag{12}$$

$$K = \frac{1}{3\pi}\left(\frac{dl}{r^2}(F(k) - E(k)\right) + \frac{4d}{l}E(k) - \frac{8r}{l} \tag{13}$$

The inductance in Henries is:

$$\mathscr{L} = \frac{\mu_0 n^2 \pi r^2}{l} K \tag{14}$$

The elliptical integrals are solved by iteration on k.

$$\begin{array}{rl} a_0 = & 1 \\ b_0 = & \sqrt{1-k^2} \\ c_0 = & k \end{array} \tag{15}$$

with the recurrence relations:

$$\begin{array}{rl} a_n = & \frac{a_{n-1}+b_{n-1}}{2} \\ b_n = & \sqrt{a_{n-1}b_{n-1}} \\ c_n = & \frac{a_{n-1}-b_{n-1}}{2} \end{array} \tag{16}$$

and run this until $c_n = 0$ or the number of bits in the values of the variables.

If the number of iterations was m, then we have:

$$F(k) = \frac{\pi}{2a_m} \tag{17}$$

$$E(k) = F(k)\left(1 - \frac{1}{2}\sum_{i=0}^{m} 2^i c_i^2\right) \tag{18}$$

Normally the series converges quickly. In what follows, this will be called the **MILLER** solution.

2.2 Statistics

I compare these values against the actual data and get the RMS error for each. For a set of m measured values L_i and the computed value M_i the error is:

$$rms = \sqrt{\frac{\sum_i^m \left(\frac{L_i - M_i}{M_i}\right)^2}{m}} \tag{19}$$

Polynomial regression fits are not good predictors outside the data set they fit. The higher the degree, the worse this gets. As a consequence every one of the new equations will have an expressed set of limitations.

For these approximations we will use the Standard Error of Estimate (SEE) formula [15]. For the predictor variable x_i (turns, diameter, length, etc.), the mean of the measured values y_i and the regression equation f, we have equation 20. Small values relative to $f(x_i)$ indicate a better fit than larger ones.

$$s_f = \sqrt{\frac{\sum_i^m \left(\frac{f(x_i) - y_i)}{y_i}\right)^2}{n-2}} \tag{20}$$

For linear equations, we may also use the slope test of equation 21 where m is the slope, f the linear equation, and p the predictor value.

$$t_e = \frac{m}{\frac{s_f}{\sqrt{\sum_i (x_i - \vec{x})}}} \tag{21}$$

3 Sources of Error

Inductance measurements are inexact at best. There are 3 important ones [16].

1. Inductance,
2. Q,
3. Self Resonant Frequency (SRF)

I'll report on all 3 though some of the measurements are *ad hoc*. A few sources of error were identified after the measurements.

Test Leads The bench top East Tester has Kelvin style probes to minimize parasitic external capacitance and inductance. The East Tester clips are gold plated to make good contact with the inductor wires. However, the contacts are scalloped and flat on the top and the spring load small. The Keysight alligator clips are sharp and the spring load large, the leads short but not Kelvin but seem to give more consistent results.

Measurement Device An East Tester ET4410 and a Keysight U1733C were used to measure inductance and Q - the results were consistently different. A nano VNA measured SRF.

Inductor wire resistance We're dealing with very low DC resistances, almost always less than one ohm so any dirt, left over enamel or finger grease alters the measurement of Q. We attempt to minimize these errors with frequent cleaning and repeated measurements.

Inductor lead length Where possible, the inductor lead lengths have been trimmed to 1" from the inductor surface and the insulating enamel removed by file and sand paper. This is a particular problem for inductors with few turns. To minimize the error a test stand forces the Kelvin probes and inductor to a fixed position.

Environment Measurements were made over the course of 20 months. During winter, the temperature and relative humidity were fairly constant. 65 degrees Fahrenheit and 28-33% relative humidity. However, for a few weeks, a series of wet winter storms raised the relative humidity to near 40% which may have affected the measurements. A further set of experiments subjected some coils to 100% humidity for at least 2 days and their inductance measured with minimal change.

Calibration I made 30 measurements of each inductor, different groups spread over a few days. The meter was calibrated once for each group and measurements made in different order to account for any changes from previous groups. In no case were more

than 15 measurements made before re-calibration. Still, the inductance varied over the course of a day, usually increasing until the early afternoon and then decreasing later in the day. The meter was allowed to "warm up" for 30 minutes before any measurements were taken.

Nearby Stuff During calibration the large body of mostly water was moved at least 10' away from the probes. Test coils were at least 12 inches from the test fixture. The test surface was composite granite. There are numerous sources of error - unknown metal nearby, the 110v power cord for the meter, LED lighting, arrangement of the probe wires, and so on.

Physical Dimensions On low cost 3D printers with default settings, resolution is a problem. The wire channels are not perfectly round and are composed of a number of cylinders subtracted from the coil cylinder. This is a particular problem for large diameters and small wires. Likewise, printer age may lead to sloppy edges and cylinder diameter variance.

Filament Shrinkage The common belief is that PLA shrinks 2% in the X and Y axes and nothing in the Z. This was factored into some of the early experiments but further experiments with a new printer and slicer challenge this assumption.

Age It appears that the forms and windings change geometry somewhat with age but only slightly. This could be expansion of the plastic with humidity change, temperature changing the diameter, or the windings sinking deeper into the channels over time.

3.1 What is a turn?

A turn has varying definitions. In [9] a straight wire is defined as $N = 1$. Others seem to define a single turn as shown in Figure 5 but this really appears to have the inductance of somewhat more than half a turn. Multiple turns have the same issue at the ends as shown in Figure 4 though the results have less influence with more turns.

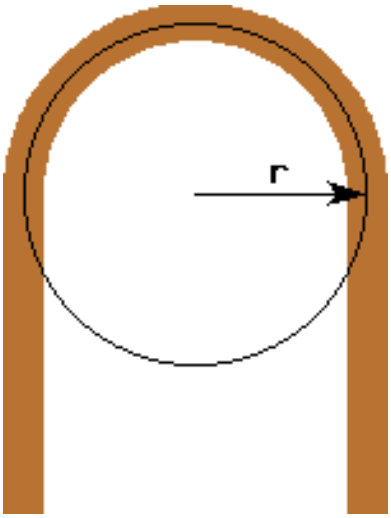

Figure 5: Single turn.

3.2 Parasitic Inductance

A straight wire has its own inductance so an inductor is complemented by its connection to the circuit. In our case the parasitic inductance is caused by the loop at each winding end.

Mounting one of these coils vertically will incur parasitic inductance from the extra length of wire. The relative permeability of copper:

$$\mu = 0.999994 \tag{22}$$

The inductance of a straight length of wire of metric radius r and length l (in centimeters) from [17] equations 94-98, [4] page 35, equation 8 is:

$$\mathscr{L} = 0.002l(\log\frac{2l}{r} - 1 + \frac{\mu}{4}) \tag{23}$$

As μ is very near 1.0 for copper we have:

$$\mathscr{L} = 0.002l(\log\frac{2l}{r} - 0.75) \tag{24}$$

Figure 6 plots inductance of a straight wire (calculated, not measured as this is not a loop) of various lengths and gauges. As you can see, the inductance for 1" is between 22 and 33 nanohenries per inch. These are summarized in Table 1. The one inch leads on the tested coils probably add about $0.05\mu H$ to the actual coil inductance.

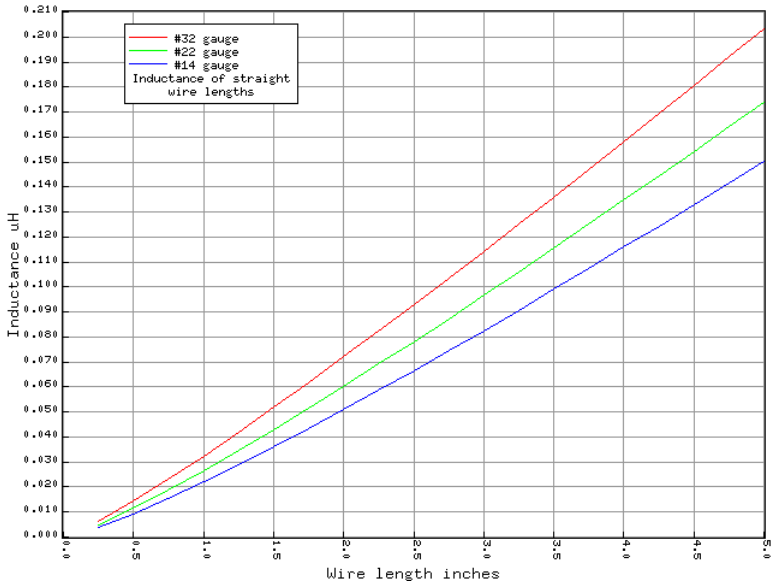

Figure 6: Inductance of three wire gauges by length.

Gauge	Inductance/inch
32	32.50 nH
30	31.36 nH
28	30.19 nH
26	29.01 nH
24	27.82 nH
22	26.65 nH
20	25.45 nH
18	23.95 nH
16	23.11 nH
14	21.92 nH

Table 1: Calculated inductance per inch of copper wire

4 Experiments

Clearly we can't explore the complete inductor parameter space, instead, we try a few parameters singly. We record the inductance and sometimes Q of an actual coil and attempt to fit a linear equation or low degree polynomial to the result. These include the obvious:

1. The number of turns.
2. The coil diameter.
3. The coil length.
4. The coil core composition.
5. The coil core fill percentage.
6. The wire gauge.

From these we attempt to derive general equations and then verify with actual construction. The data is stored in comma separated variable files with a header line and comments prefixed with double slashes (//).

Finally, we attempt to derive a multivariate polynomial that best fits the range of coils using the variables of:

Radius Coil radius in meters.

Length Coil length in meters.

Wire Size Wire radius in meters.

Turns Number of turns (an integer).

I do not attempt to include μ_r in the general polynomial solutions.

In addition to the above experiments, I attempted to characterize coil form performance and measurement including:

- Temperature and heat cycling.
- The measurement device.
- Humidity.
- Plastic permittivity.
- Composite plastic permeability.
- Internal fill percentage and geometry.

4.1 Experimental Apparatus

This consists of a MakerGear M2 3D printer (later a LULZBOT TAZ Workhorse), an East Tester ET4410 LCR meter, temperature and humidity sensor, and test stands. A second LCR, the Keysight U1733C was used on a spacing experiment for comparison.

Coil position relative to the test connectors needs to be uniform across all the tests. A 3D printed stand in Figure 7 holds both clips in a fixed position. Three different stands for different coil lengths were printed. The Keysight's leads are too short to use these stands.

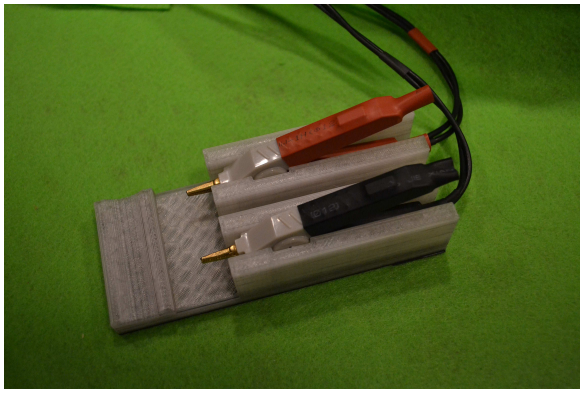

Figure 7: Holder for testing coils.

Both meters are calibrated before every group of tests. The output frequency is 100 kHz at 1 volt though for some later measurements this was reduced to 80 KHz. The East Tester instrument does appear to drift during the day even after calibration. Hence 30 measurements spread over weeks and months were taken for all tests. As noted in [16] inductance measurement can vary widely across instruments and test frequencies. Statistical analysis of the results shows the measurements near normally distributed around the mean as might be expected from the central limit theorem [15].

The MakerGear M2 3D printer is capable of printing most of the low temperature PLA filaments. However, ABS, requires a higher temperature than it can maintained and delamination is a problem. The vertical layer is about .3mm or about 0.012" which limits the spiral indent on a form to about 26 gauge wire though some experiments used small as 28 gauge. This printer was replaced for some of the final experiments by a more capable Lulzbot printer with higher resolution and greater accuracy. The newer printer has a vertical resolution of .1 mm if you're willing to wait and some of the final coils were printed at this resolution (anything in lime green).

I printed 6 types:

Plain PLA Polylactic Acid, various colors which all seem to behave the same. A test of

the dielectric values indicated they're all the same.

Conductive PLA It appears to have nearly the same permeability as plain PLA but has a much different dielectric value. This is Composite Conductive PLA CDP11705 from Protoplant.

Composite Iron PLA PLA infused with powered iron of some sort. It does have a much different permeability value than plain PLA. This came from Protoplant, FE11705.

PVA Polyvinyl Alcohol support material - used to wind coils but then dissolved in water for an air core. This is not the panacea that one might hope.

NylonG Nylon with embedded fiberglass. Also tested it's permittivity. Tested for age over time and the effects of temperature cycling.

PETG Testing of inductance change over time and temperature cycling.

The humidity test was performed in a sealed plastic box with the coils under test and a bowl of water. I used a wireless relative humidity sensor for dry and humid conditions. Typical winter Utah relative humidity is between 30% and 40% and we are at 4500' above sea level.

Temperature testing used a filament drier set at 150 Fahrenheit and a freezer set at 30 Fahrenheit. The coils were soaked at these temperatures for a day before readings were taken.

4.2 The Number of Turns

The number of turns is the most important consideration. I printed 10 coil forms - 1" in diameter, with a .125" cylinder wall in plain PLA. The cylinders were filled at 50% though this matters little as the walls are quite thin. Coils from 1 to 30 turns were created as shown in Figure 8. The coils are designed to rest on the test stand at a fixed position.

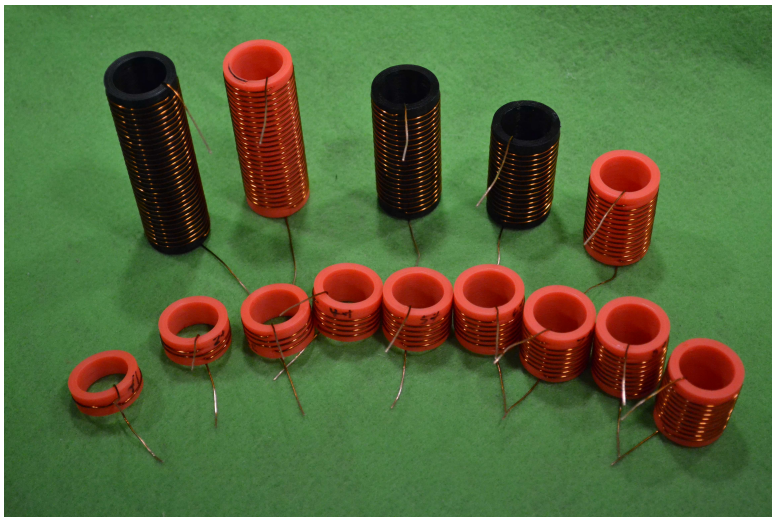

Figure 8: Turns testing coils. 1-10 turns front, 30-12 back.

The values range from about 20 nanohenries to 6.75 μH though the smaller values are below the resolution of the meters. In fact, all values below 500 nanohenries have been removed from later analysis. I measured inductance of each coil 30 times and recorded them.

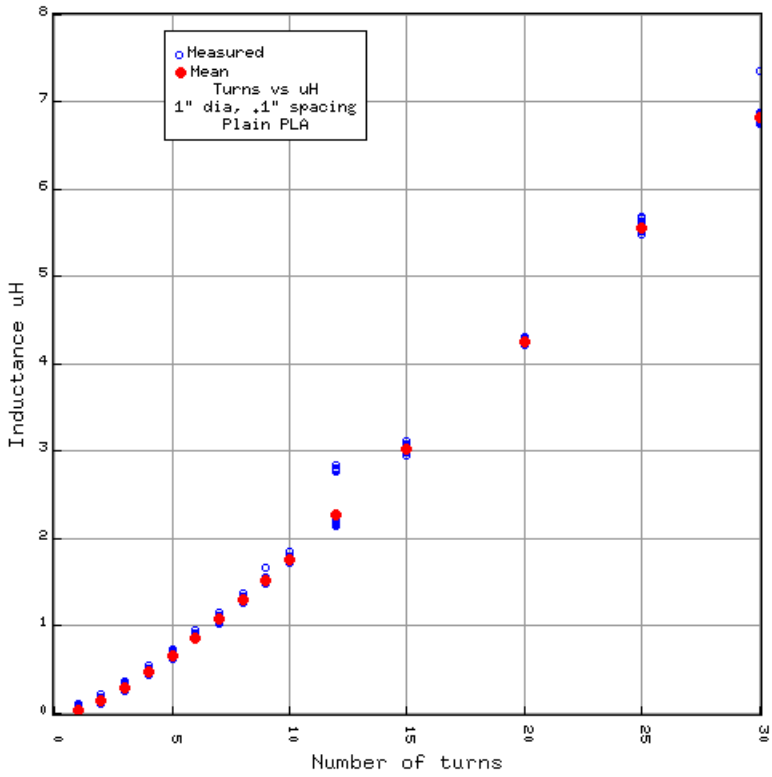

Figure 9: 1 to 30 turns inductance, 1" diameter, .1" spacing #22 wire

A linear equation fits these really well.

$$L = -0.675068 + 0.248447x \tag{25}$$

Equation	RMS error
ARRL	0.23 μH
Russian	0.19 μH
RFC1	0.24 μH
RF1	0.23 μH
Lundin	0.22 μH
Linear	0.0009 μH

Table 2: Linear fit on 1" diameter spacing

Remember that this applies only to PLA coils 1" in diameter with 0.125" wall thickness,

0.1" spacing and #22 wire. We're going to make the assumption that the curve extends beyond three inches though this is dangerous.

4.3 Turn Spacing

3D printing allows us to experiment with turn spacing. In general, for the same number of turns, the closer the spacing, the higher the inductance. In Figure 10 are some of the coils used in this experiment - 10 turns with a center to center wire spacing of 0.03" to 0.1".

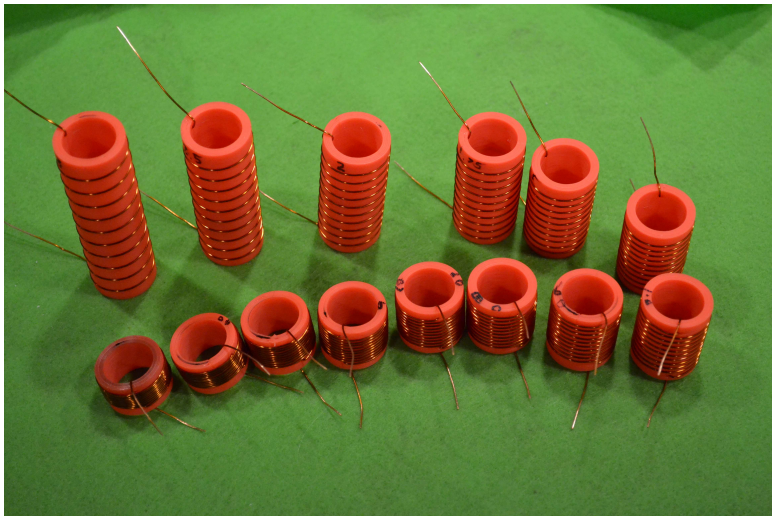

Figure 10: The forms from .3" to 3", 10 turns 1" diameter, #22 wire.

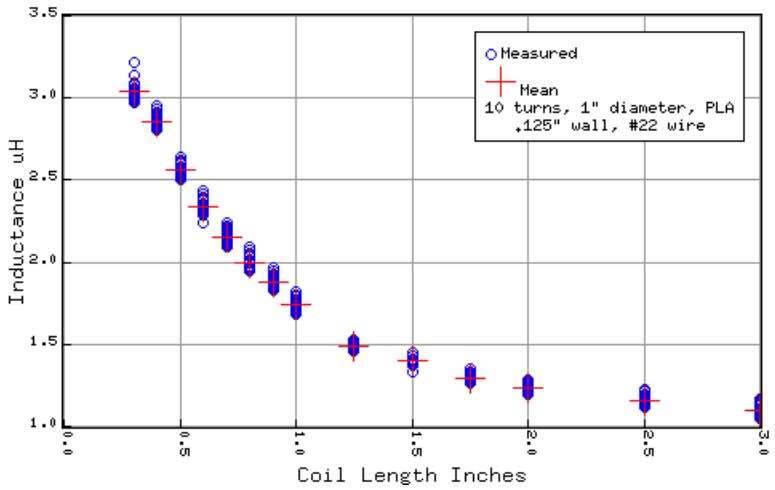

Figure 11: Length vs inductance - 10 turns.

Let's see how the different equations 1, 3, 4, 5, and 6 stack up against this experiment. The best μ_r is computed by trying values from 0.5 to 5 with the best RMS error at $\tilde{1}.422$. We also try different polynomial curve fits up to 10 degrees - the best is 5 with the results shown in Figure 12. The results are much better than any of the approximations **for this range of lengths**. However, a quintic epolynomial risks fitting to errors in measurement. In the final curve fits the best results were obtained with cubics.

$$L = 0.0432822l^5 - 0.299272l^4 + 0.480952l^3 + 0.876574l^2 - 3.34232l + 3.97903 \quad (26)$$

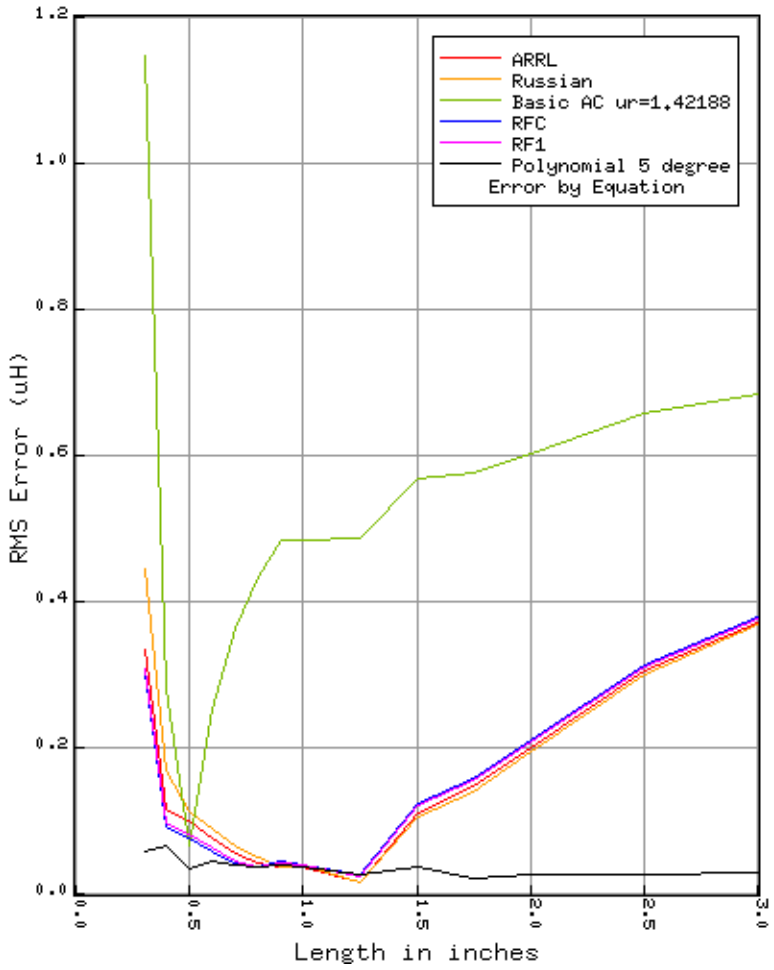

Figure 12: RMS error in length vs μH, 10 turns, 1" diameter, #22 wire

As before, 30 measurements were taken of each coil spread over a few weeks. The RMS error is computed from each measurement, not the means.

4.4 Coil Radius

Next, we try the same experiment, keeping the length and turns the same, but increasing the diameter. The wall thickness is 0.125", length 1" and 10 turns. I ran both PLA and the iron composite PLA as shown in Figure 13.

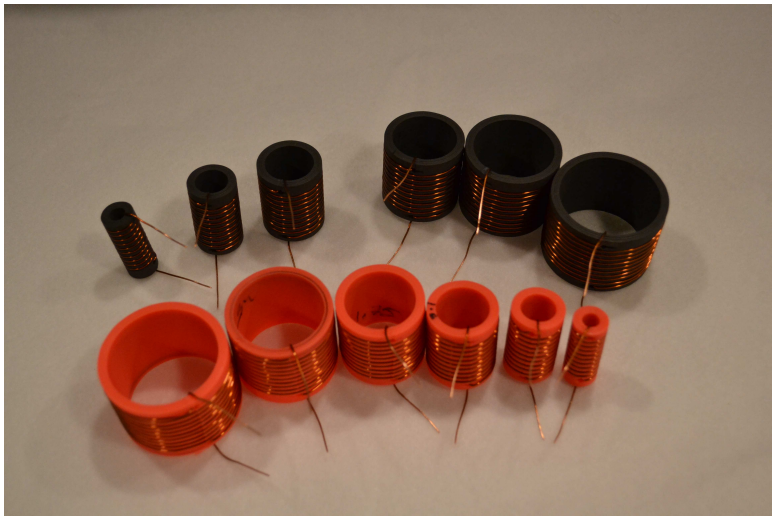

Figure 13: 10 turns, .1 spacing, diameter 0.5 to 1.75", #22 wire. Plain PLA front, Iron Composite in the back.

Performing the 30 measurements and computing the mean for both plain PLA shown in Figure 14 with a quadratic line fit in blue. An initial design of the 1.5" coil resulted in an anomolously high inductance revealed insufficient number of cylinders per turn resulting in a larger diameter. The coil was reprinted and measured.

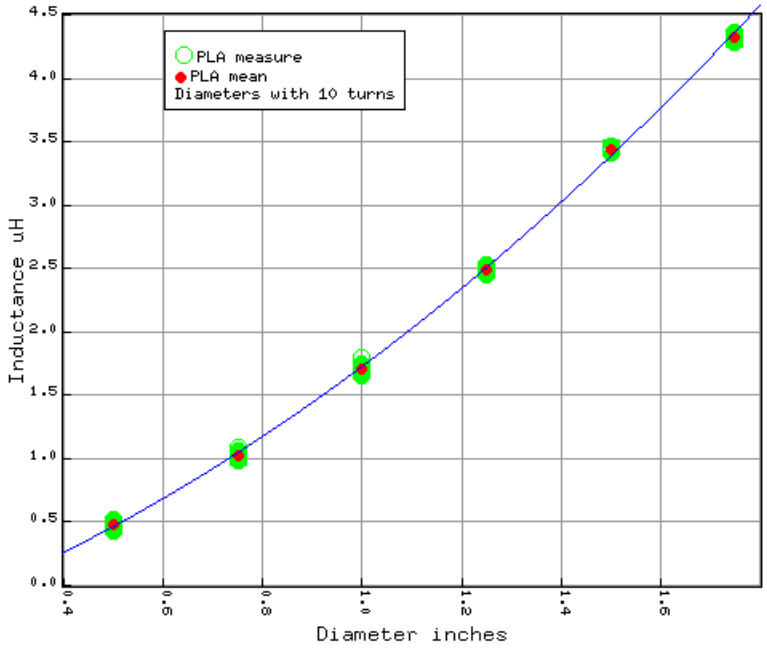

Figure 14: Diameter vs inductance

A quadratic does a fine job:

$$\mathscr{L} = 0.796771d^2 + 1.32258d - 0.400326 \tag{27}$$

Next we try the same experiment to check predictions, first with plain PLA. We compare the measured inductance (30 times) against that predicted keeping track of the RMS error and plotting it. Except for an aspect ratio of 1.0, most of the equations perform really poorly. The RF1 equations 5-6 perform nearly as well as the polynomial fit.

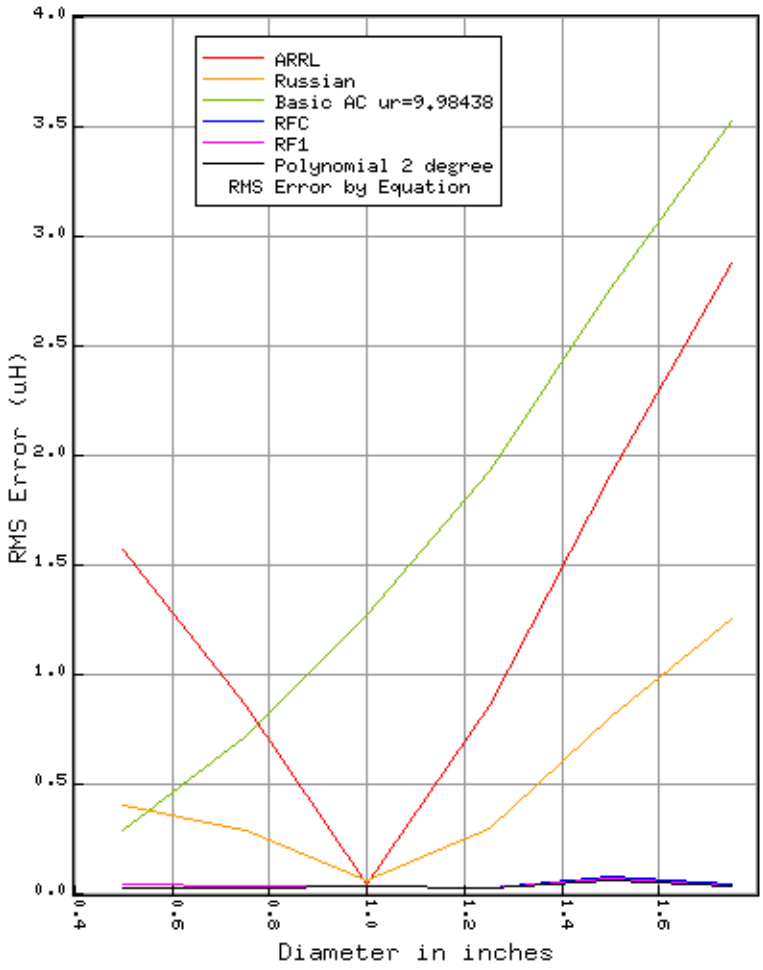

Figure 15: Really bad results except for aspect ratio of 1.0

4.5 Wire Gauge

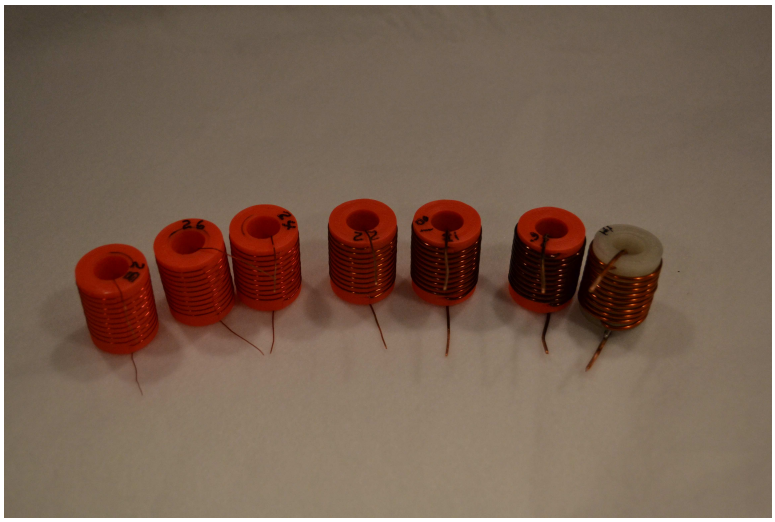

Figure 16: 10 turns, .1" spacing, wire gauges 14 to 28.

None of the equations account for wire size. What happens if we wind 10 turns on a 1" diameter PLA 50% filled, 0.125" wall 1" in length and vary the size? The inductance of these coils increases with the increasing wire gauge - that is, the thinner the wire the more inductance (See Figure 6 and Table 1). For the wire gauges I had on hand, graph 17 show increasing inductance from #14 gauge to #28 gauge (missing #20 gauge). Winding #14 on a small coil requires strong fingers and tightening it caused a wire break (fixed by soldering a new lead).

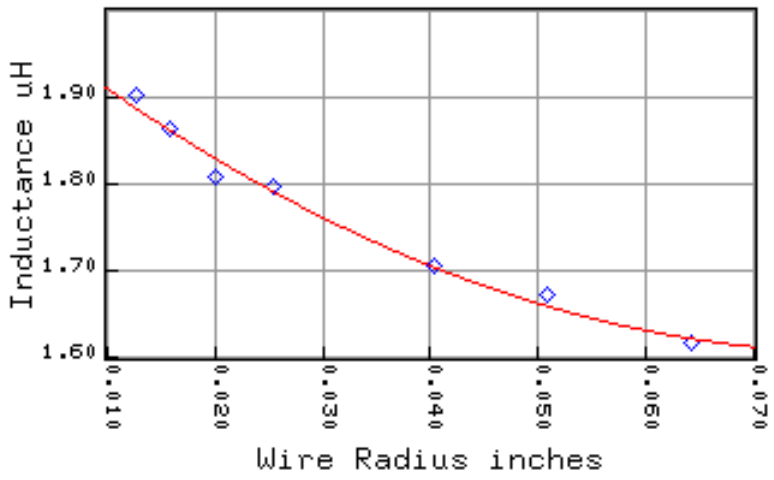

Figure 17: Wire gauge vs inductance.

Some caveats. When printing for finer gauges, we're up against the resolution of the 3D printer and some of the inductance may be a function of the wire center not being exactly at the 1" diameter. Likewise, the wire indents are made up of 20 short straight cylinders for each turn. Though these are lined up, the wind is not completely circular or even worse the channel may not extend far enough into the main cylinder.

Fitting curves to the values shows a quadratic has a reasonable fit and will be used in subsequent attempts at an all encompassing equation.

$$\mathscr{L} = 62.8303w^2 - 9.9429w + 2.00538 \tag{28}$$

To test this, I printed a 3" 10 turn coil but with #14 gauge wireb with the same 10 turns used for the #22 gauge form as shown in Figure 18. The theory being that changing the wire gauge from #22 to a smaller gauge will increase the inductance and a large gauge decrease the inductance by a linear amount.

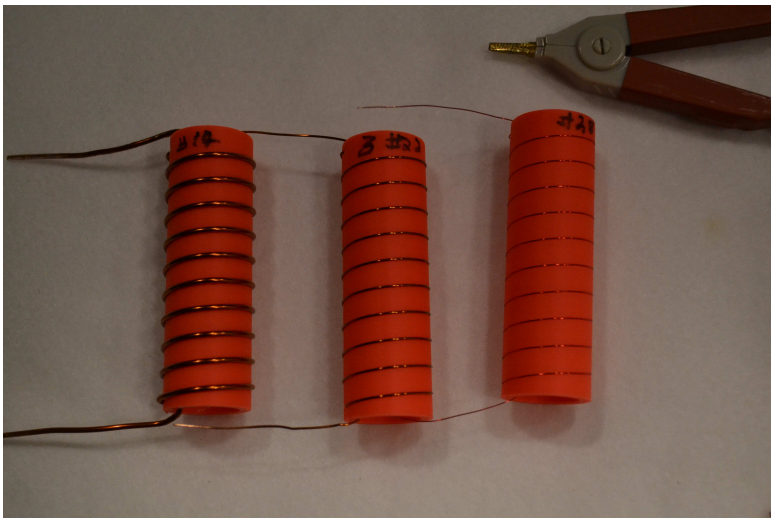

Figure 18: #14, #22, and #28 gauge 3" 10 turn form.

Measuring the inductance 30 times and showing the increase in inductance by gauge number (linear, not like radius) is shown in Table 3.

Gauge	μH	**ratio**
14	0.944367	1 %
22	1.0762	1.14%
28	1.1812	1.25%

Table 3: Inductance ratio increase by gauge, 3 inch coils, 10 turns.

4.6 Humidity

It's well known that a lot of printable plastics are hygroscopic (absorb moisture). I placed the coils in Table 9 in a tight plastic box with a bowl of water and a relative humidity sensor. I waited two days for the relative humidity to stabilize between 97% and 99% at around 65 F.

The mean of these measurements is the filled black circle in Figure 37. The measurements show that the inductance increases about 0.43% at high humidity, not good but not horrible.

Figure 19: High humidity chamber.

A further round compared larger coils with a varying number of turns. The results in Figure 20 show the same effect.

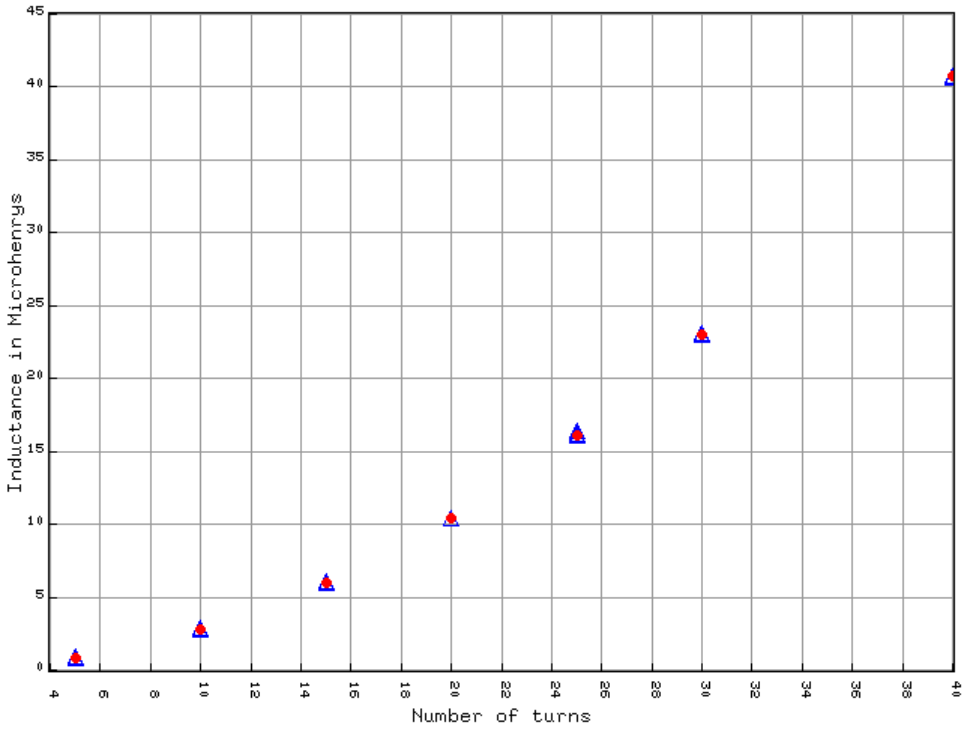

Figure 20: Inductance high vs low humidity, same coils.

4.7 Aging

Over the course of many months, I noticed or imagined that measured inductances seemed to decrease. This lead me to test 15 different coils over a month. These were printed in 3 different PLA colors (sort of yellow, melmac blue, and white), Nylon G (orange) and PETG (black) with diameters of 0.25", 0.75" and 2" with 20, 20, and 10 turns respectively. Spacing was 0.04" and all windings were #22 gauge with a helical cylinder size of 0.028" inches.

Figure 21: Age test coil sets, PLA, PETG (black), NylonG (orange).

5 measurements were taken every two days for a month. The times for Nylon G and PETG were offset by about two weeks as they were printed later.

I expect that suitable tension on the windings will reduce the radius as the wires seep into the channels over time. This might occur notably faster at higher temperatures. First, consider the 3 sizes of the 3 sets of PLA coils. In Figure 22 data sets are color coded to match the coils in Figure 21. Each set is shifted a bit horizontally so as not to cover up the others too much.

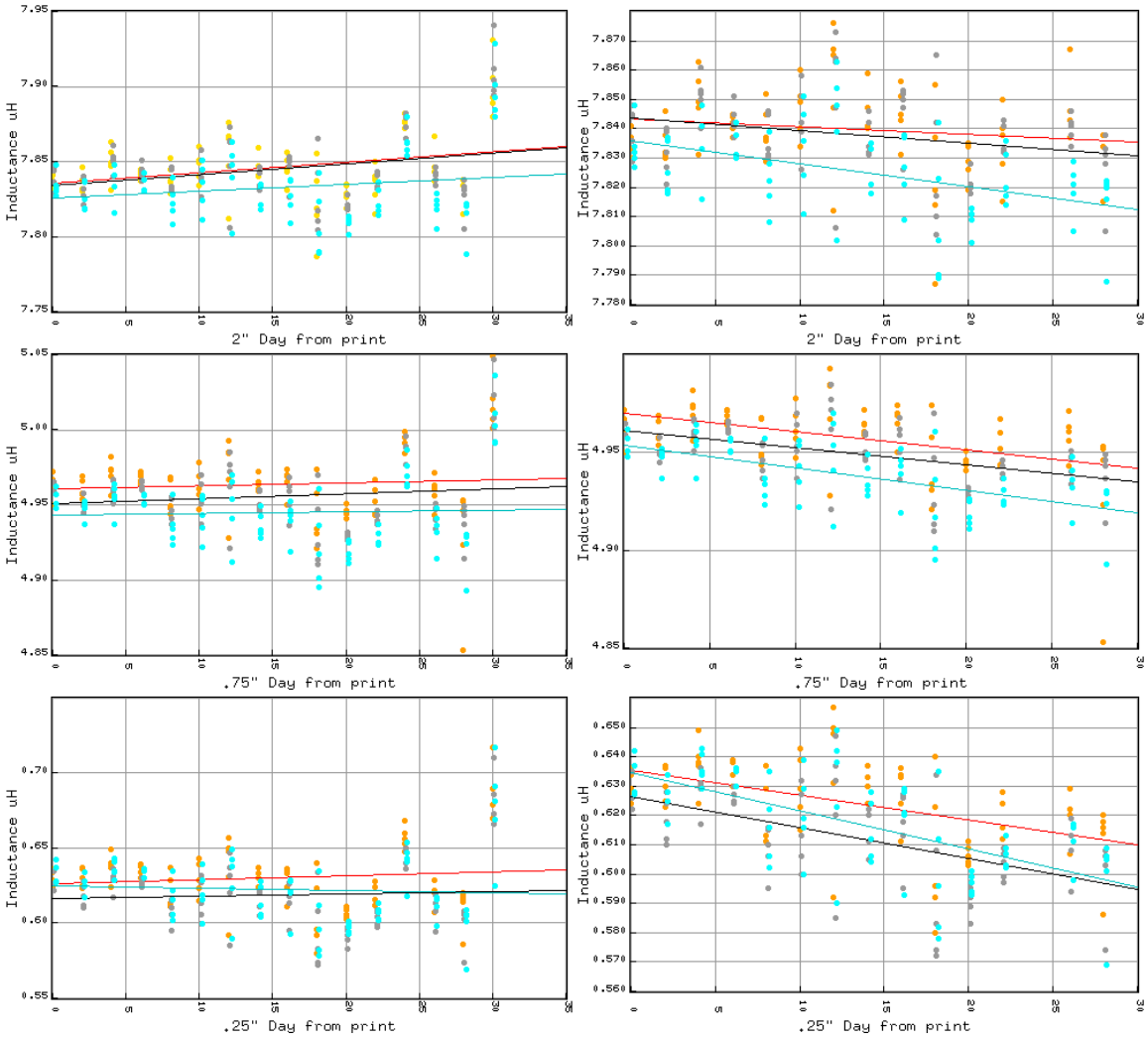

Figure 22: PLA Age test results with and without anomolous days.

Remove the data sets taken on days 24 and 30 and the results are as predicted: the inductance decreases slowly over time. We will examine this more by heating and cooling a set of coils to watch for their change if any.

In Figure 23 PETG shows a different story. Even with the anomolous days (4 and 10), there's a slight increase over time. Removing the anomolous days accentuates this even further.

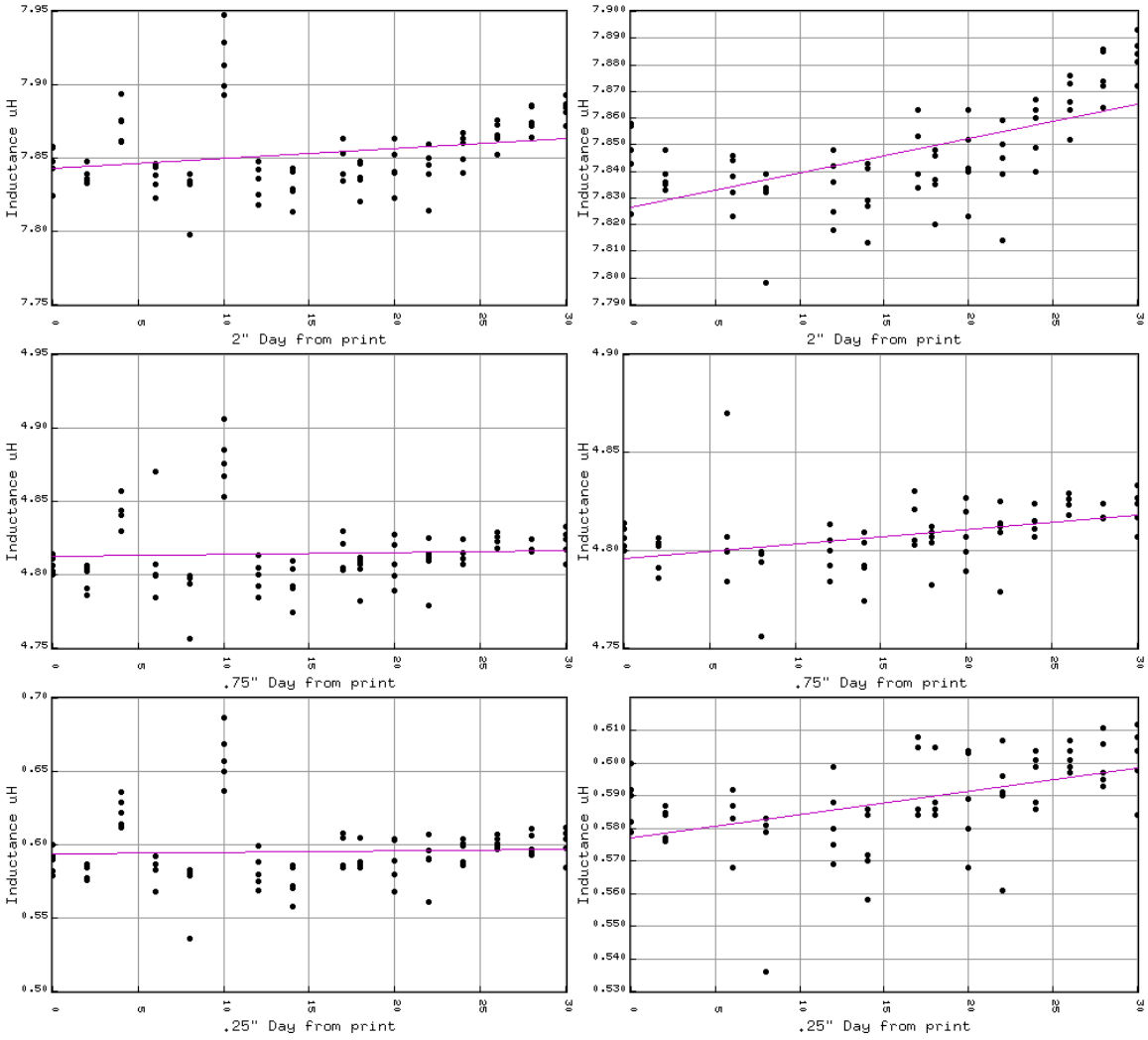

Figure 23: PETG age test results with and without anomolous days.

In Figure 24 NylonG filament shows better stability than the others.

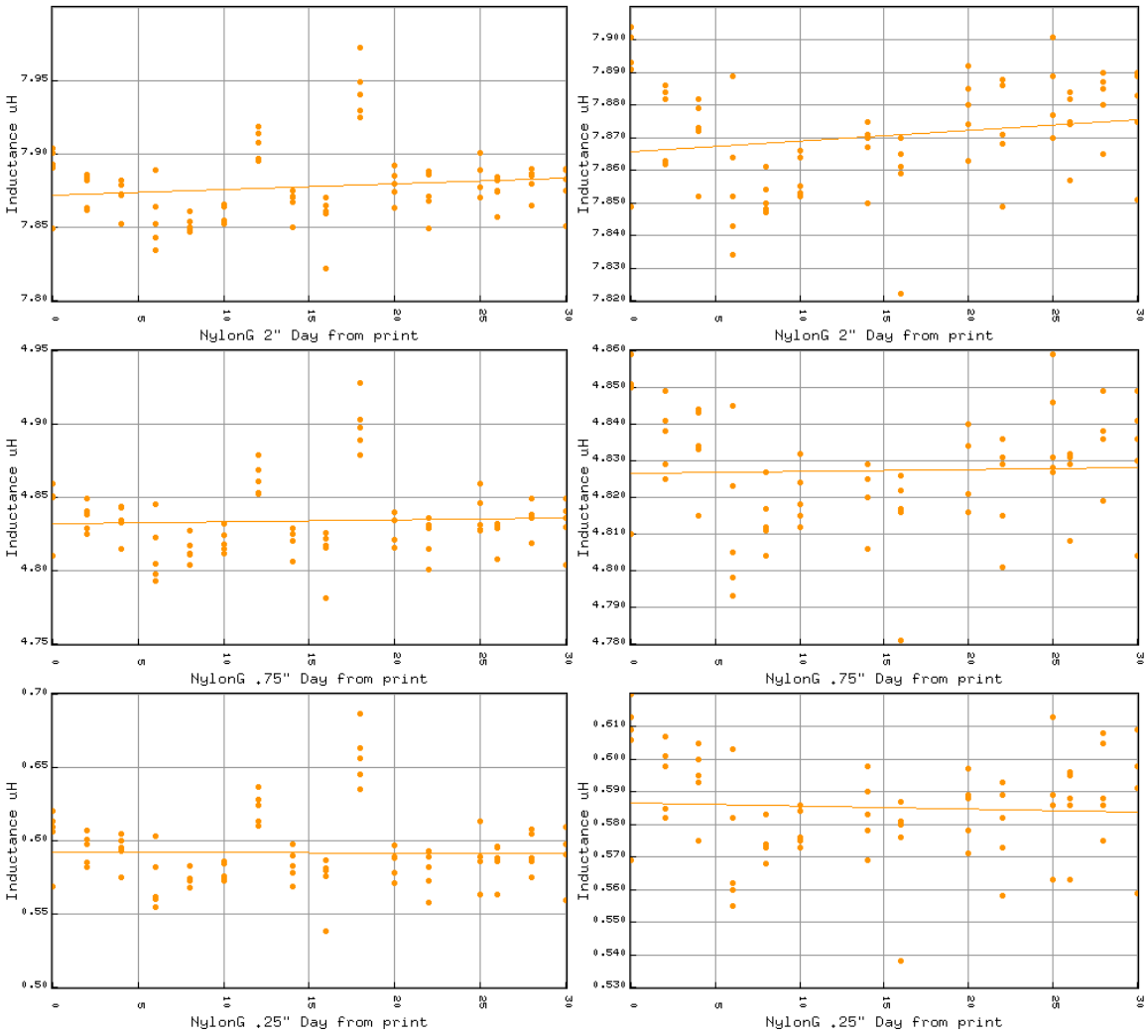

Figure 24: NylonG age test results with and without anomolous days.

There are many possible causes of the anomolous readings that all occured on the same days. I can't prove any of these were the cause or if it's the meter or coils or both or just randomness.

1. Changes in humidity. A storm passed through with over an inch of rain and the inductance increased.

2. Solar storm. At the time I had an anomolous reading on day 24, a large solar storm impacted earth. Readings were not taken in a Faraday cage.

3. Nearby electrical equipment. There are 3 refrigerators within 15’ of the test station, two furnaces a bit farther away, cheap LED bulbs lighting up the workspace.

4. Temperature change. We changed from late winter to early spring with larger indoor temperature swings.

4.8 Temperature

I printed and wound coils with 10 turns, 0.028" spacing, #22 wire and 1" in diameter. 3 identical sets of PLA, NylonG, and PETG were printed and wound with inductances varying slightly about $2\mu H$.

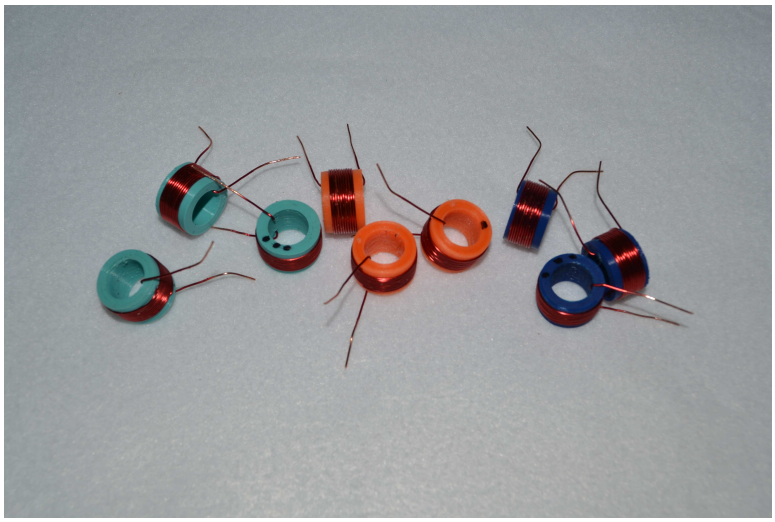

Figure 25: Temperature test coils, PLA (cyan), NylonG (orange), PETG (blue)

Do the coils have the same inductance? I took 30 readings of all 9 coils to see if they were statistically the same. While they have moderately close variances (Table 5), the means are quite different with a high probability (Table 4). Coils 1-3 are PLA, 4-6 are PETG, and 7-9 NylonG.

	1	2	3	4	5	6	7	8	9
1	*	16.0%	0.3%	0.0%	4.8%	0.0%	0.0%	44.8%	0.0%
2	16.0%	*	0.0%	0.0%	21.9%	0.0%	0.0%	16.8%	0.1%
3	0.3%	0.0%	*	0.0%	53.4%	0.0%	0.0%	3.2%	0.8%
4	0.0%	0.0%	0.0%	*	0.0%	0.0%	0.0%	0.3%	0.0%
5	4.8%	21.9%	53.4%	0.0%	*	0.0%	0.0%	0.5%	0.0%
6	0.0%	0.0%	0.0%	0.0%	0.0%	*	0.7%	0.0%	0.0%
7	0.0%	0.0%	0.0%	0.0%	0.0%	0.7%	*	0.0%	0.0%
8	44.8%	16.8%	3.2%	0.3%	0.5%	0.0%	0.0%	*	0.0%
9	0.0%	0.1%	0.8%	0.0%	0.0%	0.0%	0.0%	0.0%	*

Table 4: Probability that means are the same (Student's T).

	1	2	3	4	5	6	7	8	9
1	*	45.1%	46.7%	57.8%	60.1%	43.4%	56.9%	51.4%	58.2%
2	45.1%	*	59.7%	40.0%	44.3%	59.7%	38.6%	31.5%	40.7%
3	46.7%	59.7%	*	41.7%	46.0%	58.8%	40.3%	33.2%	42.4%
4	57.8%	40.0%	41.7%	*	58.3%	38.4%	59.8%	55.5%	60.1%
5	60.1%	44.3%	46.0%	58.3%	*	42.7%	57.4%	52.1%	58.7%
6	43.4%	59.7%	58.8%	38.4%	42.7%	*	36.9%	29.9%	39.0%
7	56.9%	38.6%	40.3%	59.8%	57.4%	36.9%	*	56.5%	59.4%
8	51.4%	31.5%	33.2%	55.5%	52.1%	29.9%	56.5%	*	55.0%
9	58.2%	40.7%	42.4%	60.1%	58.7%	39.0%	59.4%	55.0%	*

Table 5: Probability that variances are the same (F Test).

It's clear that we can't rely on one coil being a surrogate for the two others undergoing temperature changes. Instead, we will compare before and after temperature soaks.

One of each type was placed in a refrigerator freezer over night and during the experiment's course. One of each type was placed in a filament dryer set to 150 F (65 C) overnight and during the experiment's course. We then compare the base test values against the measurements taken during temperature soaking leaving one of each type at room temperature. In Table 6 I use Student's T test on 30 room temperature and 11 heated/cooled samples to test the hypothesis that the means are identical. For room temperature and cold, it's somewhat likely this is true as the values are only slightly less than the ones left at room temperature and remeasured. However for 150 F, PLA and PETG have definitely different means.

Material	**60F**	**30 F**	**150 F**
PLA	18%	3%	39%
PETG	33%	3%	70%
NylonG	62%	63%	31%

Table 6: Low values, means are different.

Comparing the room temperature one dot PLA coil and the two dot heat soaked PLA coil in Figure 26 shows the heat soaked core has significantly shrunk leaving the windings free. If wound tightly, the copper stretches and when the diameter shrinks, they relax making the coil smaller and hence with less inductance (158 nH less). The effect appears to be permanent. The PETG coil has a different problem increasing its mean inductance by 47 nH. The NylonG coil has little difference in means.

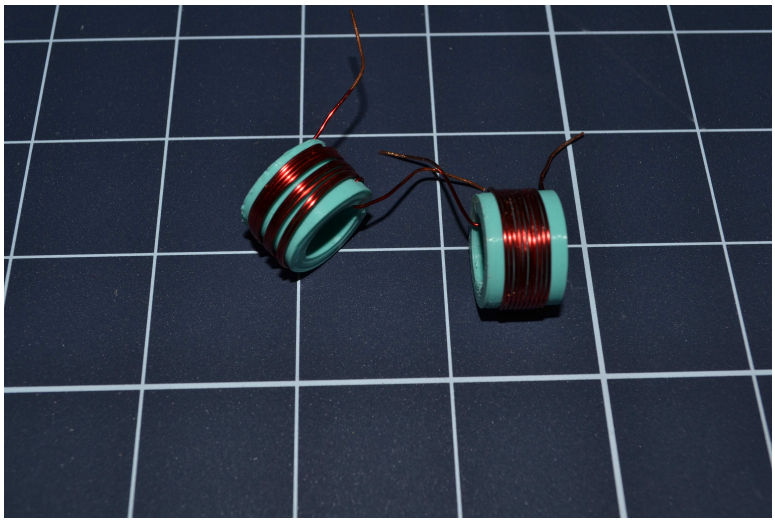

Figure 26: Heat soaked coil on left, room temperature on right.

4.9 Permeability of Core Material

The Protoplant iron composite PLA material is interesting because it can increase the Q of a coil without increasing the wire size. However, we don't know what the relative permeability of this material is. Furthermore, it can be printed with varying percentage of fill. I printed five 10 turn coils, 1" in diameter with a 0.175" hole. The fill percentages were 10, 30, 50, 70, and 100:

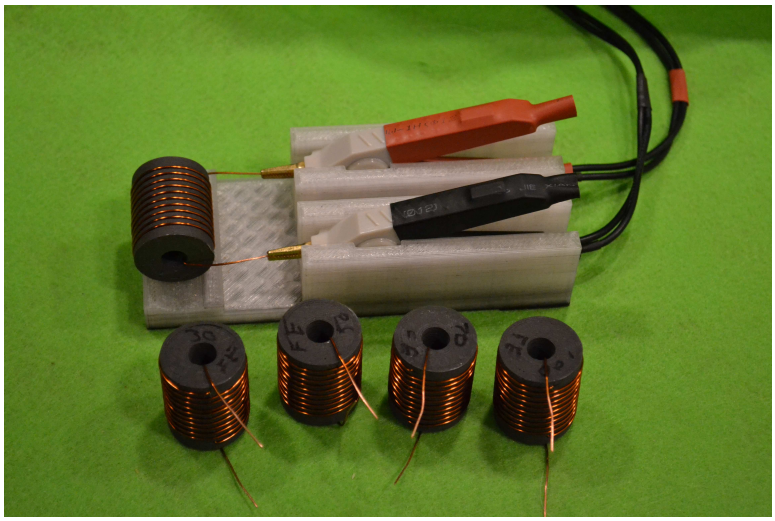

Figure 27: Iron composite PLA coils with varying fill.

The inductance increases linearly with increasing density and all other values being constant.

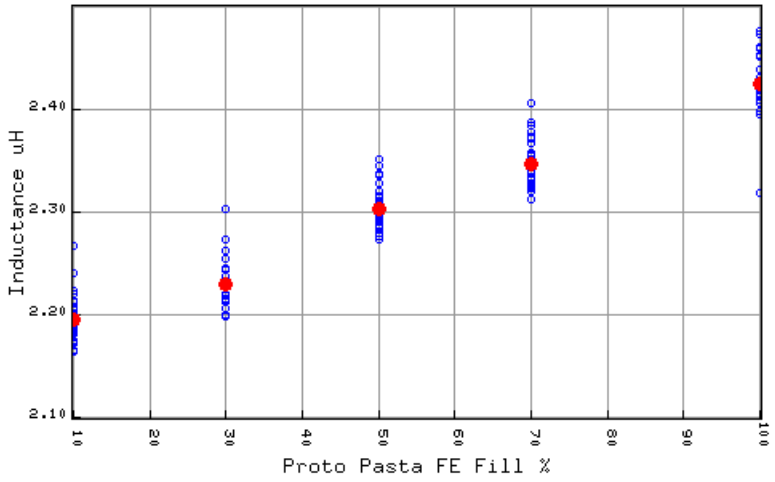

Figure 28: Inductance iron composite PLA fill percentage

Using equation 4 and optimizing for the best μ_r gives us Figure 29.

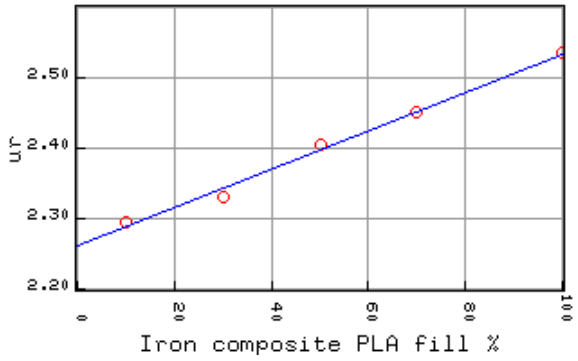

Figure 29: Inductance iron composite PLA fill percentage vs μ_r

The linear equation provides an approximation for the percent fill f for this A.

$$\mu_r = 0.00273f + 2.261 \tag{29}$$

Repeating this experiment with plain and conductive PLA indicates that the fill percentage for these plastics does not affect permeability.

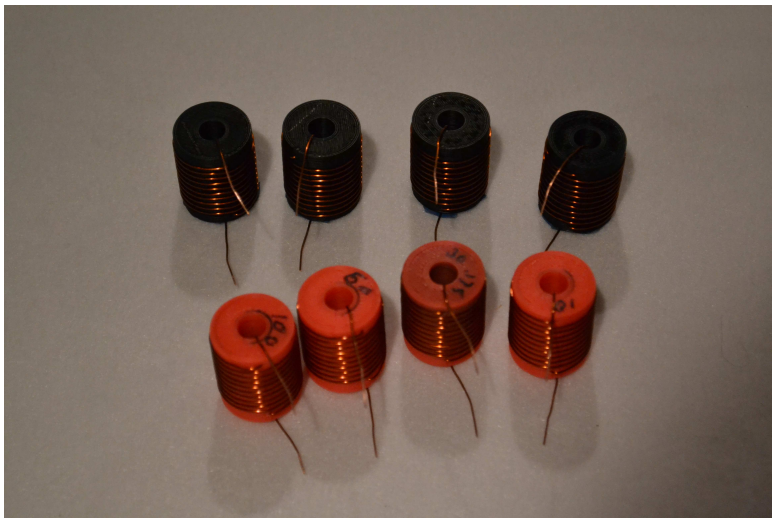

Figure 30: PLA and conductive PLA test coils.

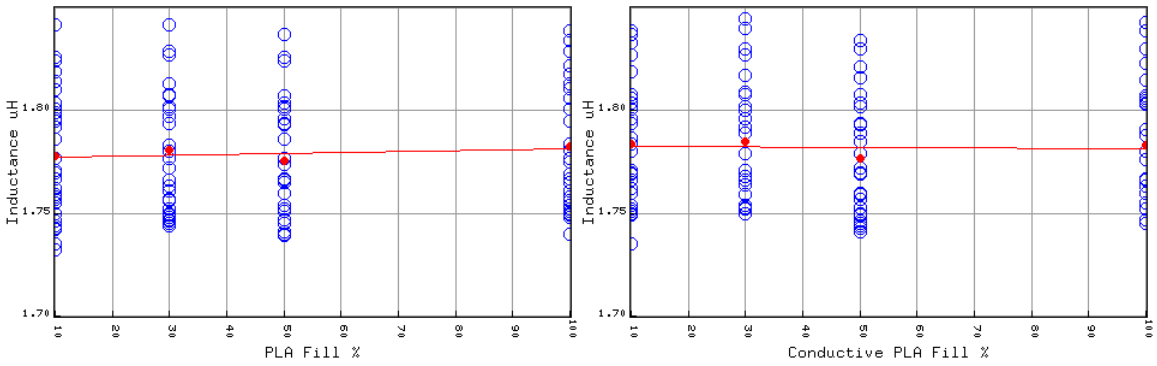

Figure 31: Fill percent vs inductance, PLA, conductive PLA

Working through equation 4, μ_r appears to be between 1.65 to 1.875 for both plastic types but this assumes the correctness of that equation for this geometry. The general guess is that plain PLA has $\mu_r \simeq 1$. linear-least-squares fit on the mean in Figure 31 is constant within the limitations of the LCR meter[4] Is this correct? My guess is that it's too high because the coil has the extra loops on the end.

Next I repeated the number of turns experiment in Figures 8-9 but with 20% fill iron composite PLA.

[4]The apparent wide spread is a consequence of the narrow value range and small inductance.

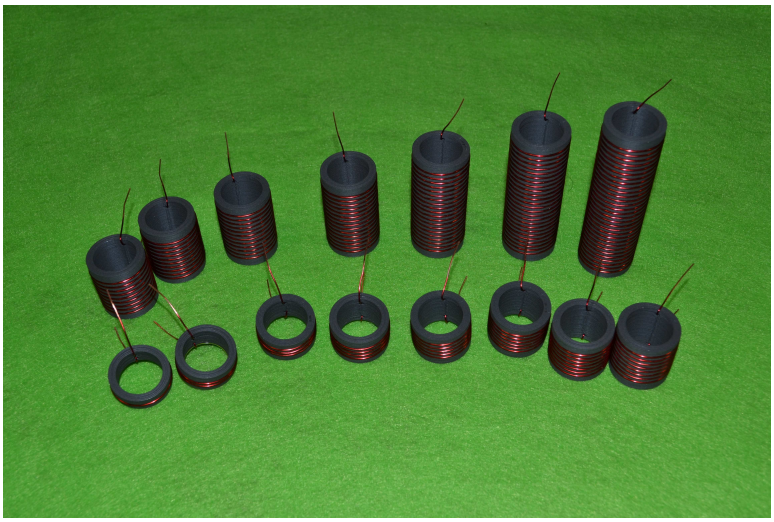

Figure 32: Iron composite PLA coils, 1 to 30 turns

These coils have the same dimensions and turns of those in Figure 8 but a 20% fill percentage - probably meaningless as the walls are mostly solid. The composite does have an effect on inductance as shown in Figure 33.

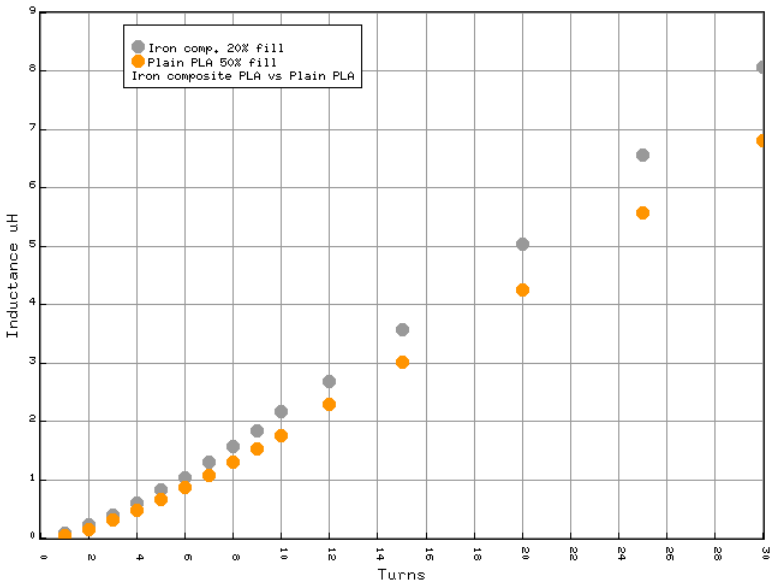

Figure 33: Inductance comparison plain PLA vs Iron composite PLA

Except for small coils, the inductance multiplier for 0.125" wall thickness, 0.1" turn spacing, #22 wire, is about 1.2. That wasn't too exciting. I replaced the .125" wall with a .25" wall with 100% fill and printed the first few coils, unfortunately running out of the expensive filament before completion. Here the multiplier is about 1.4 for bigger coils, still not very exciting but something to contemplate.

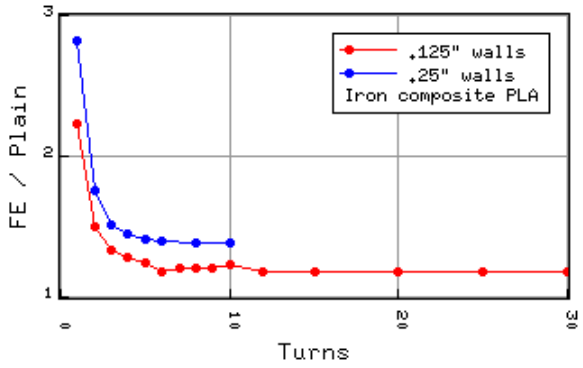

Figure 34: Multiplier for 0.125" and 0.25" wall Iron Composite PLA

4.10 Q Measurement

A coil's "quality" measurement is:

$$Q = \frac{2\pi f \mathscr{L}}{r} \tag{30}$$

where r is the coil's DC resistance and f the frequency measured at (until near the self resonant frequency). I measured some coil Q's with the East Tester, but the results tend to wander considerably so values with more resolution than integers are suspect. The resistance of most coils of #22 wire is quite small. One foot of #22 has a DC resistance of .0164 ohms so any finger grunge or bad contact can have a great variation on the measured Q. SRF measurements (see Section 7.2 on Page 75) show near 40 MHz and our excitation frequency is 100 kHz so we're not in the area where this should cause problems with skin effect and so on.

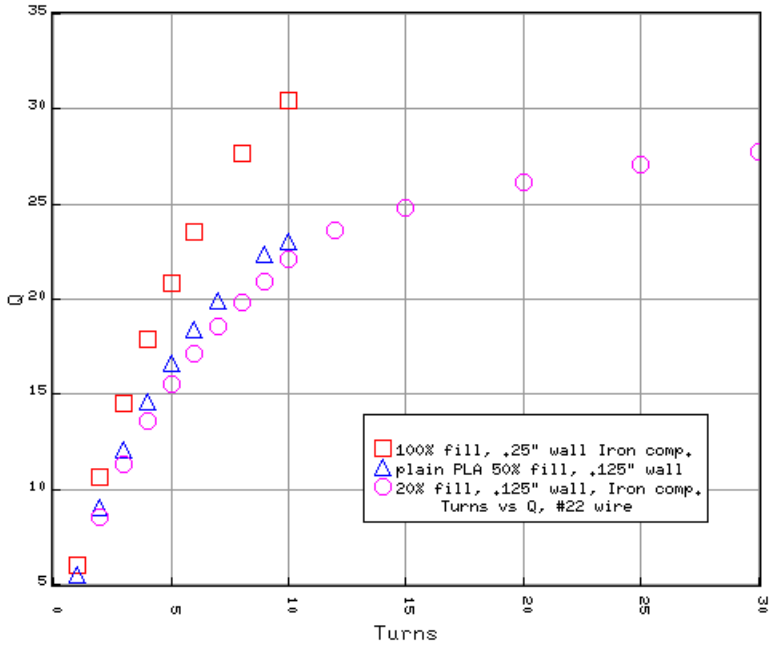

Figure 35: Q of plain PLA, .125" wall and .25" iron composite PLA

Note that the X axis in Figure 35 is number of turns, not inductance. But I'm still unable to explain why the plain PLA cores have a slightly higher Q than the 20% iron composite ones.

5 Printing Experiments

There are problems with adjustments between printing coils - repeatability can be lacking because of poor bed adjustment, tension during winding or other unknown factors.

There are also problems with printer resolution and the geometry selected. I was not able to generate a helical coil without generating many cylinders. As we're typically working near or smaller than reasonably priced printers and limited by the openSCAD CSG to STL converter, I studied the relation between the number of cylinders used to build the channel helix and the measured inductance. I also studied the relation between the cylinder core resolution and number of turns resolution.

5.1 Repeatability

I printed 8 coils with the same dimensions, wire, and number of turns. 1" diameter, 0.5 inch coil with 10 turns of #22 wire.

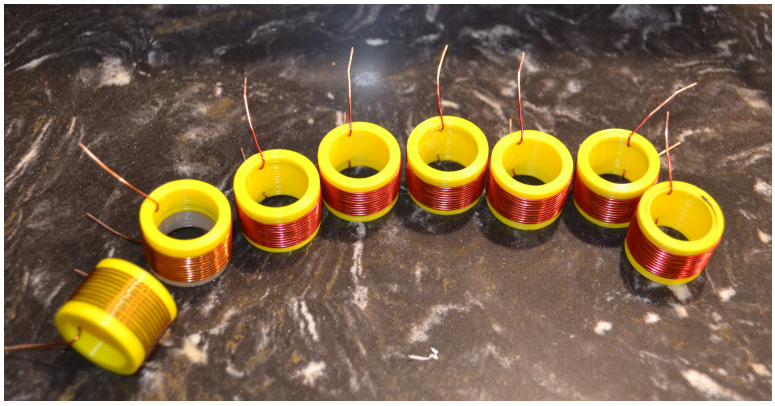

Figure 36: 8 coils, all the same.

These are labeled A-H and should measure around $2.6\mu H$.

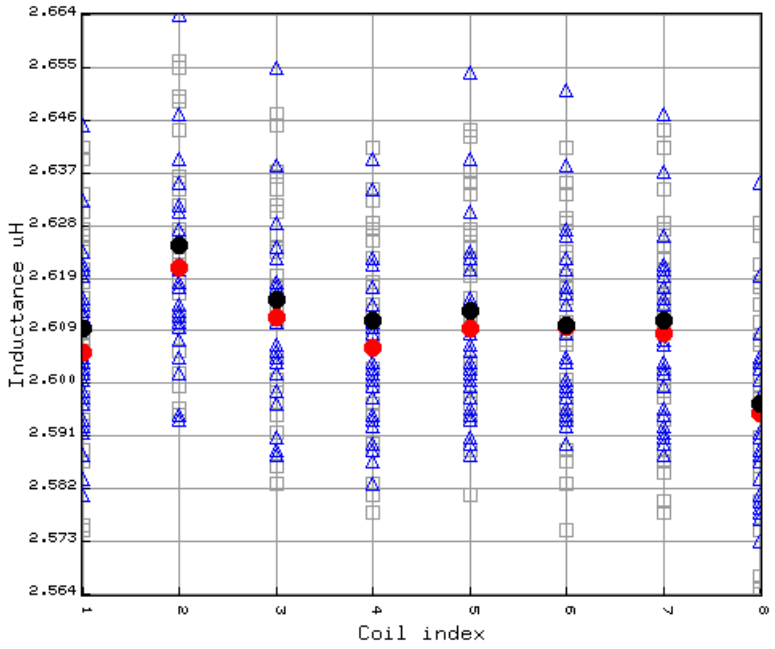

Figure 37: Measures of 8 identical coils, dry and humid

The mean value for raw data for 30 measurements of each coil is $2.602\mu H$, with a standard deviation of $0.0132\mu H$ a variation of about .5%. Removing any values with a z-Score greater than 1.25 reduces the mean to $2.601\mu H$ with a standard deviation of 0.0127 or variability of about 0.41%.

The maximum skew value was 1.52 indicating that the measurements do not have a normal distribution around the mean - they tend to have a long tail in the positive direction. This may be a function of the meter. The kurtosis values show that the 30 measures are reasonably normally distributed (Table 7).[5]

	mean	**stDev**	**skew**	**kurtosis**
1	2.60573	0.01399	0.737176	3.38026
2	2.62037	0.0152598	0.746144	3.46321
3	2.61173	0.0150171	0.805701	3.43339
4	2.60657	0.013645	0.535068	2.6187
5	2.6098	0.0152844	0.977893	3.46694
6	2.61007	0.0147366	0.87618	3.06223
7	2.60903	0.0146252	0.63661	2.73851
8	2.59517	0.0142395	0.696502	3.134

Table 7: Same coil statistics, 30 measurements.

It should be apparent from Figure 37 that coil's 2 and 8 are problematic for some unknown reason. The zTest Table 8 bears this out. Here comparisons that are at least marginally different are in bold.

	1	2	3	4	5	6	7	8
1	*	**-3.872**	-1.601	-0.234	-1.075	-1.168	-0.893	**2.899**
2	**3.872**	*	2.209	**3.692**	**2.680**	**2.659**	**2.937**	**6.613**
3	1.601	-2.209	*	1.395	0.494	0.434	0.705	**4.385**
4	0.234	**-3.692**	-1.395	*	-0.864	-0.955	-0.675	**3.166**
5	1.075	**-2.680**	-0.494	0.864	*	-0.069	0.199	**3.837**
6	1.168	**-2.659**	-0.434	0.955	0.069	*	0.273	**3.983**
7	0.893	**-2.937**	-0.705	0.675	-0.199	-0.273	*	**3.721**
8	**-2.899**	**-6.613**	**-4.385**	**-3.166**	**-3.837**	**-3.983**	**-3.721**	*

Table 8: zTest all 8 against each other

[5]Tables 7 and 9.

The discrepancies can be accounted for by the measured diameters of the wire at the coil center, i.e. the diameter outside the wire hence the larger value. Figure 38 shows the relation between mean diameter and inductance with coils 2 and 8 being the outliers.

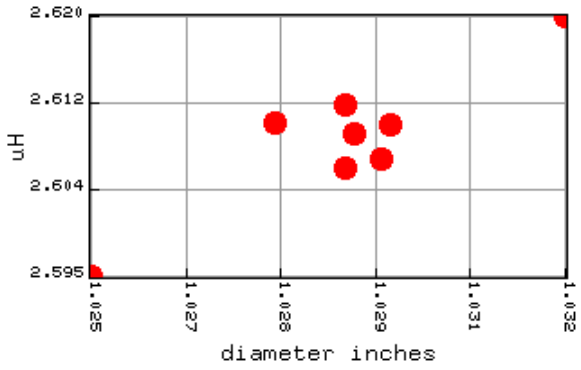

Figure 38: Diameter vs inductance, 8 coils the same.

I also examined coil diameter for those in Figure 36 as shown in the following table with diameters in inches. The coils were printed with each dimension multiplied by 1.02 to account for shrinkage. Measurement was at the 90 degree point from the wire exit and does not include the wire.

Coil	Diameter "	Humid "
A	0.997	1.000
B	1.000	1.002
C	0.999	1.000
D	1.000	1.002
E	1.000	1.000
F	1.000	1.001
G	0.997	1.001
H	0.996	1.001
Mean	0.9986	1.00087
Median	0.9995	1.001

Table 9: Caliper measured coil diameters for 1" nominal.

The average dimension is within about 0.14% of the specified diameter. However exposing the coils to 97% - 99% relative humidity for 1 day results in an average increase in diameter of about 0.25%. A paired T test indicates the means are different to about 99% probability.

5.2 Number of Cylinders per Turn

I tested coils of 0.125", 0.25", 0.375", and 0.625" radii with varying cylinder counts. This experiment fixed the total cylinder faces at 90, that is, a rectangle every 4 degrees no matter the main diameter.

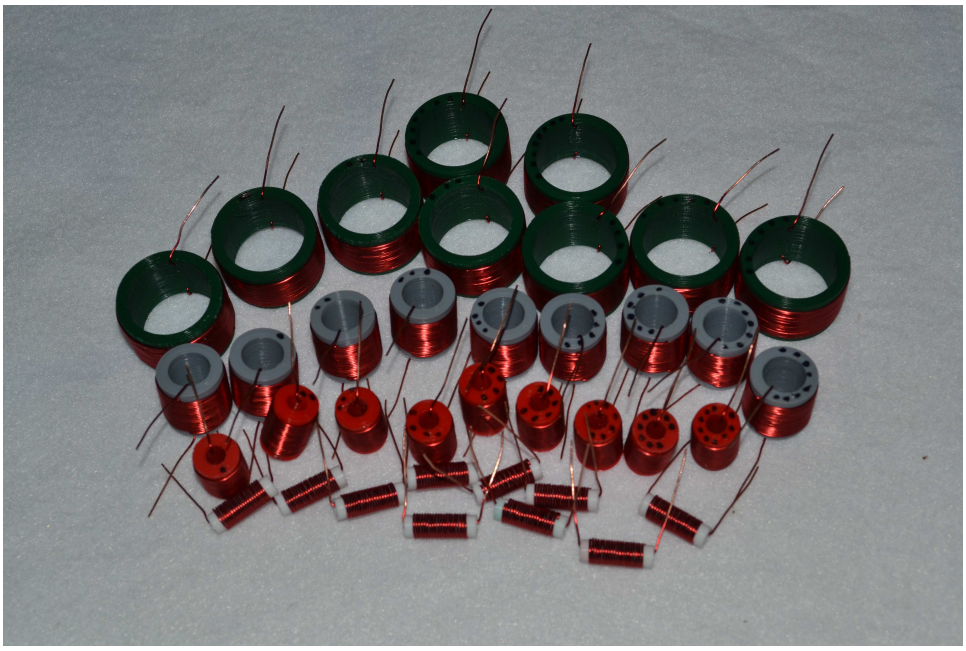

Figure 39: Coils, 20 turns varying helix cylinder count.

The goal is to find the minimal number of cylinders per winding as a function of diameter. The theory: too few gives a higher inductance, larger diameters require more cylinders for consistent inductance. We vary the number of cylinders per turn while fixing the other dimensions and number of turns. The inductance is measured in the usual fashion and then linear least squares is used to find the minimum number leading to consistent results. The results are somewhat odd but explainable.

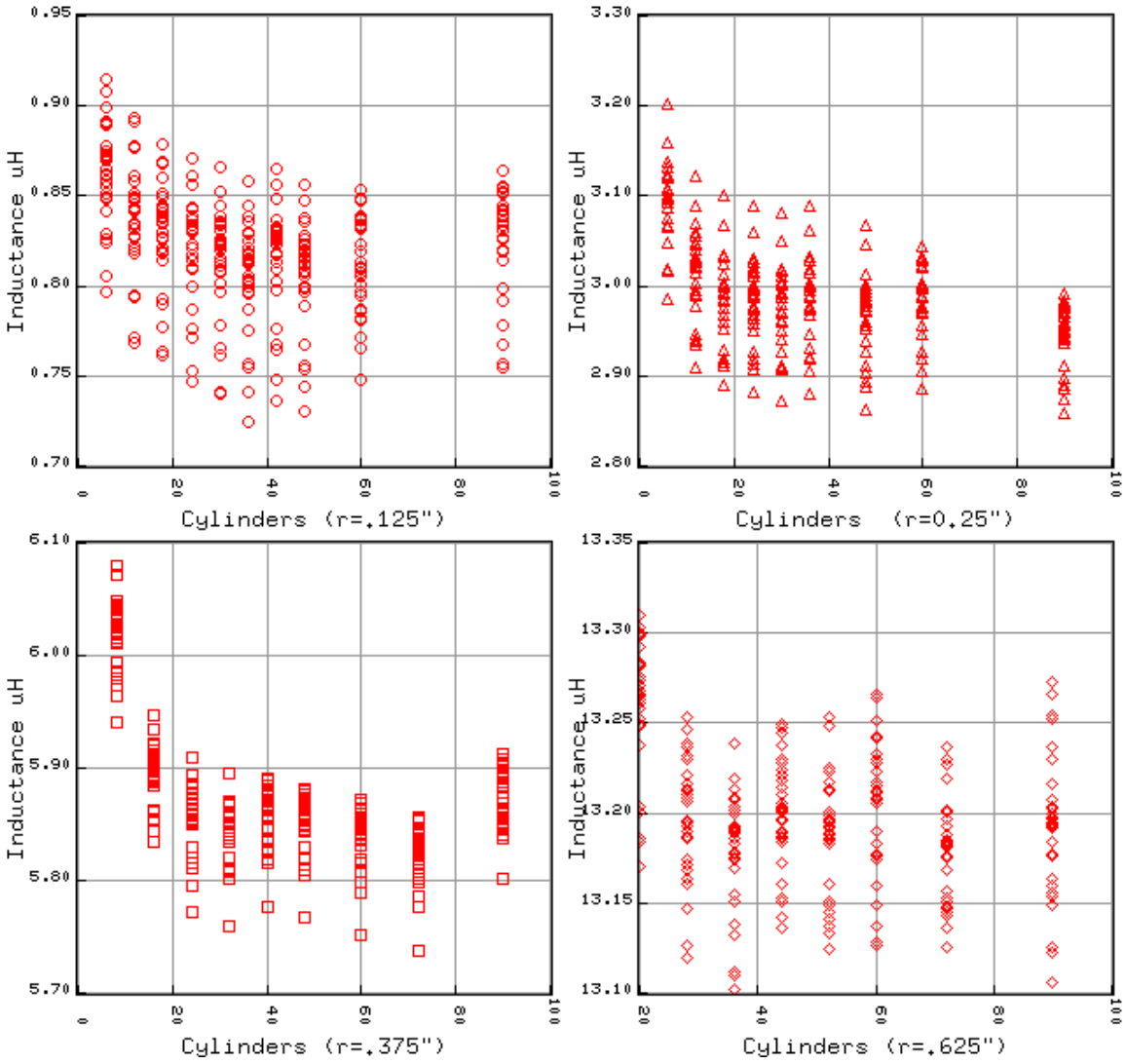

Figure 40: Cylinder count vs inductance, fixed radii.

To help understand the problem, consider the two versions of Figure 41. The topmost has a limited number of cylinders forming the helix with the result that the mean radius is larger larger than the bottom with many more. Even worse, the channel disappears every so often making it difficult to keep the windings properly separated. A larger radius gives more inductance than a smaller so there is more inductance in the fewer which is born out by the graphs in Figure 40. The number of cylinder faces is a second problem. In this section's experiments, the cylinder core had 90 faces - one every 4 degrees with the radius determined at every face corner. Hence the mean radius is somewhat less than that requested.

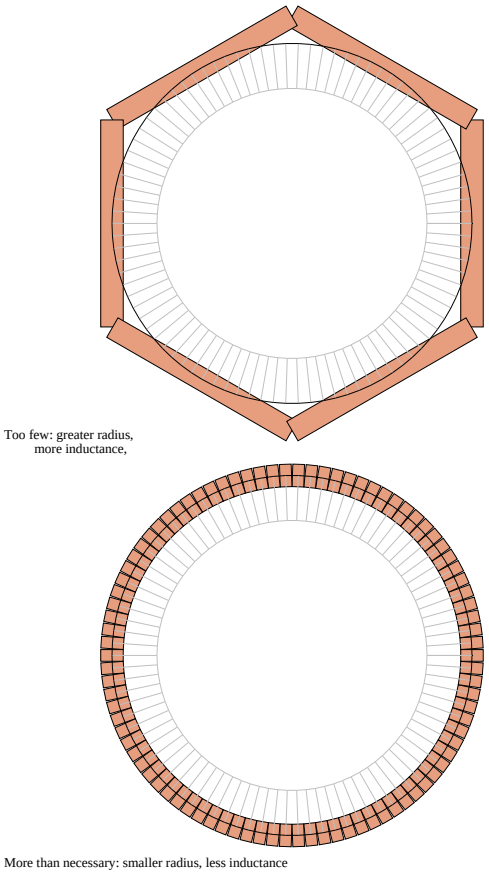

Figure 41: Helix cylinder count vs cylinder faces

During the initial experiments, the number of cylinders per turn increased haphazardly as the radius increased but only guessed at. Figure 42, shows the data set for the .375" radii cores and the linear least squares fits for subsets from the first to the last in light grey. The one with a slope closest to zero is used as the most probable point of diminishing returns, it this case 24 cylinders per turn.

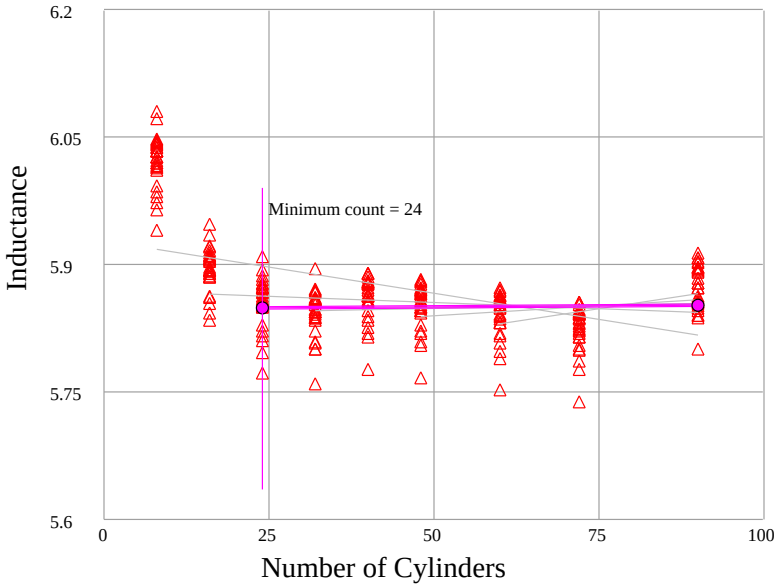

Figure 42: Using linear least squares to find minimal cylinder count.

Performing this on all four datasets and using polynomial regression of degree 2 is shown in Figure 43.

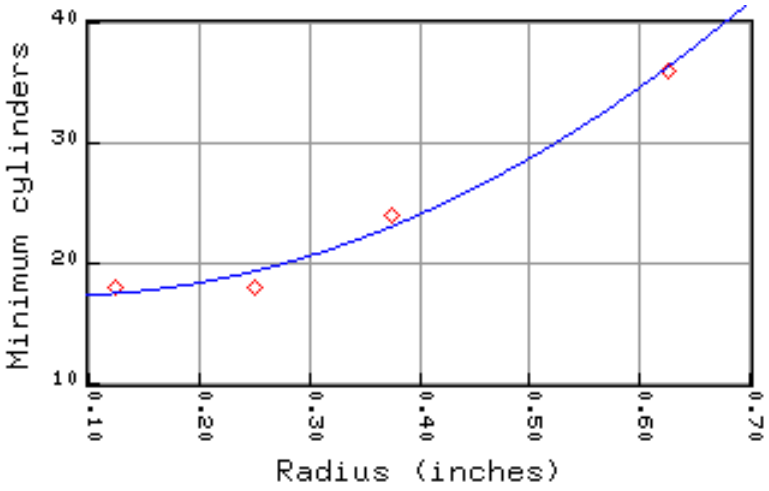

Figure 43: Recommended cylinder count vs radius.

The following equation was added to the **coil** program that issues a warning if the number of "-cylindersPerTurn" is less than specified. If no value was given, then this

approximation is used.

$$c_{recommended} = 17.6 - 8.5r + 61.1r^2 \tag{31}$$

5.3 Form Faces

The number of rectangles used to define the cylinder core affects conversion time so it behoves us to understand the relation between the cylinders per turn and the face count. In particular - what's the minimal number of faces and is there a relationship between face count and cylinders per turn?

I printed a number of coils with face counts varying between 6 and 40 with 36 cylinders per turn and with radii of 0.125", 0.25", and 0.5". Some of these are obviously not reasonable (the 6 face version of the larger set) but are designed to magnify the differences.

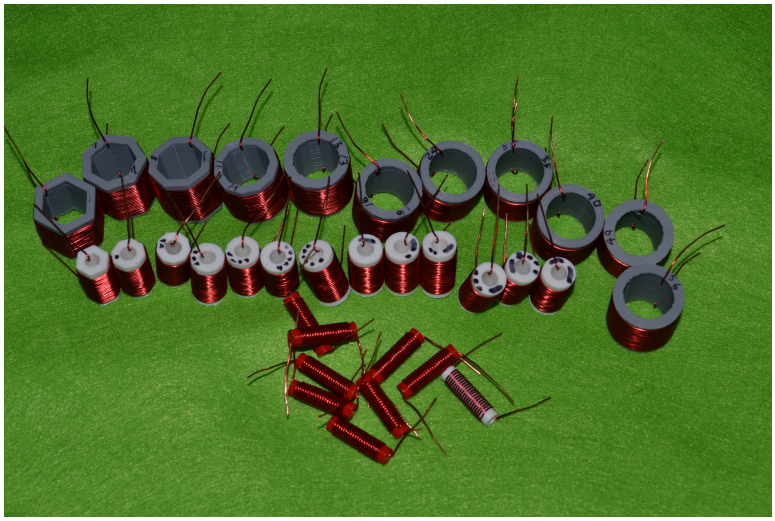

Figure 44: Coils varying diameter and faces. 20 turns, #22 wire.

The measured inductance of the .25" radius coils is shown in Figure 45. The blue line is a 5th degree polynomial fit to mean inductance measurements. Lower degree polynomials have a bad fit.

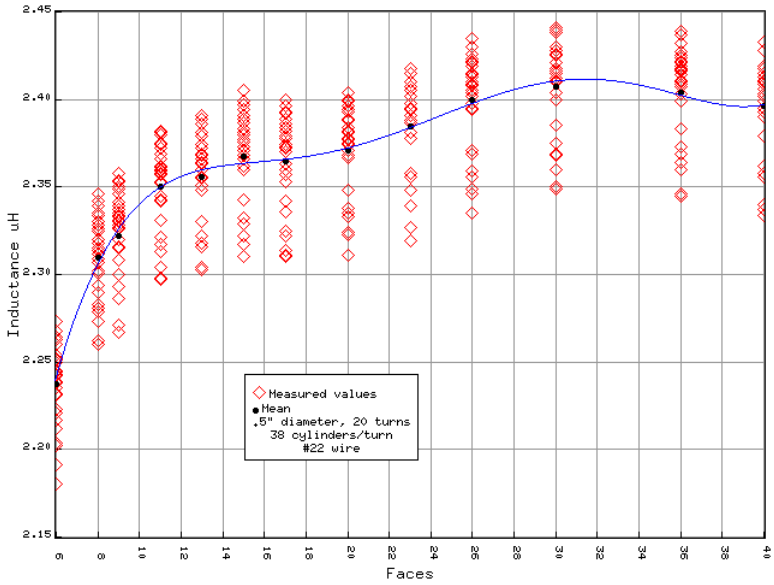

Figure 45: Varying number of faces with 38 cylinders per turn, .5" diameter.

There are two effects here. A very small number of faces means the coil turns flatten out at less than the specified radius and there is less wire for self inductance hence a lower inductance. This effect goes away rather quickly.

There is also a relation between the number of faces and the number of cylinders per turn (which can be different). The more of the turn cylinders whose centers fall on a core face edge, the smaller the coil diameter and the less inductance. Hence the wavering inductance values at higher face counts.

The smaller coil has similar variations though we're near the lower limit of reliability for the LCR meter.

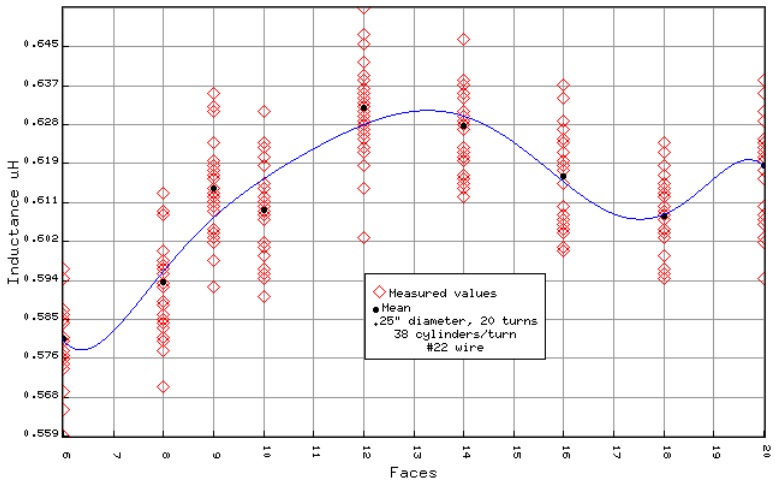

Figure 46: Varying number of faces with 38 cylinders per turn, .125" diameter.

A larger diameter gives a chance to explore the large effects of reduced number of faces.

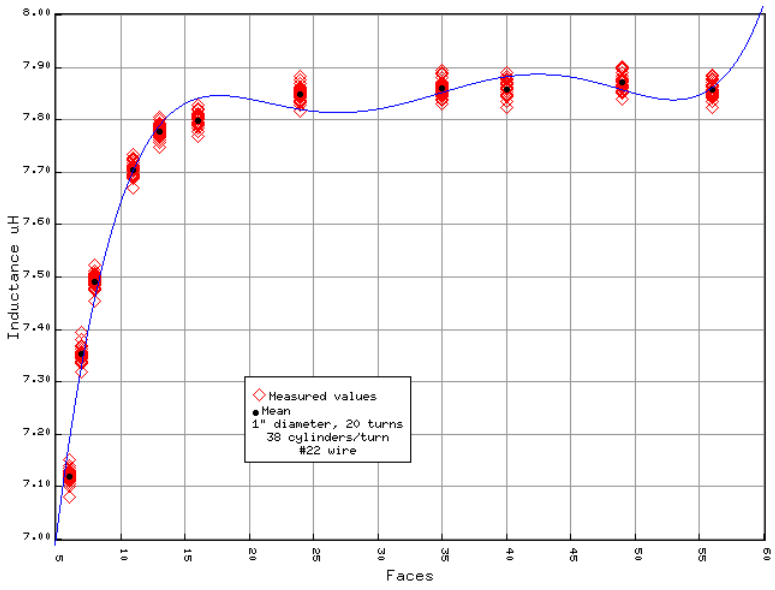

Figure 47: Varying number of faces with 38 cylinders per turn, 1" diameter.

The fact that a high degree polynomial was needeed indicates that the relation between the number of faces and cylinders per turn is important. To give an approximation of the

requirement, linear least squares was applied to the data as done in Figure 43 on page 58 shown in Figure 48.

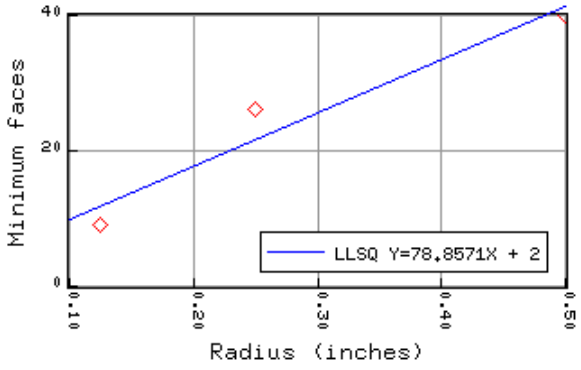

Figure 48: Minimal faces vs Radius.

So the coil section will recommend or automatically set the number of faces to:

$$Faces = 78.86r + 2 \tag{32}$$

and will give warnings if less or greatly more than this.

5.4 Shrinkage

Different PLA plastics seem to have slightly different shrinkage characteristics. To test this hypothesis, I printed a number of 1" cubes with 2.85 mm PLA from different manufacturers and different colors. The fill was set to 100% and resolution to the highest for a .5mm nozzle.

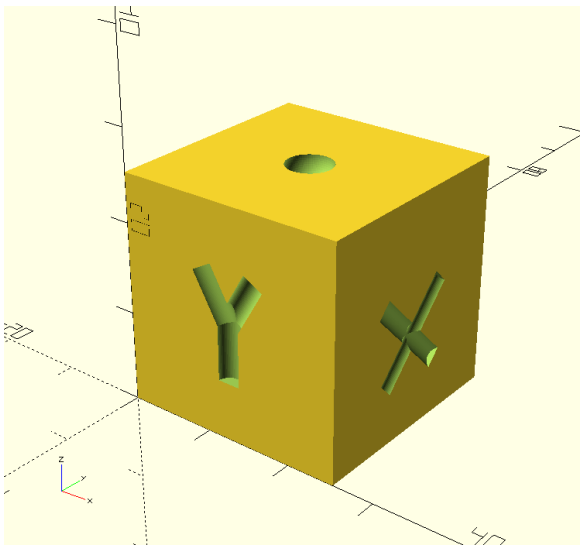

Figure 49: Cube with side markers. Design 1" x 1" x 1"

Filament	**Fill**	X	Y	Z
PolymakerLite lime green	100	0.998	0.994	0.995
	20	0.998	0.995	1.005
PolymakerLite white	100	0.998	0.995	0.992
	20	1.000	0.995	0.992
	highres	1.001	0.997	1.009
Unknown clear	100	1.000	0.997	0.988
	20	0.995	0.994	0.965
MH BuildSeries Forest Green	100	1.007	1.007	.980
	20	.998	1.001	0.994

Table 10: Cube measurements at top/center

I also printed plain cylinders to measure length and diameter using a test stand and a dial indicator to measure every 5 degrees around the circumference. For a 1" diameter

cylinder printed at 2 different resolutions the results are shown with the cylinder deviation 10 times normal.

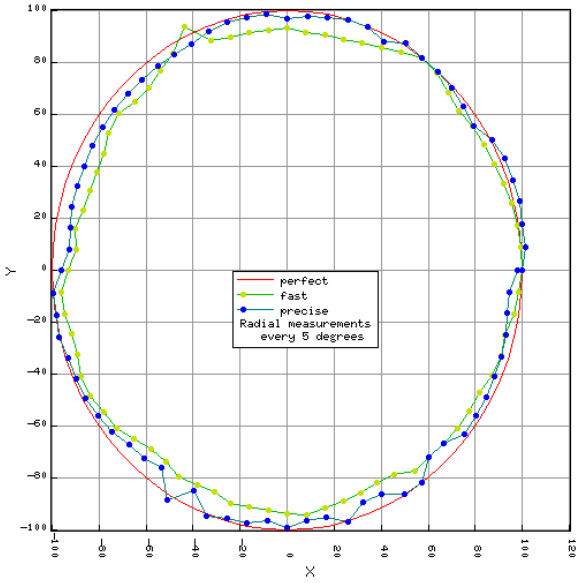

Figure 50: 1" cylinder at 5 degree increments.

I measured the lengths vs the predicted length on a number of coils and found that the length was accurate to 0.001" in all cases. However, as shown in Table 10, the total Z varies considerably. I expect this has to do with the Z axis adjustment and the first few layers. It also appears that filament from the printer manufacturer performs better than generic. If you're used to the .001" or better accuracy of a milling machine, don't expect such from retail additive printing.

6 LCR Meters

Earlier measurements were made with the East Tester ET4410. As a check I borrowed a hand held Keysight U1733C LCR meter and later purchased a bottom of the line CAMWAY BM4070.

Figure 51: Keysight U1733C LCR meter

I repeated the measurements on the 10 turn coils with lengths varying from 0.3" to 3" (Figure 10) and recorded the set 30 times. Comparing the mean of each set of 30 measurements shows that the Keysight averages some 4% higher than the East Tester.

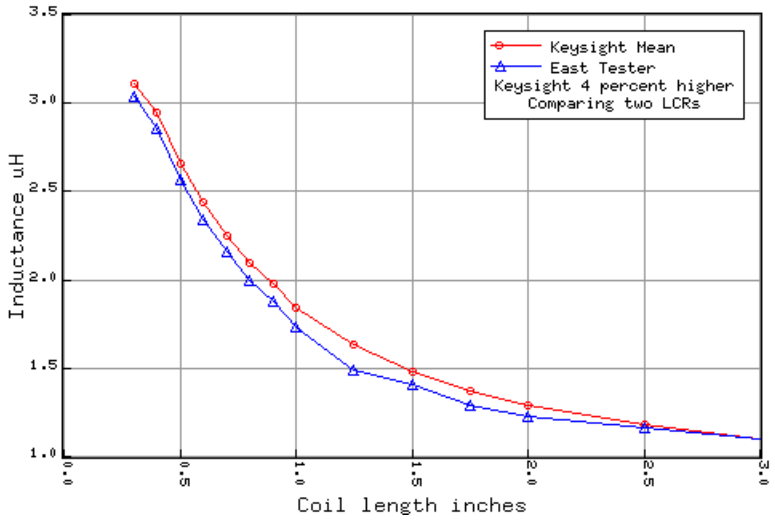

Figure 52: Varying coil length, East Tester vs Keysight LCRs

It appears that the Keysight measurement is more stable than the East Tester. Figure 53 shows the median values of each series of tests, the minimum and maximum, and the standard deviation. The mean of the standard deviations is about 6.4 nanohenries.

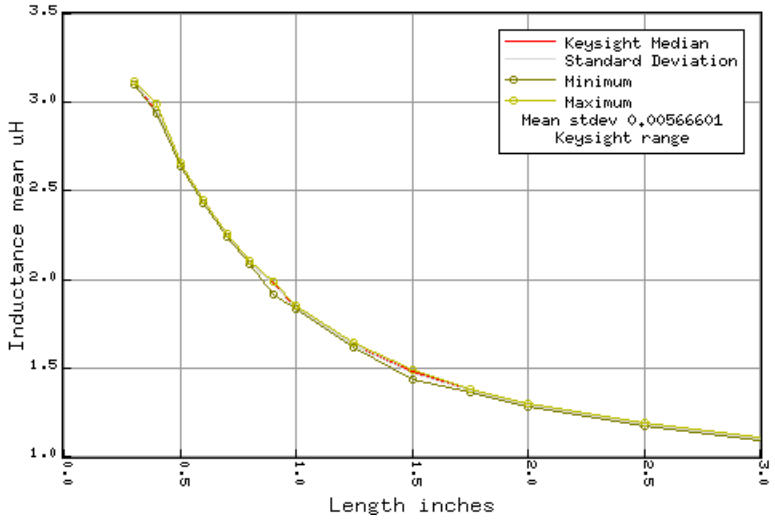

Figure 53: Varying coil length, Keysight variability each size.

On the other hand, the East Tester, in Figure 54, has a standard deviation of 32.5 nanohenries, about 5 times worse.

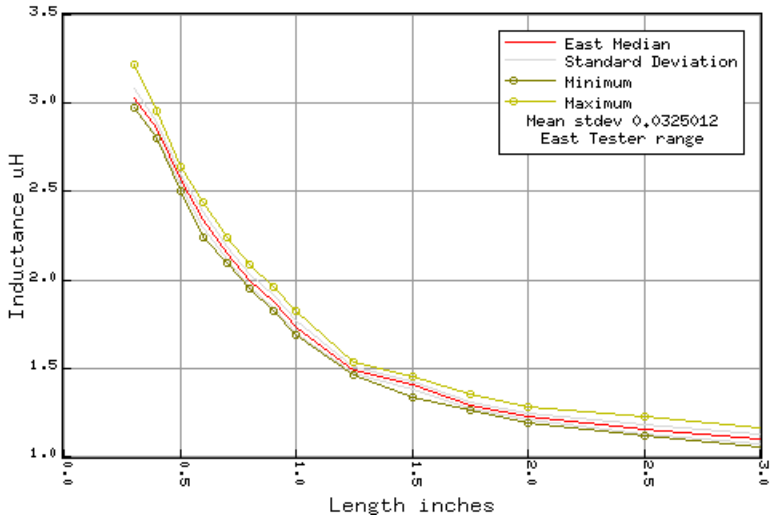

Figure 54: Varying coil length, East Tester variability each size.

I wondered if the ranges returned for each inductor varied with inductance. A wide range would indicate either insufficient calibration, uncompensated temperature variations, poor connections or varying parasitics from the orientation or connection length. In Figure 55 it's clear the East Tester has greater variability as the inductance goes up - perhaps a sign of insufficient digital capture, but the Keysight goes down somewhat but for unknown reasons. Perhaps the inductance range isn't sufficient to draw conclusions.

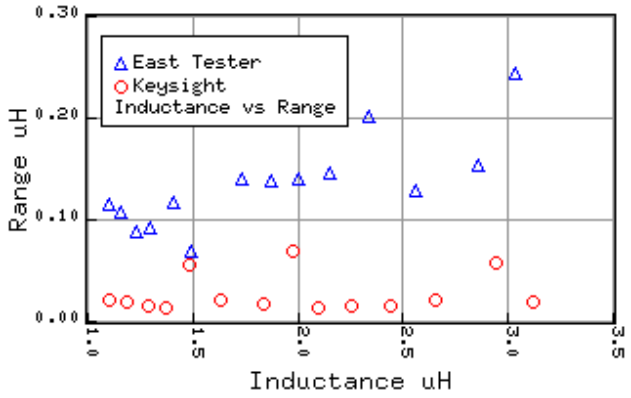

Figure 55: Range per inductance value for two testers

The CAMWAY LCR has good agreement with both the East Tester and Keysight but much less resolution. I measured the same coils as above with calibration between each

measurement plotted in Figure 56. Like the Keysight, the CAMWAY measured slightly above the values shown in green multiplied by 10.

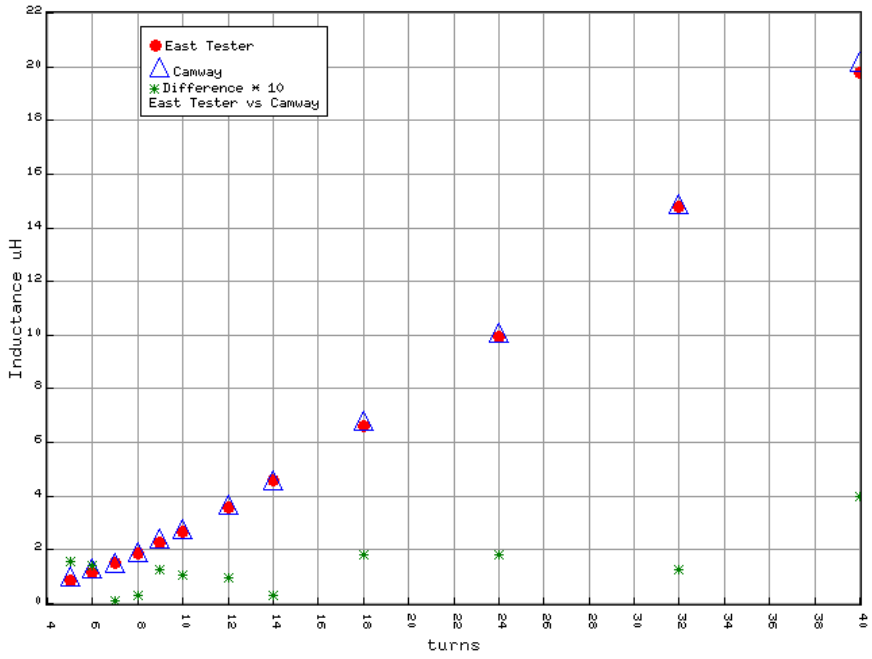

Figure 56: Comparing CAMWAY BM4070 to East Tester ET4410

This is insufficient evidence to convict any instrument reviewed. Just because one has more stable readings than the other, doesn't make it more accurate. After all, a clock that's stopped is accurate at least once a day. Potential causes:

1. **Probes** The East Tester probes are Kelvin whereas the Keysight probes are short lead alligator clips. The East Tester probes are gold plated but do not have sharp teeth. They are spring loaded but not strong. The Keysight alligator clips are chrome plated, sharp and have a very strong spring, enough to make your hand cramp when testing a number of coils. The CAMWAY probes are similar but not as strong.

2. **Drift** Per its instructions, the lines powered East Tester is turned on once in the morning, wait 30 minutes before a test and then the calibration routine run. The Keysight tester is battery powered, the calibration period is short and is turned off between tests. The East Tester appears to drift during the day though in no recognizable pattern even when calibrated between runs. The CAMWAY tester drifts with battery discharge. It is best to calibrate between every measurement. Just remember to subtract the calibration value from the final reading.

7 Permittivity

As the PLA used is an insulator and most inductor calculations are based on air or iron cores. The parasitic capacitance associated with PLA becomes particularly important at higher frequencies. I measured the permittivity of PLA and NylonG blocks of various fill percentages.

7.1 Testing Permittivity

The test stand is two 4"x4"x0.25" aluminum plates nestled in a PLA test stand separated by a 0.25" air gap.

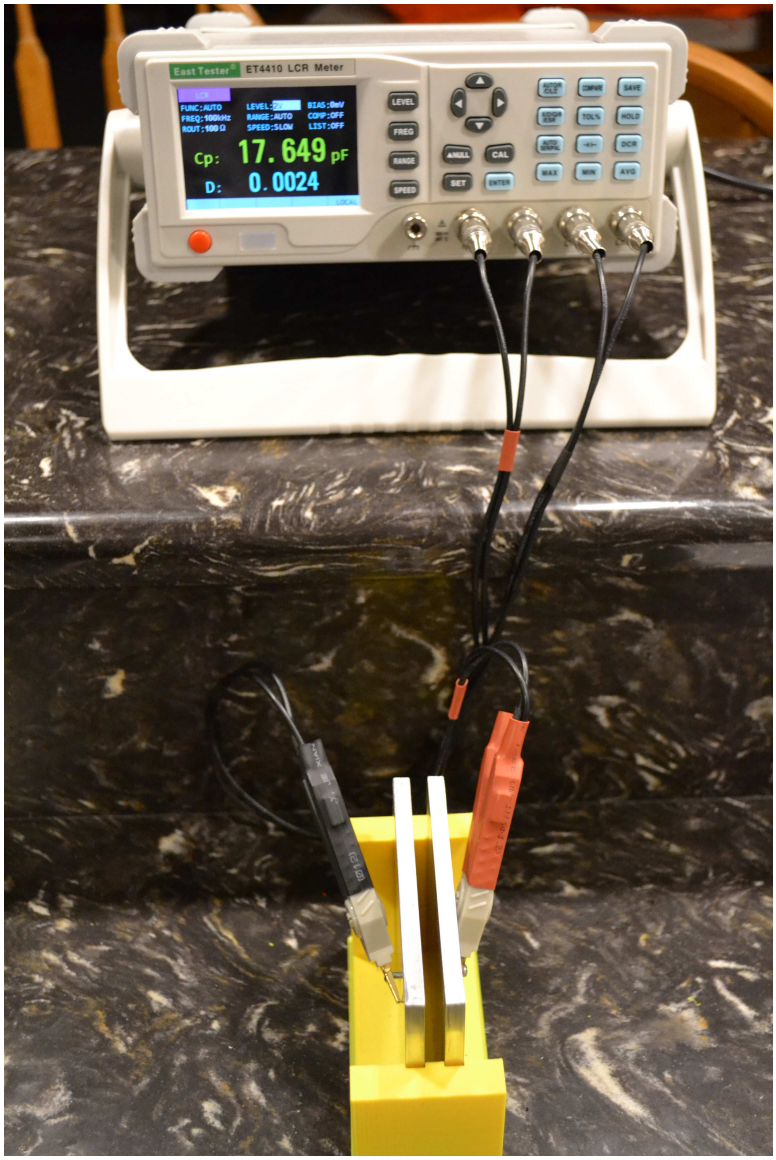

Figure 57: Permittivity test stand.

A number of 0.25" panels were printed with varying degrees of fill from 3% to 100%. The capacitance values were then compared to the air gap capacitance of some $\approx 17.5pf$.

The measurements were taken with a 100 kHz excitation frequency with 2 volts output.

Figure 58: PLA permittivity test panels.

The permittivity does go up (PLA is more of an insulator than air) when measured against fill percentage. The PLA fills half the air gap between coils - used to keep them from slipping around. The odd colors come from using up various PLA spools with only short lengths left.

Figure 59 is a cross section of the coil form. The space between wires is nearly 100% fill but core wall interior may be some percentage less.

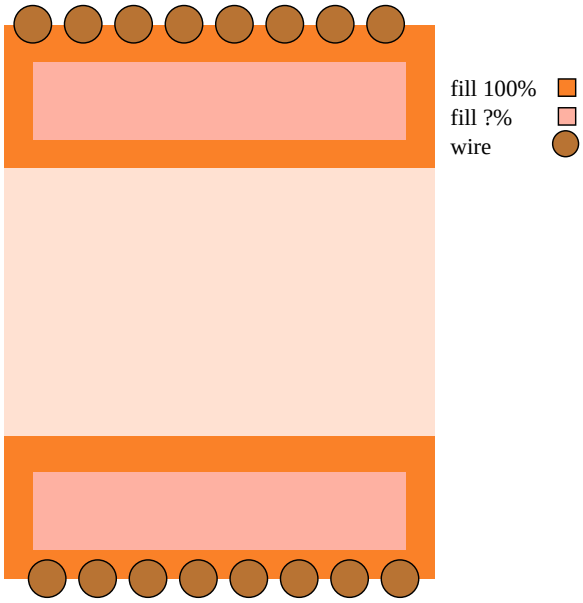

Figure 59: Cross section of printed coil forms with solid outside, variable inner fill.

The weight per panel vs fill percentage is not linear, nor is the relative permittivity.

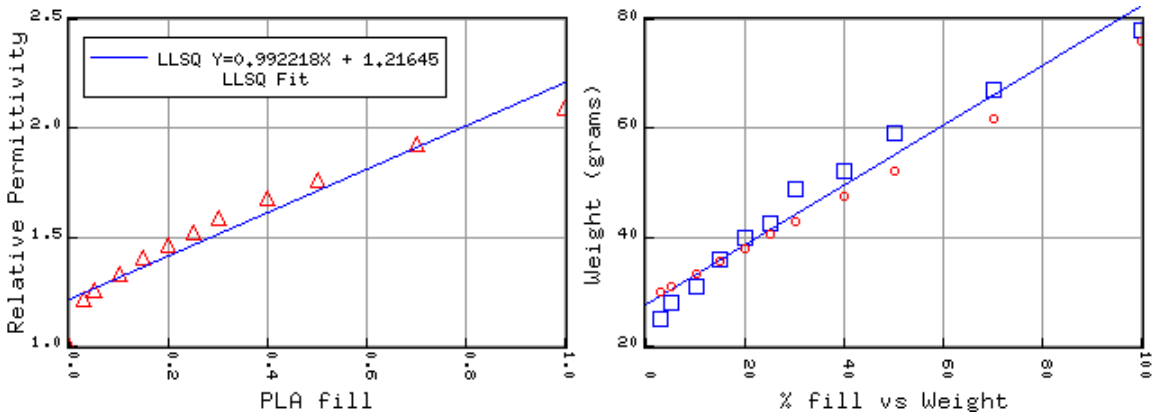

Figure 60: Capacitance vs fill percentage and weight (in grams).

However, from the previous demonstrations, the value of μ_r is not much affected by the fill PLA percentage unless the material is the iron composite type. However, given that dry PLA is a better insulator than air, the parasitic capacitance of a coil may be greater thus causing problems at frequencies higher than the 100 kHz of the measurements.

NylonG has slightly different permittivity. Again, fill panels were created with different fill percentages (but not 100% due to running out of expensive filament). The fill geometry is somewhat different than the hexagons used for the PLA which may account for most of the difference.

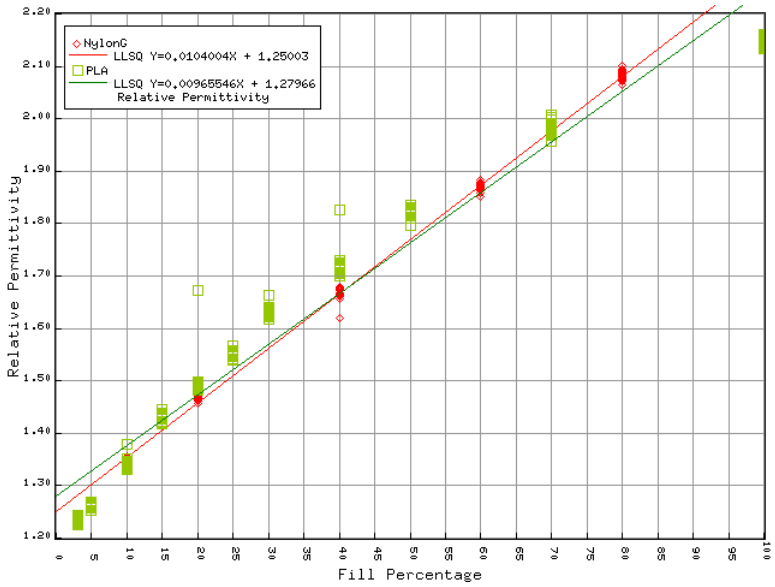

Figure 61: Comparing PLA to NylonG permittivity by fill percent.

7.2 Self Resonant Frequency

As the permittivity of PLA is higher than air, we would expect the self resonant frequency (SRF) do decrease. To test the SRF, each coil was hooked to a calibrated nanoVNA and we look for the first 180 degree phase change. The sample size was set to 501, and the range adjusted so that the change is in the approximate middle of a 1 MHz sweep.

Most of this capacitance is between the coil winding's which are half air and half PLA. I first tested the SRF of the variable length 10 turn coils shown in Figure 62. Here there are 10 turns of #22 on 1" diameter. As shown in Figure 10, the SRF increases as the distance between turns expands indicating less capacitance.

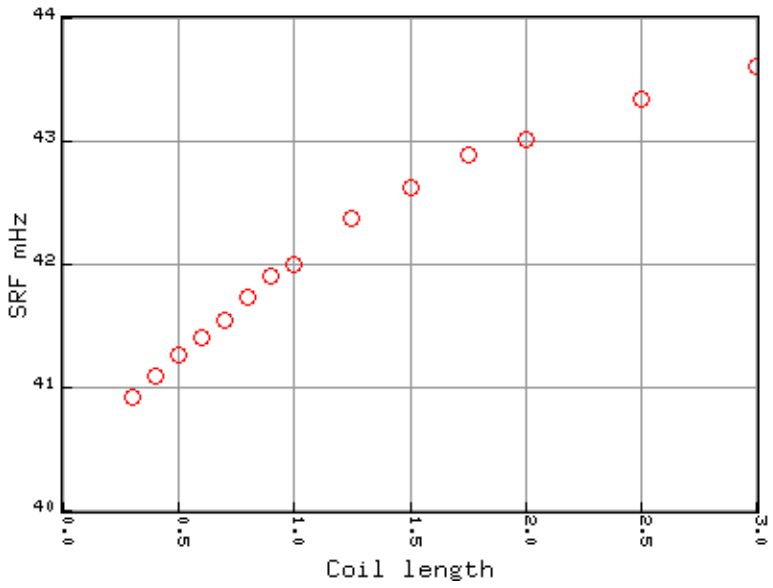

Figure 62: Coil length vs self resonant frequency

The type of core matters as well. In Figure 63 Are measurements of three coil types. The single air core coil serves as a baseline at 41.717 mHz (shown at fill=50%). The iron composite PLA is fairly close to this value though somewhat lower as it is not very conductive. The conductive PLA fills half the space between turns making a near multi-plate capacitor thus reducing the SRF considerably. The effect increases somewhat with the fill density. The variability between 5% and 10% fill is difficult to explain but may have to do with the internal orientation of the "star" fill pattern. Two identical prints have nearly the same SRF and inductance.

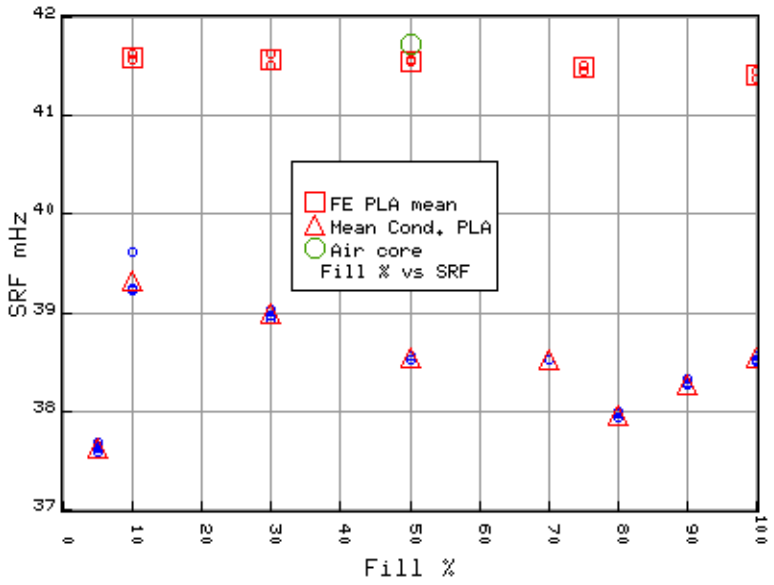

Figure 63: Coil core type and fill percentage vs SRF.

8 Exploring Other Shapes

3D printing opens up the possibility of odd inductor shapes. One can imagine printing toroids with the iron composite PLA and making them other than circular. In Figure 64 are 3 inductors: a base line circular one, two with 6 cog and a third (yellow) with 12 and an inner radius of .5". This proved too difficult to wind. The inner and outer radii are scribed with the normal helix though with a significantly greater diameter, especially on the inner core. The inner helix makes a hole through the part sticking out.

Figure 64: Cog shape test. Two I could wind, one too hard.

The leftmost is a plain circular inductor with 5 turns of #26 wire. The center and right coils have 6 cogs evenly spaced at 60 degrees. The outer radius is 1", the inner radius 0.75". To wind, you start with enough wire to complete the task - for these about 9 feet. The wire is wrapped around each cog with the end running underneath it to the next. The blue core is wound with the wire to the next cog on the outside core rather than the inner. All three have roughly the same footprint, yet the inductances are wildly different. The inner winding coil has more than twice the inductance of the plain circular. We can expect that increasing the number of cogs and reducing the inner diameter would further increase this ratio.

Coil	μH	Ratio
Base line	1.92	1
Inner cog	2.79	1.45
Outer cog	4.09	2.13

Table 11: Inductance ratios for cog cores.

However, these are desparate measures. Winding these cores is a long process. Like winding a toroid, you must draw long lengths of copper through small holes and avoid creating snags and kinks. This is nearly impossible. I wound the blue core with shorter copper pieces and soldered them together during winding.

Furthermore, none of the equations examined will even remotely model this geometry. Any coil with multiple holes will have this problem, including toroids with winding channels.

And finally, odd geometries require complex calculations to position the channels. Most likely, these are done on a per geometry basis and won't resemble each other. For example, an egg or dumbbell shape might have interesting SRF properties but matching wire channels to the surface would be a lot of work.

3D printing is ideal for outdoor chokes where you wrap coax on a form rather than just a circle with cable ties. These choke forms have a beveled hole for the coax entrance and exit rather than trying for a 90 degree bend. These were printed with glow in the dark plastic and are supposed to be in the $5-6\mu H$ range.

Figure 65: 6" diameter choke forms.

9 Modeling Inductors

There are 4 variables to approximate a coil's inductance $\mathscr{L}$.

R Coil radius in meters.

L Coil length in meters.

W Wire radius in meters.

N The number of turns.

I assume that R, L and W are continuous and N is an integer though in truth, the continuous values are modeled as double-precision floating-point of which there are a finite number.

Assuming a generic cubic equation for each variable V with coefficients a_i:

$$a_3V^3 + a_2V^2 + a_3V + a_4 \tag{33}$$

Each term could be in the numerator or denominator which gives 4096 possible equations. My goal was to find the optimal values for all coefficients for a subset of these equations to accurately match the the closed loop inductance of the coils measured. For the moment, we ignore μ_r though all the equations tested will include μ_0 as a constant the (possibly incorrect) view that μ_r will just be a linear multiplier.

It should be apparent that optimizing 16 parameters for 4096 equations to match 175 coils is intractable for any but the largest super computer. I used some of the on-line and published approximations as starting points for eliminating many of the possible equations.

9.1 Data Sets

I built 6 data sets from the coils deemed to be appropriate for modeling. These did not include coils used for permeability testing, other geometries or experiments with aging, temperature, or setting print parameters.

turntest.csv Fixed spacing, radius, #22 gauge wire, vary turns. 8 coils.

turntestall.csv As above, but individual coil measurements not averaged. 241 records.

cspacing.csv #22 gauge coils, 0.028 spacing only, no inductance below .5 μH. 61 coils.

cspacingall.csv #22 gauge coils, as above but coil measurements not averaged. 938 records.

all22.csv All coils with #22 wire. No inductance below .5 μH. 149 coils.

all.csv All coils, different wire sizes, PLA cores only. 173 coils.

All approximations have limitations. Table 12 gives the limits for equations by the file they were optimized against. Attempting a value beyond any of the limits is tempting fate.

Subset	Entries	Turns	Gauge	Diameter	Length	μH
turntest.csv	8	8-50	22	0.5"	.32" - 2"	0.612 - 7.06
turntestall.csv	240	8-50	22	0.5"	.32" - 2"	0.612 - 7.06
cspacing.csv	61	5-40	22	.258" - .866"	.14" - 1.12"	.516 - 19.8
cspacingall.csv	937	5-40	22	.258" - .866"	.14" - 1.12"	.516 - 19.8
all22.csv	149	5-40	22	.261" - 2"	.14" - 3"	.502 - 40.73
all.csv	173	5-50	14-28	.261"- 2"	.14" - 3"	.502 - 40.73

Table 12: Optimization subset limits

9.2 Raw Datasets

The following raw datasets form the basis of the analyses. These are all on-line and are in a modified CSV format. Comments are prefixed with //.

15p15.csv Plain PLA coils. 1.5" diameter, 1.5" length, vary turns (5,10,15,20,25,30,40). 0.125" walls, #22 wire. Inductance from $0.8\mu H \rightarrow 40\mu H$.

15p175.csv 1.5" diameter, 1.75" long, vary turns. 0.125" walls, plain PLA, #22 wire. Turns (5, 10, 15, 20, 30, 40), 5 turns commented out for measurement problems. Inductance from $2.6\mu H \rightarrow 36.5\mu H$.

1in.csv 1" diameter, 1" length, 0.125" wall, plain PLA, #22 wire. Turns (5, 15, 20, 25), 5 turns commented out for measurement problems. Inductance from $3.9\mu H \rightarrow 11\mu H$.

1p25in.csv 1" diameter, 0.125" walls, 1.25" length, plain PLA, #22 wire. Turns (5, 10, 15, 20, 25) with 5 commented out for measurement problems - less than $0.5\mu H$. Inductance from $1.5\mu H \rightarrow 9\mu H$.

1p5in.csv 1.5" diameter, 1" long, 0.125" plain PLA walls, #22 wire. Turns (5, 10, 15, 20, 25). Inductance from $1\mu H \rightarrow 19.5\mu H$.

1p75in.csv 1" diameter, 1.75" length, 0.125" walls, plain PLA, #22 wire. Turns (5, 10, 15, 20, 25, 30, 40), 5 commented out because less than $0.5\mu H$. Inductance from $1.3\mu H \rightarrow 18\mu H$.

2in.csv 2" diameter, 1" length, walls 0.125", plain PLA, #22 wire. Turns (5, 10, 15, 20, 25), 5 commented out for measurement problems (probably should be retained). Inductance from $1.5\mu H \rightarrow 32.5\mu H$.

2p15.csv 2" diameter, 1.5" length, 0.125" walls, plain PLA, #22 wire. Turns (5, 10, 15, 20, 25, 30). Inductance from $1.3\mu H \rightarrow 37\mu H$.

3inws.csv 10 turns, #14, #22, #28, plain PLA, 0.125" walls. Inductance from $0.9\mu H \rightarrow 1.2\mu H$.

3inwsQ.csv 10 turns, #14, #22, #28, plain PLA, 0.125" walls. Q from $4 \rightarrow 35$. Same coils as *3inws.csv*.

age25melmac.csv, age25nylon.csv, age25petg.csv, age25white.csv age25yellow.csv These are .25" diameter coils measured over the course of 30 days. Two days of anomalous readings are commented out on some files. Days are from the experiment start and are not the same for each coil set.

age75melmac.csv, age75nylon.csv, age75petg.csv, age75white.csv age75yellow.csv These are .75" diameter coils measured over the course of 30 days. Two days of anomalous readings are commented out on some files. Days are from the experiment start and are not the same for each coil set.

age2melmac.csv, age2nylon.csv, age2petg.csv, age2white.csv age2yellow.csv These are 2" diameter coils measured over the course of 30 days. Two days of anomalous readings are commented out on some files. Days are from the experiment start and are not the same for each coil set.

cplafill.csv Conductive PLA fill percentage. 1" diameter, 10 turns, #22, wire 0.175" hole. Vary fill percentage (10, 30, 50, 100). Inductances all about $1.75\mu H$.

fe25turns.csv Composite Iron PLA. 1" diameter, 0.1" turn separation, turns 1-10, 0.25 wall thickness, #22 wire. Note that we ran out of filament so 7 and 9 are missing. 100% fill.

fe25turnsq.csv Composite Iron PLA Q measurements. 1" diameter, 0.1" turn separation, turns 1-10, 0.25 wall thickness, #22 wire. Note that we ran out of filament so 7 and 9 are missing. 100% fill. Q from $2 \rightarrow 32$.

fedia.csv Protopasta iron fill diameter vs inductance. 50% fill, 0.125 wall thickness. 10 turns. Inductance from $0.6\mu H \rightarrow 4.8\mu H$.

fepla175.csv Protopasta Iron fill. 1" radius, 0.175" radius hole, fill percentage variable from (10, 30, 50, 70, 100) percent. 10 turns, 0.1" spacing.

feturns.csv Composite Iron PLA. 1" diameter, 0.1" turn separation, turns from (2, 3, 4, 5, 6, 7, 8, 9, 10, 12, 15, 20,25, 30) 0.125" wall thickness, #22 wire. 20% fill. Inductances $0.143\mu H \rightarrow 8\mu H$.

feturnsq.csv Composite Iron PLA. 1" diameter, 0.1" turn separation, turns from (2, 3, 4, 5, 6, 7, 8, 9, 10, 12, 15, 20,25, 30) 0.125" wall thickness, #22 wire. 20% fill. Q from about 5 to 36.

g18.csv Plain PLA, fixed spacing, radius, varying turns (10, 15, 20, 30, 40), #18 wire. Inductance from $0.7\mu H \rightarrow 4.6\mu H$.

g22.csv Plain PLA, fixed spacing, radius, varying turns (10, 15, 20, 30, 40), #22 wire. Inductance from $0.8\mu H \rightarrow 4.6\mu H$.

g26.csv Plain PLA, fixed spacing, radius, varying turns (10, 15, 20, 30, 40), #22 wire. Inductance from $0.8\mu H \rightarrow 4.7\mu H$.

humid2p15.csv 2" diameter, 1.5" length PLA coils, #22 wire, turns (5, 10, 115, 20, 25, 30) in 100% humidity. The humid version of *2p15.csv*. Inductance from $1.3\mu H \rightarrow 37\mu H$.

highaspect.csv Number of turns on high aspect ratio coils. Diameter 1.0", spacing 0.1", plain PLA, 0.125" wall thickness, 50% fill, #22 wire, turns from (10, 12, 15, 20, 25, 30).

humid.csv 1" diameter, 0.5" length, 10 turns #22 wire. All identical. This is the humid version of *same.csv*.

keysight.csv 10 turns, .3 to 3" length, #22 wire, 1" diameter, 0.125" walls, plain PLA. Measured with Keysight LCR. Inductances from $3.2\mu H \rightarrow 1.3\mu H$.

lspacing.csv #22 wire, 1" diameter, 10 turns. Spacing is length / 10. Lengths from 1.25" $\rightarrow$ 3". Inductance from $1.5\mu H \rightarrow 1.1\mu H$.

p125.csv .125" radius coils, #22 wire, 0.028" spacing per turn. The outside diameter of each coil is measured 8 times and is included. Turns (5, 6, 7, 8, 9, 10, 12, 14, 18, 24, 32, 40). Coils with turns 5-12 removed because of bad inductance readings. Only 16 measurements made. Inductances from $0.5\mu H \rightarrow 2\mu H$.

p125cyls.csv Test number of cylinders per turn for 0.125" radius coils from (6, 12, 18, 24, 30, 36, 42, 48, 60, 90). Measure inductance on 0.027" spacing, #22 wire.

p125faces.csv Test number of faces on coil cylinder from (6, 8, 9, 10, 12, 14, 16, 18, 20). 0.125" radius, 20 turns, 18 cylinders per turn.

p1875.csv 0.1875" radius (0.375" diameter),#22 wire, 0.028" spacing. Turns from (5, 6, 7, 8, 9, 10, 12, 14, 18, 24, 32, 40) with 5, 6, 7, 8 removed because inductance too low for LCR meters. Diameter measured around 8 angles and averaged. Uncommented inductances from $0.55\mu H \rightarrow 4.3\mu H$.

p1875b.csv A revamp of some coils in *p1875.csv* - same values but turns of 18, 24, and 32.

p25.csv 0.25" radius, #22 wire, 0.028 spacing/turn. Coil diameters measured and averaged. Turns (5, 6, 7, 8, 9, 10, 12, 14, 18, 24, 32) with 5 and 65 removed because of low inductance. Inductances from $0.63\mu H \rightarrow 7.3\mu H$.

p25cyls.csv Test number of cylinders per turn for 0.25" radius coils from (6, 12, 18, 24, 30, 36, 42, 48, 60, 90). Measure inductance on 0.027" spacing, #22 wire.

p25faces.csv 0.25" radius, 20 turns, #22 wire, vary face count from (6, 8, 9, 11, 13, 15, 17, 20, 23, 26, 30, 36, 40). Inductance around $2.4\mu H$.

p3125.csv Measure diameter test. 0.3125" radius, #22 wire, 0.028" spacing/turn. Turns from (5, 6, 7, 8, 9, 10, 12, 14, 18, 24, 32, 40). 5 removed because of low inductance. Inductance from $0.7\mu H \rightarrow 11.4\mu H$.

p375_1_18.csv #18 wire, 0.375" radius, 1" length, turns from (5, 10, 15, 20, 23), inductance from $0.29\mu H \rightarrow 5.4\mu H$.

p375b.csv Diameter test again. 0.375" radius, #22 wire, 0.028" spacing/turn. Turns from (5, 6, 7, 8, 9, 10, 12, 14, 18, 24, 32, 40), inductances from $0.7\mu H \rightarrow 15.7\mu H$. Only 15 measurements.

p375.csv Plain PLA, 0.375" diameter, 0.08" walls, #22 wire, 1" length, turns from (5, 10, 15, 20, 25, 30), 5 and 10 removed because of low inductance. Inductances from $0.69\mu H \rightarrow 2.5\mu H$.

p375cyls.csv Test number of cylinders per turn for 0.375" radius coils from (8, 16, 24, 32, 40, 48, 60, 72) inductance on 0.027" spacing, #22 wire.

p4375.csv Diameter measurement. 0.4375" radius, #22 wire, 0.028" spacing per turn. Inductances from $0.8\mu H \rightarrow 19.8\mu H$.

p5_1_26.csv #26 wire, 0.5" diameter, 1" length, vary turns from (5, 10, 15, 20, 25, 30, 35, 40). Inductances $0.2\mu H \rightarrow 8.8\mu H$.

p5faces.csv Fixed cylinders per turn 36, 0.5" radius, 0.8" length, turns 20, coil form faces from (6, 7, 8, 11, 13, 16, 24, 35, 40, 49, 56). Inductances from $7.1\mu H \rightarrow 7.9\mu H$.

p5in.csv 0.5" diameter, 1" length, 0.125" walls, #22 wire, plain PLA, turns from (5, 10, 15, 20, 25), 5 turns removed because of low inductance. Inductance from $0.57\mu H \rightarrow 3\mu H$.

p625cyls.csv Test number of cylinders per turn for 0.625" radius coils from (12, 20, 28, 36, 44, 52, 60, 72, 90), 12 removed for display purposes as it has high inductance. 0.027" spacing, #22 wire. Inductance about $13\mu H$.

pladia.csv Regular PLA 50% fill, diameters from (0.5", 0.75", 1.0", 1.25", 1.5", 1.75") 0.125" walls, 10 turns, #22 wire. Inductances from $0.5\mu H \rightarrow 4.3\mu H$.

plafill.csv Vary plain PLA fill percentage from (10, 30, 50, 100). 1" diameter, 10 turns, #22 wire, 0.175" hole. Inductance around $1.75\mu H$.

qex3.csv Some fixed spacing 0.5" diameter. Measuring at 80 kHz. Turns from (8, 10, 15, 20, 25, 30, 40), inductances from $0.6\mu H \rightarrow 7\mu H$.

qex3k.csv Same as above but using Keysite tester at 100 kHz.

same.csv 8 coils, all 1" diameter, 0.5" length, 10 turns, #22 wire. Inductance around $2.6\mu H$.

samedia.csv Same 8 coils as above, measuring diameter in dry and 97% humidity soak.

spacing.csv 10 turns, 1" diameteter. Lengths from 0.3" $\rightarrow$ 1.0" in increments of 0.1". 0.125" thick walls, #22 wire. Inductances from $3\mu H \rightarrow 1.7\mu H$.

specials.csv Unusual coil forms. #26 gauge wire.

srfcond.csv Conductive PLA self resonant frequency test., % fill from (5, 10, 30, 50, 70, 80, 90, 100). 1" length, 10 turns, #22 wire, 0.375" core. Measure in mHz, SRF around 38 mHz. 12 measurements of each coil.

srffe.csv SRF of Iron composite PLA. 1" diameter, 10 turns, fill percentage (10, 30, 50, 75, 100). SRF average around 41 mHz. Only 2 measurements.

t10.csv 10 turns, 2" diameter, #22 wire, 0.028 spacing. Measured diameter slightly larger than requested.

t10d.csv Diameter measure of eight 10 turn coils at 45 degree increments (see *same.csv*.

t50p125.csv 50 turns, 0.0257" diamete, #22 wire, 0.028 spacing. 15 measurements, one coil. Inductance about $2.5\mu H$.

tempnylonbase.csv Base line measurement for temperature test of Nylon G coils. 10 turns, room temperature.

tempnylong.csv Room temperature, 31 F temperature, 150 F temperature of 3 Nylon G coils. Only 11 measurements. Generally $2\mu H$.

temppetgbase.csv Base line measurement for test coils, PETG. 3 coils, 10 turns at room temperature.

temppetg.csv Room temperature, 31 F temperature, 150 F temperature of 3 PETG coils. Only 11 measurements. Generally $2\mu H$.

tempplabase.csv Base line measurement for temperature test of plain PLA coils. 10 turns, room temperature. Inductance about $2\mu H$.

templa.csv Room temperature, 31 F temperature, 150 F temperature of three plain PLA coils. Only 11 measurements. Generally $2\mu H$.

turns.csv 1" diameter, 50% fill, 0.125" walls, plain PLA, 0.1" spacing, #22 wire. Turns from (1, 2, 3, 4, 5, 6, 7, 9, 10). Inductances from $0.02\mu H \rightarrow 1.8\mu H$.

turnsq.csv Number of turns on variable length coil. 1" diameter, 50% fill, 0.125" walls, plain PLA, 0.1" spacing, #22 wire. Turns from (1, 2, 3, 4, 5, 6, 7, 9, 10). Q values from 4.5 to 23.

urcyan.csv Data from cyan PLA coil - 10 turns, 0.1" spacing, #22 wire, 0.325" wall thickness.

urgreen.csv Data from greeb PLA coil - 10 turns, 0.1" spacing, #22 wire, 0.325" wall thickness.

uryellow.csv Data from yellow PLA coil - 10 turns, 0.1" spacing, #22 wire, 0.325" wall thickness.

weight.csv Weight of coils with different fill percentages from (5, 10, 30, 50, 70, 80, 90, 100). 1" diameter, 0.325" hole, conductive PLA, 10 turns, #22 wire. Weight in grams measured with wire and 1" leads.

wiresize.csv 10 turns with different wire gauges (14, 16, 18, 22, 24, 26, 28). Inductance around $1.8\mu H$ but varies with gauge.

9.3 Optimizing the ARRL Equation

Equation 1 on page 9 can be modified with different integer coefficients to better fit the data. Using an exhaustive search with limited integer values shows the limits of this equation. Repeats using the genetic algorithm resulted in different floating-point coefficients but with nearly identical results.

In general:

$$\mathscr{L} = \frac{Ad^2n^2}{Bd + Cl} \tag{34}$$

I wrote a multi-process program to search for optimal values for the various data sets. The limits were 1-1000 for A, 1-10000 for B, and 1-10000 for C. Table 13 shows good improvement for the small datasets with lesser improvement as the number of variables goes up.

Subset	Original RMS	New RMS	A	B	C
turntest.csv	10.24%	1.82%	44	1283	1585
cspacing.csv	12.52%	5.54%	43	864	1909
all22.csv	13.06%	10.44%	11	229	456
all.csv	14.42%	11.88%	16	337	664

Table 13: Modified ARRL coefficients for different subsets

The ARRL equation is probably OK for general purposes but tends to predict higher values than those read by LCR meters. For truly accurate values, it is insufficient.

9.4 Tukey Plots

In the following analyses I'll present errors usually by inductance for the best of each equation. These use a complex display mechanism developed for display of normal distribution values [18]. These are an attempt to show the errors within a restricted bin of values, usually 2 μH. The rectangular box holds 50% of the error values, the bar across the middle is the median of all bin values. Above and below the box there may be a T (if there are more than 3 values). Values that lie within 1.5 times the box range lie within this area. If there are any values that fall outside this range, they appear as solid black circles. A plain circle indicates that only one value occurred in that bin.

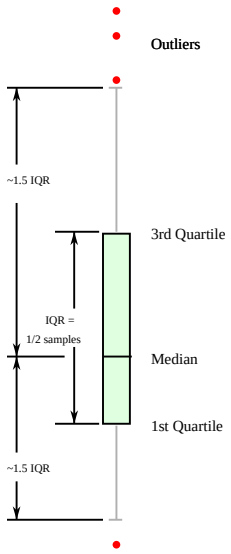

Figure 66: Tukey box plot detail.

9.5 The Optimization Algorithm

For a generic polynomial f I'm attempting to minimize the value of:

$$v = \sqrt{\frac{\sum_i (f_{l,r,n,w}(L_i, R_i, N_i, W_i) - m_i)^2}{n}} \tag{35}$$

where:

m_i The mean inductance from 30 measurements of coil i in Henries.

L_i The length of coil i in meters.

R_i The radius of coil i in meters.

N_i The integer number of turns in coil i.

W_i The radius of the winding wire of coil i in meters.

l The set of coefficients for the length polynomial.

r The set of coefficients for the radius polynomial.

n The set of coefficients for the turns polynomial.

w The set of coefficients for the wire radius polynomial.

To develop the coefficients of f's polynomial I developed code based on the genetic algorithm concepts in [19]. Similar complex problems using this and other similar approaches proved useful for many multivariate problems [2, 3, 20].

For a particular polynomial the algorithm needs limits on each coefficient and the granularity of values between the limits. To understand the exponential growth of this problem consider the simplest polynomial of two variables - radius in a cubic and number of turns in a quadratic. This needs 8 values. Suppose the range of each value is $-1000 \leq v \leq 1000$. Matching this against $n = 8$ coils using an exhaustive search requires about 2 octillion evaluations of the polynomial. At 1 μ second per evaluation, that's about 65 trillion years.

In summary, the Genetic Algorithm approach starts with completely random coefficient values l, r, n, w within the ranges specified. The base data set and measurements compute v for each of these which are sorted into increasing (less good) values. This is called a *generation*. The best of these, typically 7, create a new generation by pairs or mutating some of the coefficients of an old one. And just in case we're getting stuck, we generate a few new completely random ones. To avoid re-computation, any new coefficient set is matched against those already done. If a match occurs, the set is rejected and the the offending process tried again.

To speed the process, the control program starts a number of subprocesses usually between 8 and 32 depending upon the processor's capabilities. The evaluation of equation 35 happens very quickly. To avoid spending a lot of time on interprocess communication, an exhaustive search in a small neighborhood around l, r, n, w is conducted - usually between 1 and 2 million tests. The best of these is returned for the next generation. The size of these tests and their granularity is set with the coefficient ranges. A typical test may take between 1 and 10 seconds.

The process continues for a number of generations set by the configuration file or until a number of generations have passed without improvement of the results.

There's a degree of manual operation. Initially I don't know the coefficient ranges that lead to good solutions but exploit a number of recylcled multi-processor serrvers to work my way towards it. This proceeds as follows:

1. Create an initial configuration file with very broad positive and negative ranges and coarse local optimization.

2. For as many processors as feasible, select different random number seeds run for a fixed number of generations.

3. Examine the results. Select one or more that show the greatest promise and use their solution as the starting points for the next.

4. After a run, if any coefficients are near their range limits, expand their range in the direction nearest the limit and move the other range in the same direction.

5. If a coefficient is not near the range limits, reduce the range limit and decrease the granularity of the local search.

6. Run the new configuration and repeat at step 4 until satisfied with the result. Termination occurs when the results don't improve over the existing results.

Only one equation at a time is optimized - selected at compile time from all those implemented. Compilation is with gcc's -Ofast option for hardware double-precision floating point. The use of Linux processes precludes this from running on Windows.

9.6 Simple

For the #22 with fixed spacing coils I note that $l = 0.027N$ so remove length from the equation. This performs reasonably well but not killer. It appears to have some trouble at small values (perhaps the fault of the LCR meters) and consequently at the larger ones as well. In the code, this is called the SIMPLE model and was optimized against the *cspacing.csv* test file that contains only coils with identical spacing.

$$\mathscr{L} = \mu_0 \frac{(r_0 + r_1 R + r_2 R^2 + r_3 R^3)(t_0 + t_1 N + t_2 N^2)}{c_d} \tag{36}$$

Coefficient	Value
r_0	0.04577932701610
r_1	-3.47318092941792
r_2	-32586.59629999914978
r_3	990000.68900003179442
c_d	459987.89609983825358
t_0	81262.26570000193897
t_1	-30132.44869999826915
t_2	-1717.08300000000872
t_3	21.00967900000605

Table 14: SIMPLE coefficient values.

The best cumulative SEE so far is 2.38% for the *cspacing.csv* data set. If that's your coil style, you can't do better. Against the other data sets, it's atrocious.

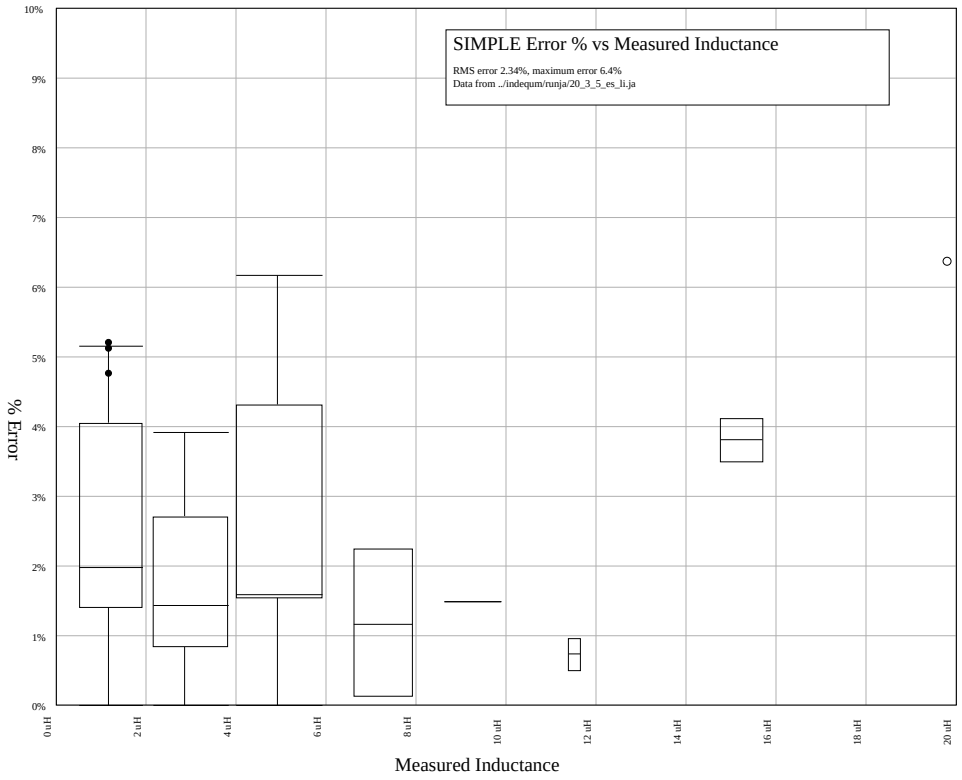

Figure 67: SIMPLE Equation error bars (Tukey) optimized for *cspacing.csv*.

For the coils measured, the result is much more accurate than the ARRL equation.

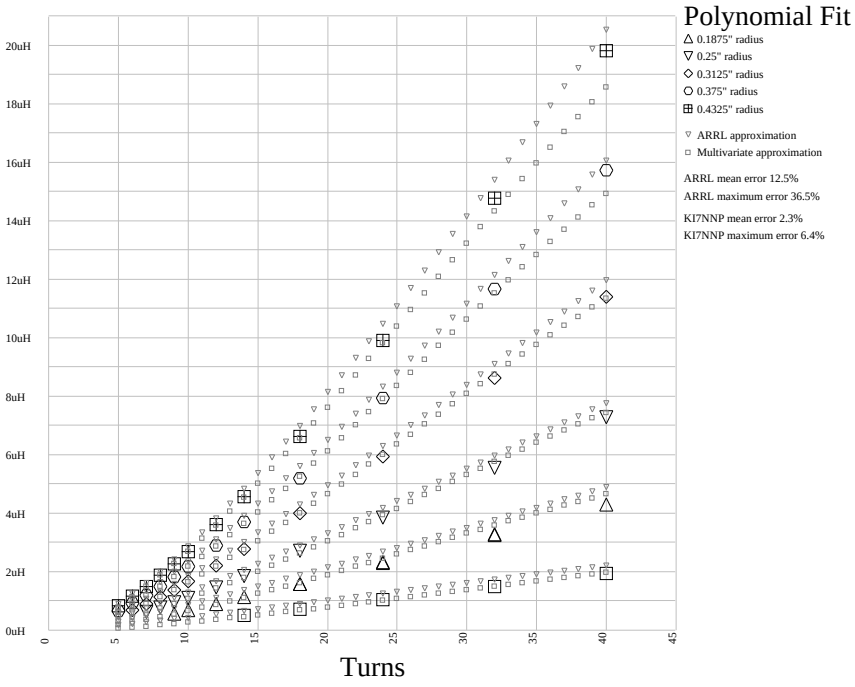

Figure 68: SIMPLE Equation vs ARRL equation.

9.7 Equation 8

Equation 8 (1-7 do not appear here) mirrors ARRL formula but with extra powers on the terms. Optimized against all #22 gauge coils in *all22.csv* and called EQUATION8 in the code. The results are reasonable and can be used for #22 gauge coils as the wire size is not included in the equation.[6]

$$\mathscr{L} = \mu_0 \frac{(rn_0 + rn_1 R + rn_2 R^2 + rn_3 R^3)(t_0 + t_1 N + t_2 N^2)}{(rd_0 + rd_1 R + rd_2 R^2) + (l_1 L + l_2 L^2 + l_3 L^3)} \tag{37}$$

Coefficient	Value
rd_0	-407.04509076938336
rd_1	-47300.28250000364642
rd_2	-996508.40000000002328
l_1	-73233.56241363284062
l_2	199806.98573789244983
l_3	-1099730.00000000000000
rn_0	0.00682643308813
rn_1	-1.30673958074054
rn_2	-37699.90661940674181
rn_3	-184104.91928571878816
t_0	-19.36749549088033
t_1	12.13749991044755
t_2	5.37301893791146

Table 15: Equation 8 coefficient values optimized against *all22.csv*.

The results for the *cspacing.csv* being worse than all the #22 gauge coils indicating some attention made to the many more coils in the bigger set.

Subset	SEE
turntest.csv	7.09%
cspacing.csv	6.20%
all22.csv	3.81%
all.csv	6.13%

Table 16: Equation 8 Results

[6]Equation G is actually the same as equation 8 and has been removed.

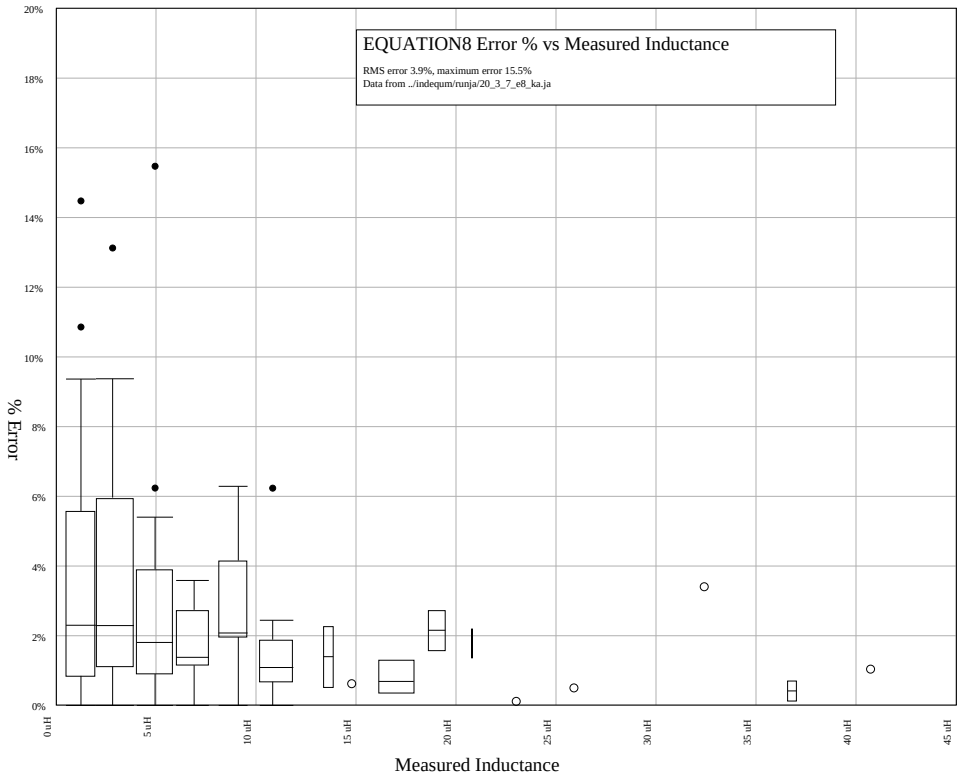

Figure 69: Equation 8 error bars (Tukey).

9.8 Equation 9

An extraordinary simple one with marginal results. No wire gauge, but:

$$\mathscr{L} = \mu_0 \frac{(2R)^2 N^2}{2d_0 R + d_1 L} \tag{38}$$

This was optimized against *all22.csv* and performed poorly against more complicated polynomials, but better than the optimized ARRL equations.

Coefficient	Value
d_0	0.66490392427040
d_1	1.33028471078599

Table 17: Equation 9 coefficient values optimized against *all22.csv*.

Subset	SEE
turntest.csv	7.26%
cspacing.csv	6.34%
all22.csv	10.52%
all.csv	11.95%

Table 18: Equation 9 Results

As shown in Figure 70, the equation has a rough time with small values in *all22.csv*.

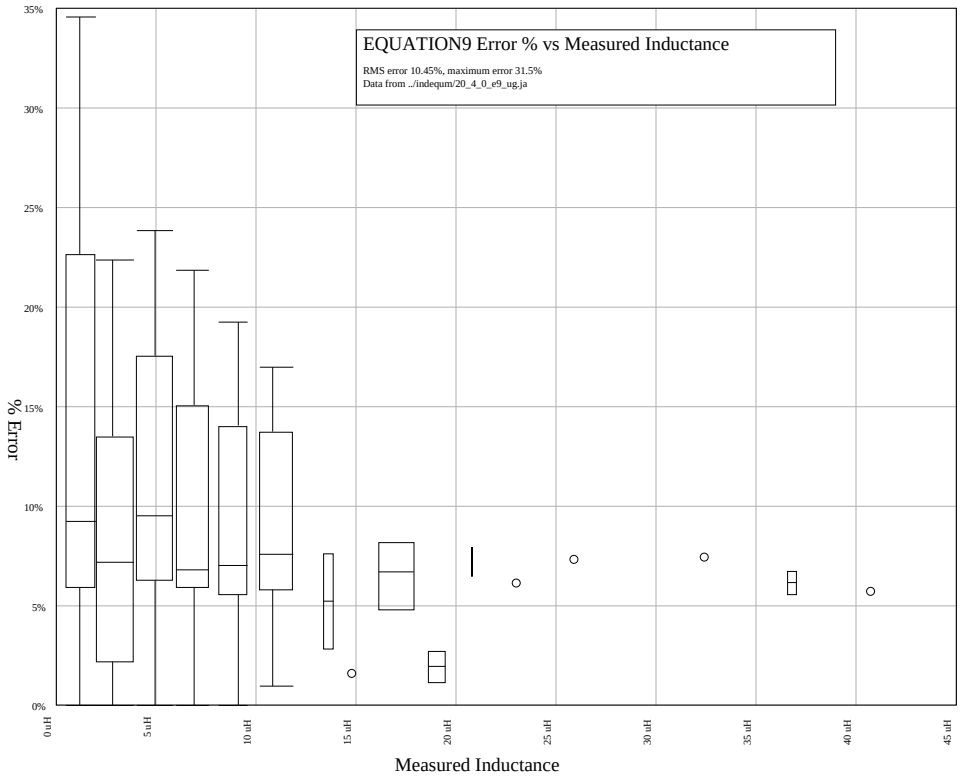

Figure 70: Equation 9 error bars (Tukey).

9.9 Equation A

Not a good idea as 5 degrees tends to fit well but will have many oscillations between measurements that don't bode well for predictions inside the measured range. Because the wire gauge is not included, we run this only against #22 gauge coils. Called EQUATIONA in the code.

$$\mathscr{L} = \mu_0 \frac{(r_0 + r_1 R + r_2 R^2 + r_3 R^3 + r_4 R^4 + r_5 R^5)(t_0 + t_1 N + t_2 N^2)}{l_0 + l_1 L + l_2 L^2 + l_3 L^3 + l_4 L^4 + l_5 L^5} \tag{39}$$

Subset	RMS Error
turntest.csv	5.08%
cspacing.csv	6.88%
all22.csv	4.63%
all.csv	6.34%

Table 19: Equation EQUATIONA Results

Coefficient	Value
r_0	-0.46000000000000
r_1	182.99999999999596
r_2	0.00000000000000
r_3	226674.20000000012806
r_4	100000.00000000000000
r_5	50047.39999999787688
t_0	3.72000000000000
t_1	-1.88000000000000
t_2	-0.52000000000000
l_0	-450.99999999999881
l_1	-24924.80000000019209
l_2	-0.20000000000000
l_3	0.60000000000000
l_4	19.60000000000000
l_5	-20.20000000000001

Table 20: Equation A coefficient values from 20_3_8_ea_kc.txt.

Of the 5 worst performers, 4 were in the group that measured actual radius rather than the printer specified one suggesting that all unmeasured radii are somewhat suspect.

Error	Measured	Compute	Turns	Dia.	Len	Gauge	File
3.9%	4.618	5.529	40	0.509"	1.6"	#22	*g22.csv*
2.3%	3.305	3.810	30	0.509"	1.2"	#22	*g22.csv*
2.2%	0.876	0.747	5	1.5"	1.5"	#22	*15p15.csv*
1.6%	0.772	0.870	10	0.509"	0.4"	#22	*g22.csv*
1.0%	2.039	2.247	20	0.509"	0.8"	#22	*g22.csv*

Table 21: 5 worst coils for Equation A

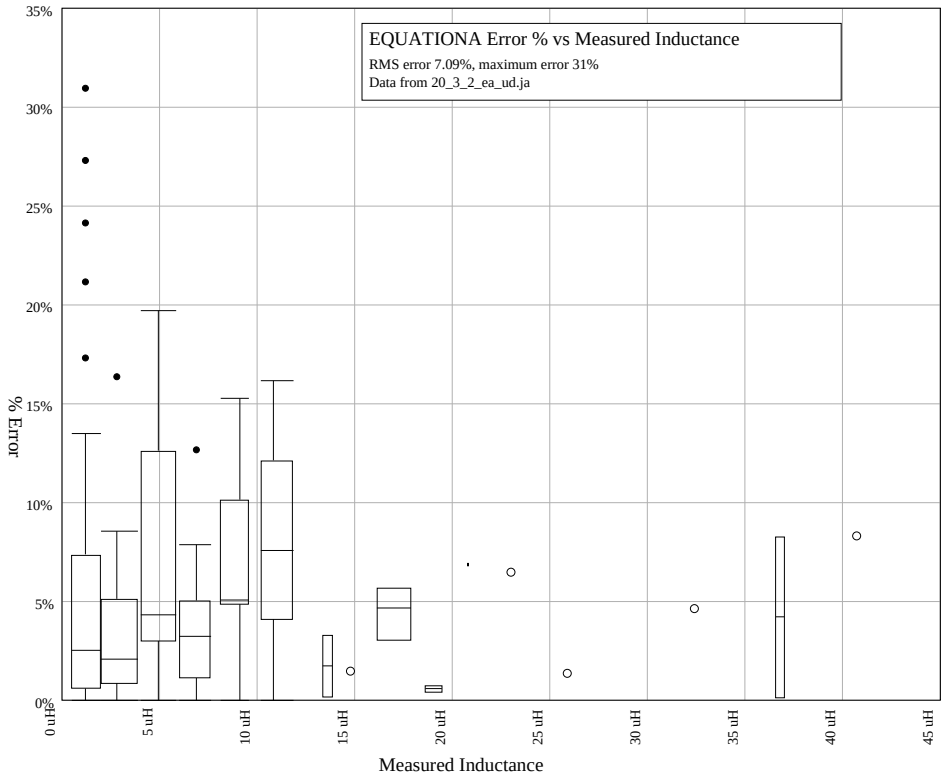

Figure 71: Equation A error bars (Tukey).

9.10 Equation C

Add wire gauge to Equation A. Called EQUATIONC in the code and is the slowest computationally requiring some extended processing times even when the equations are unrolled. This was optimized against *all.csv*.

$$\mathscr{L} = \mu_0 \frac{(r_0 + r_1 R + r_2 R^2 + r_3 R^3 + r_4 R^4 + r_5 R^5)(t_0 + t_1 N + t_2 N^2)(w_0 + w_1 W + w_2 W^2)}{l_0 + l_1 L + l_2 L^2 + l_3 L^3 + l_4 L^4 + l_5 L^5} \tag{40}$$

Coefficient	Value
r_0	-3.78425610055474
r_1	1730.13463110271277
r_2	199538.23918580383179
r_3	-3399848.35999976471066
r_4	-149989.00000000081491
r_5	4909.86891871382340
t_0	903.56309019975549
t_1	-395.63677420390195
t_2	-103.73733704737968
w_0	0.01207370432147
w_1	-0.13655337273057
w_2	2.11620166340000
l_0	-2225.09808363423281
l_1	-128589.90168644346704
l_2	-1003.00000000000000
l_3	-1008.29292763376998
l_4	2483.63690288608086
l_5	490.30826633053363

Table 22: Equation C coefficient values.

The results against all the subsets are reasonable with the caveat of using quintics to fit to errors of winding and measurement.

Subset	SEE
turntest.csv	2.72%
cspacing.csv	6.11%
all22.csv	5.67%
all.csv	5.42%

Table 23: Equation C Results

Looking for the most trouble, the worst 5 entries are on the fringes of measured data:

- High aspect ratio (≥ 2.75), low inductance ($< 1\mu H$).
- Small or large gauge wire.

Error	Measured	Compute	Turns	Dia.	Len	Gauge	File
8.5%	1.181	0.837	10	1"	3"	#28	*3inws.csv*
5.0%	1.076	0.836	10	1"	3"	#22	*3inws.csv*
2.3%	4.040	4.651	10	0.398"	1.12"	#22	*p1875.csv*
2.1%	8.821	7.551	40	0.5"	1"	#26	*p5_1_26.csv*
1.6%	1.616	1.820	10	1"	1"	#14	*wiresize.csv*

Table 24: 5 worst coils for Equation C.

Greatest variability between prediction and measurement is for low inductance coils.

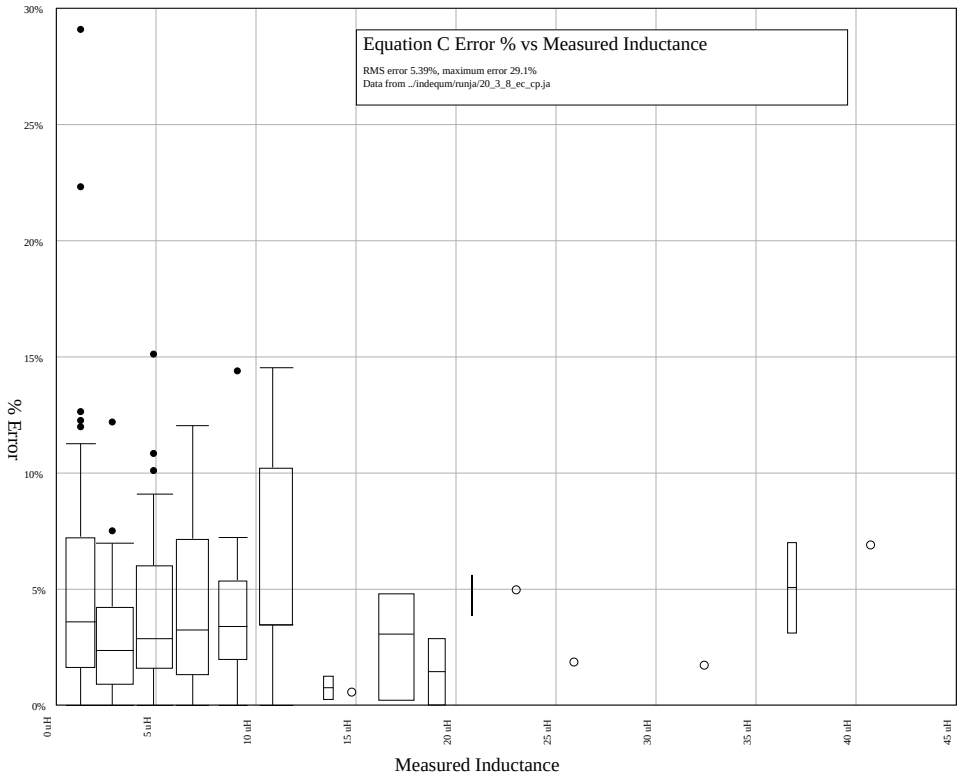

Figure 72: Equation C error bars (Tukey).

9.11 Equation D

This accounts for wire size and variable spacing but removes the quintics on the radius and length of Equation A. Optimize against *all.csv* except those with less than .5 μH. In the code, this is called EQUATIOND.

$$\mathscr{L} = \mu_0 \frac{(r_0 + r_1 R + r_2 R^2 + r_3 R^3)(t_0 + t_1 N + t_2 N^2)(w_0 + w_1 W + w_2 W^2)}{l_0 + l_1 L + l_2 L^2 + l_3 L^3} \tag{41}$$

Coefficient	Value
r_0	0.01794
r_1	-8.31722000000232
r_2	-804.89380000006770
r_3	-0.0379
t_0	-5.25855999999957
t_1	1.52247999999994
t_2	0.73276000000004
w_0	-1.03136000000004
w_1	1.54125999999996
w_2	88.01792000000133
l_0	3.55340000000013
l_1	425.52679999991551
l_2	-1036.50319999997032
l_3	-18481.68420000031620

Table 25: Equation D coefficient values from 20_3_3_ed_cj.txt.

The results are reasonable across all data sets.

Subset	SEE
turntest.csv	10.43%
cspacing.csv	6.17%
all22.csv	9.90%
all.csv	8.98%

Table 26: Equation D Results

The worst performing coils are ones with more accurate diameter measurements suggesting that we're fitting the equations to more coils without accurate measurement.

Error	Measured	Compute	Turns	Dia.	Len	Gauge	File
26.2%	4.674	5.898	40	0.509"	1.6"	#22	*g26.csv*
23.3%	0.876	0.672	5	1.5"	1.5"	#22	*15p15.csv*
20.1%	4.618	5.544	40	0.509"	1.6"	#22	*g22.csv*
18.7%	3.371	4.00	30	0.509"	1.2"	#26	*g26.csv*
17.7%	0.784	0.923	10	0.509"	0.4"	#26	*g26.csv*

Table 27: 5 worst coils for Equation D.

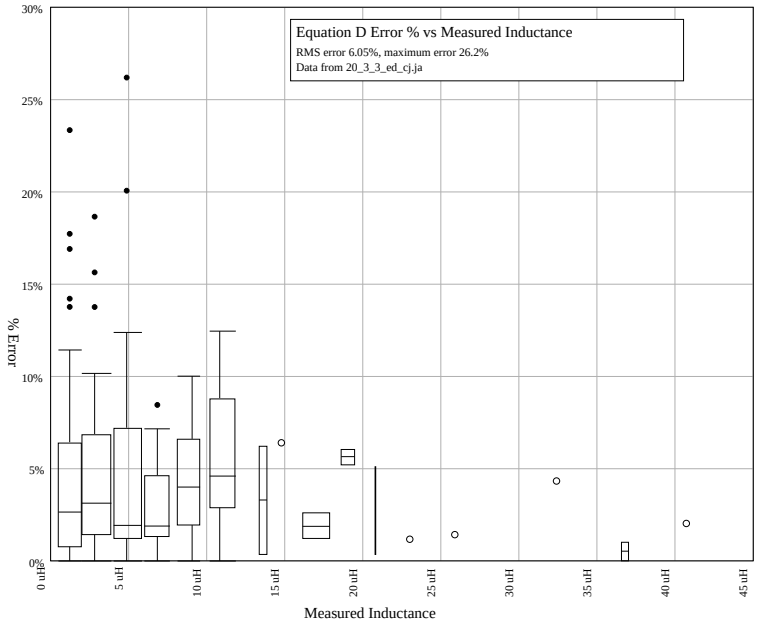

Figure 73: Equation D Tukey plot measured inductance vs error %

9.12 Equation E

Try to fit with a log of the radius. Fit was against *all22.csv*. This is an example of an equation with no hope of a fit - not just because of the log function but I tried it anyway.

$$\mathscr{L} = \mu_0 \frac{(r_0 \log(r_1 R))(t_0 + t_1 N + t_2 N^2)}{l_0 + l_1 L + l_2 L^2 + l_3 L^3 + l_4 L^4 + l_5 L^5} \tag{42}$$

After a few runs it became clear this isn't the gift to inductance prediction one would hope. As there's no wire size, I attempted to fit this to *all22.csv*.

Coefficient	Value
l_0	0.00395483165663
l_1	0.34500000000000
l_2	-10.74143633681195
l_3	25.67099690499859
l_4	3238.75043977776795
l_5	-30621.34388796867643
r_0	-0.00001505876902
r_1	336.80000000000001
t_0	64.33864199999695
t_1	-37.02649487999803
t_2	-1.50169943034172

Table 28: Equation E coefficient values.

Nowhere does this approach reasonableness.

Subset	SEE
turntest.csv	27.52%
cspacing.csv	23.06%
all22.csv	30.24%
all.csv	30.09%

Table 29: Equation E Results

This turned out to be more of a test of the system rather than a useful approximation. However, it did spur research into including the equation in the optimization scheme.

9.13 Equation F

This has a fixed wire #22 only. In the code this is called EQUATIONF. The equation was fit against the *all22.csv* data file with a resulting RMS error of 0.051144.

$$\mathscr{L} = \mu_0 \frac{(r_0 + r_1 R + r_2 R^2 + r_3 R^3)(t_0 + t_1 N + t_2 N^2)}{l_0 + l_1 L + l_2 L^2 + l_3 L^3} \tag{43}$$

Coefficient	Value
r_0	0.09800000000000
r_1	-57.40291999999053
r_2	-10949.29838000065320
r_3	-7000.13919999999962
t_0	-10.00000000000000
t_1	4.91220000000005
t_2	1.75840000000000
l_0	-134.06080000003760
l_1	-9000.00020000434233
l_2	-1501.47499999999991
l_3	49.510

Table 30: Equation F coefficient values from 20_3_3_ef_ca.txt.

The results aren't horrible but not always the best so this is not the recommended solution.

Subset	SEE
turntest.csv	4.40%
cspacing.csv	6.18%
all22.csv	5.72%
all.csv	7.66%

Table 31: Equation F Results

As usual, the equation has a lot of trouble with small inductances - either an equation problem or LCR errors.

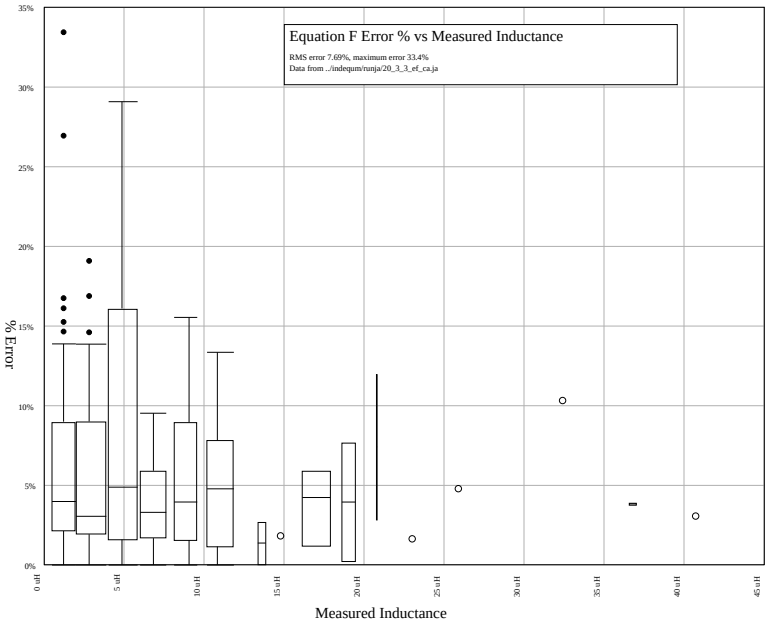

Figure 74: Equation F Tukey plot measured inductance vs error %

9.14 Equation H

Trying random things here, I put the length in the numerator and the radius in the denominator where the number of turns is a linear function of the length with constant spacing[7]. This was fit, not very successfully, against *cspacing.csv*.

$$\mathscr{L} = \mu_0 \frac{l_0 + l_l L + l_2 L^2 + l_3 L^3}{r_0 + r_1 R + r_2 R^2 + r_3 R^3} \tag{44}$$

With an RMS error of 0.0881938, the results are pretty poor even for the constant spacing.

Coefficient	Value
r_0	200.05999999999764
r_1	-32705.05999999758569
r_2	1493771.60000001755543
r_3	-1490874.40999975963496
l_0	-15.54000000000006
l_1	7163.15999999994983
l_2	106422.55999998308835
l_3	51945.70000000068831

Table 32: Equation H coefficient values

As one might expect, the results are dreadful for non-constant spacing (0.1"). If one were automating the equation search, this one and ones like it would be rejected quickly.

Subset	SEE
turntest.csv	106.29%
cspacing.csv	17.42%
all22.csv	476.12%
all.csv	931.46%

Table 33: Equation H Results

A few small inductances caused trouble, but in general, performance is not that good.

[7]Equation G turned out to be the same as another equation but with a different variable name and was removed.

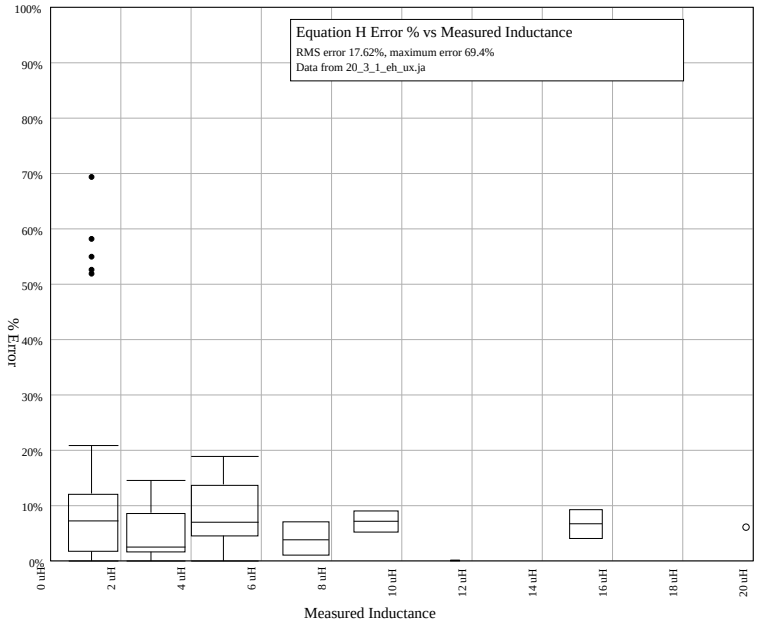

Figure 75: Equation H Tukey plot measured inductance vs error %

9.15 Equation I

Do cubic's for all 4 parameters. Reasonable results all around when fit against *all.csv*.

$$\mathscr{L} = \mu_0 \frac{(r_0 + r_1 R + r_2 R^2 + r_3 R^3)(t_0 + t_1 N + t_2 N^2 + t_3 N^3)}{(l_0 + l_1 L + l_2 L^2 + l_3 L^3)(w_0 + w_1 W + w_2 W^2 + w_3 W^3)} \tag{45}$$

Coefficient	Value
r_0	-0.12439606855974
r_1	59.34165136966276
r_2	6842.26394817989058
r_3	-16522.11014265214544
w_0	-2000.50704210045296
w_1	-1960.86505488237162
w_2	-35099.56997791079630
w_3	-5060482.57904209569097
t_0	-2828.82066302971543
t_1	722.31593558954432
t_2	1454.66890894125208
t_3	-4.40302929936243
l_0	-24.50983300791553
l_1	-2818.19194986313141
l_2	9286.00347049571428
l_3	93039.70835298359452

Table 34: Equation I coefficient values.

Results are not particularly good but reasonable.

Subset	SEE
turntest.csv	7.23%
cspacing.csv	4.49%
all22.csv	8.54%
all.csv	8.00%

Table 35: Equation I Results

As typical, the low inductance coils have the largest error.

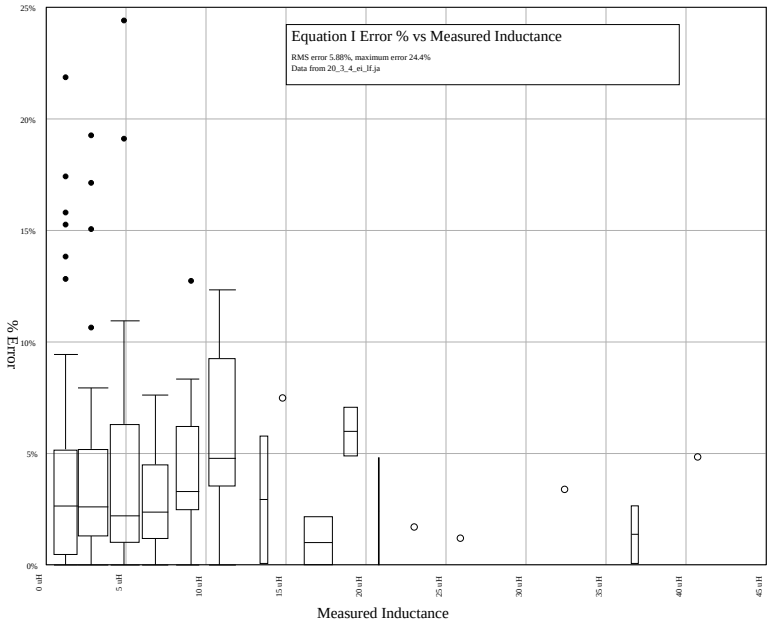

Figure 76: Equation I Tukey plot measured inductance vs error %

9.16 Equation J (cubic)

Here I try cubics for everything except wire size with reasonable results. This is also called the "Cubic" equation.

$$\mathscr{L} = \mu_0 \frac{(r_0 + r_1 R + r_2 R^2 + r_3 R^3)(t_0 + t_1 N + t_2 N^2 + t_3 N^3)}{(w_0 + w_1 W + w_2 W^2)(l_0 + l_1 L + l_2 L^2 + l_3 L^3)} \tag{46}$$

Coefficient	Value
r_0	0.06874935911182
r_1	-33.54915030573340
r_2	-6014.91131494658657
r_3	39348.09999999596039
w_0	-335.85286243928442
w_1	-1993.67721199933703
w_2	11.98000000000000
t_0	11.99000000000000
t_1	336.91508219616071
t_2	538.22967240256025
t_3	-2.23075127004639
l_0	49.88575262532289
l_1	4131.31057855364907
l_2	-16915.37200213107280
l_3	-12248.33510236051552

Table 36: Equation J coefficient values.

The results are generally quite good for all subsets.

Subset	SEE
turntest.csv	2.86%
cspacing.csv	5.92%
all22.csv	4.77%
all.csv	4.38%

Table 37: Equation J (Cubic) Results

Equation J is the best all around performer, however, the use of cubics threatens to fit

the equation against some anomalous data points. I recommend the use of Equation K (Quadratics) in Table 38 on page 38 instead.

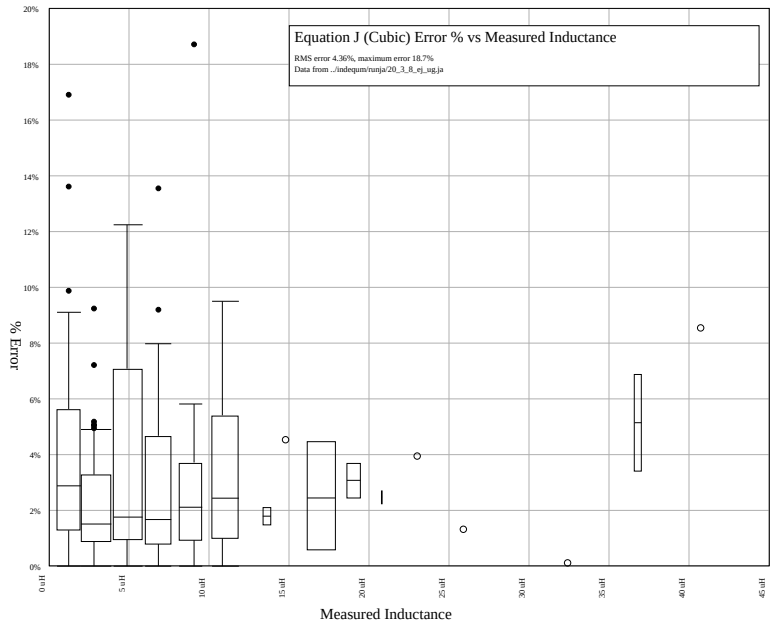

Figure 77: Equation J (Cubic) Tukey plot measured inductance vs error %

9.17 Equation K (quadratic)

Here all variables have a quadratic approximation. This is called the "Quadratic" approximation.

$$\mathscr{L} = \mu_r \mu_0 \frac{(r_0 + r_1 R + r_2 R^2)(t_0 + t_1 N + t_2 N^2)}{(w_0 + w_1 W + w_2 W^2)(l_0 + l_1 L + l_2 L^2)} \tag{47}$$

I fit this equation against *all.csv* as we now have the wire size parameter.

Coefficient	Value
r_0	0.17441641068426
r_1	-83.04622923581972
r_2	-9011.64600000499013
w_0	534.47547661359704
w_1	7025.29740000000129
w_2	-108295.0733700038254
t_0	3351.63767400000143
t_1	-1261.22039999999993
t_2	-316.92996598636881
l_0	43.87868302222068
l_1	3601.75520024868956
l_2	-15315.16458101996977

Table 38: Equation K coefficient values.

Subset	SEE
turntest.csv	4.85%
cspacing.csv	5.86%
all22.csv	5.23%
all.csv	4.49%

Table 39: Equation K Results

Note that the values for the cubic equation J (see Table 37 are somewhat better but a cubic starts the risk that wee're fitting a better equation to some bad data points. Hence the recommendation that you use this quadratic version.

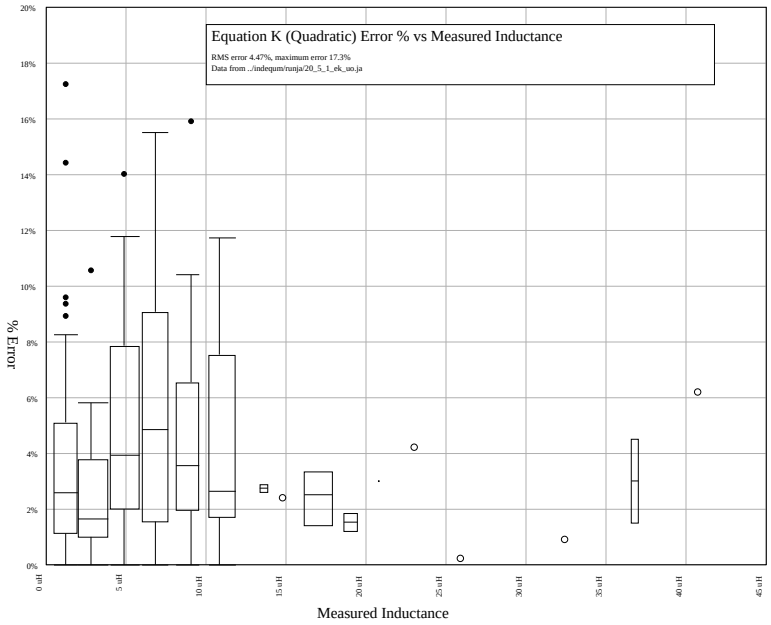

Figure 78: Equation K (Quadratic) Tukey plot measured inductance vs error %

9.18 Equation Summary

Some of the polynomials shown in the preceding sections are better predictions of our particular geometry as compared to the standard ARRL polynomial. To squeeze the table in the Simple equation 36 is labeled **S** and Equation E 42 is not listed for its very poor results.

Data	ARRL	S	8	9	A	C	D	F	H	I	J	K
turntest	11.8	29.9	7.1	7.3	5.9	2.8	10.4	4.4	106	7.2	2.9	4.8
cspacing	12.7	2.4	6.2	6.3	7	6.1	6.2	6.2	17.4	4.5	5.9	5.9
all22	13.4	52.7	3.8	10.5	4.6	5.7	9.9	5.7	476	8.5	4.8	5.2
all	14.5	60.8	6.1	12	6.4	5.4	9	7.7	931	8	4.4	4.5

Table 40: Result summary, SEE percent.

I conclude that Equation K 47, though not the best overall, is the appropriate choice if wire gauge is to be included as it is less effected by anomalous values than Equation J 46.

10 The Programs

The 5 programs are written in plain C without reference to any but standard libraries. Except for the optimization routines, they are portable to Windows and Linux. All are command line programs, the interfaces very simple. You will find their documentation in [21]. In the following I discuss their use and implementation.

10.1 Subset CSV Files

The following programs require a different set of CSV columns for operation. The first row must contain the column headings separated by commas. Subsequent rows contain numbers and file names separated by commas.

Column	Description
Henrys	A coil value in Henries.
Radius	The coil radius in meters.
wireRadius	The wire radius in meters.
gauge	The wire gauge (an integer).
Turns	The number of turns.
Length	The coil length in meters.
FileName	The origin CSV file - a string.

Table 41: Program CSV file format.

The rows can be for a single coil with the mean of multiple measurements, median by your choice, or one row for each measurement. However, all measurements are expected to be metric.

10.2 compare: Comparison of Equations

The equations in this document are implemented in the *compare* program. As a command line argument, it takes a CSV file of the format in Table 41.

For example, *turntest.csv* gives something like the following:

compare turntest.csv

```
compare V2.00.009
Limits:
  Turns             8 -> 50
  Gauge             #22 -> #22
  Diameter          0.5" -> 0.5"
  Length            0.32" -> 2"
  Ind.              0.6123 uH -> 7.06123 uH

Working turntest.csv for SEE
  Original ARRL error    11.83%
  ARRL Turns error       2.10%
  ARRL cspacing error    9.48%
  ARRL all22 error       7.06%
  ARRL all error         7.28%
  RFC error              11.89%
  RF1 error              12.06%
  Lundin error           11.87%
  Miller error           11.87%

  Simple error           29.91%
  Equation 8 error       7.09%
  Equation 9 error       7.26%
  Equation A error       5.87%
  Equation C error       2.72%
  Equation D error       10.43%
  Equation E error       9353800.23%
  Equation F error       4.40%
  Equation H error       106.29%
  Equation I error       7.23%
  Cubic Error (J)        2.86%
  Quadratic Error (K)    4.82%
```

Initially, it summarizes the input CSV file. It then runs through all known equations giving their SEE for that file.

Original ARRL error is Equation 1 on page 9.

ARRL Turns error is the general ARRL Equation 34 on page 87 optimized for *turntest.csv* in Table 13 on page 87.

ARRL cspacing error is the general ARRL Equation 34 on page 87 optimized for all constant spacing coils*cspacing.csv* in Table 13 on page 87.

ARRL all22 error is the general ARRL Equation 34 on page 87 optimized for all #22 gauge coils *all22.csv* in Table 13 on page 87.

ARRL all error is the general ARRL Equation 34 on page 87 optimized for all coils *all.csv* in Table 13 on page 87.

RFC error from [10] is Equation 5 on page 14.

RF1 error is from [11] is Equation 6 on page 14.

Lundin error is from Lundin's paper [13] is Equation 8 on page 14.

Miller error is from Miller's paper [14] is Equation 11 on page 15.

Simple error is a 2 variable polynomial in Equation 36 on page 91 with coefficients in Table 14.

Equation 8 error is a 3 variable polynomial (no wire gauge) with Equation 37 on page 94 with coefficients in Table 15.

Equation 9 error is a 3 variable polynomial similar to the ARRL. Equation 38 on page 96 with coefficients in Table 17.

Equation A error is a 3 variable polynomial. Equation 39 on page 98 with coefficients in Table 19.

Equation C error has all 4 variables but quintics in Equation 40 on page 100 with the coefficients in Table 22.

Equation D error has all 4 variables but quartics in Equation 41 on page 103 with the coefficients in Table 25.

Equation E error a truly dreadful one but here to show how bad it can be. Equation 42 on page 105 with coefficients in Table 28.

Equation F error has no wire size with Equation 43 on page 106 with suboptimal coefficients in Table 30.

Equation H error Just length and radius with the number of turns a linear function of length. Equation 44 on page 108 with coefficients in Table 32.

Equation I error cubics for all 4 variables in Equation 45 on page 110 with coefficients in Table 34.

Cubic Error (J) all 4 variables with quadratic wire radius, the rest cubic in Equation 46 on page 112 with coefficients in Table 36.

Quadratic Error (K) all 4 variables quadratic in Equation 47 on page 114 with coefficients in Table 38.

10.3 inductor: Optimal Form

This program does an exhaustive search to build the coil of your dreams. You give it your required inductance (in μH), some limits on size, and which equation to use for the determination. Its output is a command line to call the *coil* program that generates the OpenSCAD form description.

Using defaults and Equation K (quadratics) for a $5\mu H$ coil we have:

inductor 5 -equation EquationK

```
inductor V1.00.007
For equation EquationK:
Best result 5.00002 uH, 40 turns, length = 1.9675", radius = 0.25"
Recommendations:
  ARRLOriginal          : marginal
  ARRLTurns             : marginal
  ARRLcspacing          : recommended
  ARRLall22             : reasonable
  ARRLall               : marginal
  Simple                : marginal
  Equation8             : highlyRecommended
  Equation9             : marginal
  EquationA             : highlyRecommended
  EquationC             : highlyRecommended
  EquationD             : notRecommended
  EquationE             : notRecommended
  EquationF             : recommended
  EquationH             : notRecommended
  EquationI             : notRecommended
  EquationJ             : notRecommended
  EquationK             : highlyRecommended
  RFC                   : marginal
  RF1                   : marginal
  Lundin                : marginal
Execute this:
coil inductor.scad -radius 0.25 -length 1.9675 -turns 40
```

The recommendations are based on your requirements and may vary with what you request. You can expand or contract the search range, make for finer resolution of the search, set the wire size, and minimum or maximum turns.

The program will list the options if you execute it with no command line arguments. You can cut and paste the execution of the *coil* program or change it as you like.

10.4 coil: Generate OpenSCAD

The *coil* program creates an OpenSCAD file. This contains the coil cylinder minus the core hole, the two holes for the leads and a helical set of cylinders as the wire channels. Depending upon the options, this can be a rather large file and take forever to convert to

STL. Executing the result from the *inductor* program yields the following:

```
coil inductor.scad -radius 0.25 -length 1.9675 -turns 40
 Using 19 cylinders per turn
 theta = 1.79356
 wire length = 62.8627
 Cylinder length 0.0992568 inches
 Cylinder offset Z 0.00258882 inches
```

You'll find the file *inductor.scad* as a result of some 118k bytes. The prolog shows the parameters used.

```
// Coil cylindersPerTurn 19
// Coil wireSize 0.028"
// Coil wallThickness 0.125"
// Coil wireIndentFaces 9
// Coil formFaces 90
// Coil end overhang 0.1
// Coil radius 0.25"
// Coil length 1.9675"
// Coil turns 40
// Coil extensions 0.1
```

Following this is the master cylinder, the center hole, and the two lead holes.

```
scale([25.4, 25.4, 25.4])
difference() {
 // The master coil cylinder.
 cylinder($fn=90, r=0.25, h=2.1675);

 // The hole through the center
 translate ([0,0,-0.1]) cylinder($fn=90, r=0.125, h=2.4675);

 // The two wire holes.
 translate([0,0,0.1]) rotate([0,90,0])
    cylinder($fn=9,h=0.5,d=0.042);
 translate([0,0,2.0675]) rotate([0,90,0])
    cylinder($fn=9, h=0.5, d=0.042);
    ⋮
```

And then lots of little cylinders. Converting this to STL took 59 minutes on a 3.6 GHz Xeon processor (only one thread).

10.5 Parameter Optimization

There are many optimization strategies for multivariate polynomials. I've used two: exhaustive search for integer optimization and genetic optimization with many modifications for floating-point solutions.

10.5.1 ARRL Optimization

The multi-process *arrl* program runs only on Linux. It requires 3 command line arguments. For example, optimizing the coefficients for Equation 34 on page 87 against all the #22 gauge printed coils for small coefficients (< 100) requires the configuration file:

```
# A quick run. Values up to 100 allowed.
lownum 1 100
highnum 100
incnum 2

lowdia 1
highdia 100
incdia 1

lowlen 1
```

```
highlen 100
inclen 1
```

A short run using 8 processes gives the following:

arrl cspacing.csv vars 8

```
arrl V2.01.002
RMS errors
Original equation 12.52%
   301.046%:  13 100 100
   239.689%:  11 100 100
   178.401%:  9 100 100
   117.291%:  7 100 100
   56.932%:  5 100 100
   12.2852%:  3 80 100
   5.5801%:  1 20 45
Best RMS error 5.58%
   numerator (A)    1
   diameter (B)     20
   length (C)       45
```

signifying a better set of values:

$$\mathscr{L} = \frac{d^2 n^2}{20d + 45l} \tag{48}$$

Large ranges in the configuration file will require exponential search time as will increasing the size of dataset being optimized.

10.5.2 Multivariate Optimization

The *indequ* program is simple multi-process genetic algorithm program to optimize multivariate polynomials against inductor datasets. The input dataset must have the format in Table 41 on page 117. The configuration file format is defined in [21].

The general flow for optimizing a new equation.

1. Define the new equation in the *indequ* source and compile selecting it.
2. Build a configuration file with broad ranges and coarse granularity for each coefficient.

3. Run the optimization against your selected ranges for a limited number of generations. If nothing is happening, you can prematurely terminate by typing escape.

4. (a) In the configuration file, if any coefficient is very near its limits adjust the limit(s) in that direction.
   (b) Compare each coefficient to previous values. If they haven't changed much, reduce the range and decrease their granularity.
   (c) Change the random number seed (64 bit integer).
   (d) Change the output file names.
   (e) Copy the best coefficients from the generated *.txt* file into the configuration file.
   (f) If the system was still reliably decreasing the RMS error when it finished, increase the number of generations you allow.

5. Verify that *indequ* is not running or has left any subtasks running. Kill any processes still running.

6. If you're still converging, or believe you are, run the system again and repeat at step 4.

7. Document the results!

11 Conclusions

For a restricted range of length, diameters, numbers of turns and wire gauge, equation provides a reasonable solution.

Diameters .375" to 2" with increasing errors on the outer edges somewhat matching the error margins published for the East Tester LCR.

Lengths .25 to 3" with increasing errors on the ends.

Turns Ok except where the turns are widely spaced.

Wire Size Mostly OK except where larger gauges significantly decrease the spacing between turns. Wire gauges #14 to #28 tested.

Humidity PLA is not a good plastic for devices in widely varying humidity.

Exceed these ranges at your own risk. Polynomial curve fits rarely good predictors much beyond the range of data points.

11.1 Do your own

If you're winding your own coils on a different form, perhaps with different core material or geometry a simple approach works as follows.

1. Print and wind a few coils varying only one parameter: turns, length, radius, or wire gauge. A minimum of 3 is required, more if possible. The coils should explore both the minimum and maximum inductances you need.
2. Measure their inductance multiple times and average.
3. Measure the parameter you varied. Counting turns is easy, measuring the radius less so.
4. Perform a univariate polynomial regression or linear least squares on the data with a maximum power much less than the number of coils.
5. For an inductance in the range tested, vary the parameter until you get what you want. The *turntest.csv* data set example varies only the number of turns. A linear equation gives an RMS error of 4.68% for the 8 coils while a cubic degree polynomial reduces the error to 1.52%, greatly superior to any of the equations tested. The more test coils you print the better your results will be.

As previously stated, using much more than cubic equations threatens to model randomness in your printing and winding tension.

11.2 Further Research

I did not have time, money, or space to explore stereo lithography (SLA) approaches for coil forms. These promise higher resolution and would help reduce the problems with poor winding channels.

I felt limited to coils with convex shapes that can be wound by hand but 3D printing opens up possibilities not previously explored.

- Irregular shapes to fit on circuit boards.
- Irregular spacing.
- Internal threads to match ferrite screws for variable inductance.
- Geometries for transformers and tapped inductors.
- Convex shapes to increase inductance in small spaces. This might require printing both conductive and high permittivity plastics.

Index

References

[1] ARRL, *The ARRL Handbook for Radio Communications*. Newington, CT 06111: The National Association for Amateur Radio, 2017.

[2] S. Kim, S. Kim, C. H. Green, and J. Jeong, "Multivariate polynomial regression modeling of total dissolved-solids in rangeland stormwater runoff in the colorado river basin," *Environmental Modelling & Software*, vol. 157, p. 105523, 2022. [Online]. Available: https://www.sciencedirect.com/science/article/pii/S1364815222002237

[3] P. Kövesárki and I. Brock, "Multivariate polynomial regression regularized via fit function uncertainty," *Journal of Physics: Conference Series*, vol. 523, p. 012029, 06 2014.

[4] F. W. Grover, *Inductance Calculations*. Mineola, New York: Dover, 2009, originally published 1946.

[5] C. R. Paul, *Inductance Loop and Partial*. Hoboken, New Jersey: Wiley, 2010.

[6] "How to calculate coil inductance," *http://zpostbox.ru/how_to_calculate_inductors.html*.

[7] S. R. Fulton and J. C. Rawlins, *Basic AC Circuits*. 201 W. 103rd Street, Indianapolis, Indiana 46290: SAMS, 1981.

[8] E. Magnetica, "Database of magnetic properties," *https://e-magnetica.pl/doku.php/database*.

[9] "Inductor sizing equation," *https://www.allaboutcircuits.com/textbook/reference/chpt-1/inductor-sizing-equation*.

[10] C. Bowick, J. Blyler, and C. Ajluni, *RF Circuit design*. Burlington, MA: Elsevier, 2008.

[11] R. Ludwig and G. Bogdanov, *RF Circuit Design Theory and Applications*, 2nd ed. Pearson.

[12] "Coil inductance calculator," *https://www.eeweb.com/tools/coil-inductance/*.

[13] R. Lundin, "A handbook formula for the inductance of a single-layer circular coil," *Proceedings of the IEEE*, vol. 73, no. 9, pp. 1428–1429, 1985.

[14] H. C. Miller, "Inductance formula for a single-layer circular coil," *Proceedings of the IEEE*, vol. 75, no. 2, pp. 256–257, February 1987.

[15] S. K. Kachigan, *Multivariate Statistical Analysis, A Conceptual Introduction*, 2nd ed. New York: Radius Press, 1991.

[16] C. J. Kaiser, *The Inductor Handbook*. Rogersville, MO 65742: CJ Publishing, 1996.

[17] E. B. Rosa and F. W. Grover, "Formulas and tables for the calculation of mutual and self-inductance," pp. 150–152, 1912.

[18] R. McGill, J. Tukey, and W. A. Larsen, "Variations of box plots," *The American Statistician*, vol. 32, no. 1, pp. 12–16, February 1978.

[19] D. E. Goldbert, *Genetic Algorithms in Search, Optimization & Machine Learning*. Addison-Wesley, 1989.

[20] P. Sinha, "Multivariate polynomial regression in data mining: Methodology, problems and solutions," *International Journal of Scientific & Engineering Research*, vol. 4, no. 12, 12 2013.

[21] J. Marti, *Inductor Software Manual*, *https://www.cog9llc.com*.